“ Hydrothermal liquefaction of lignin ”

zur Erlangung des akademischen Grades einer

DOKTORIN DER INGENIEURWISSENSCHAFTEN

von der KIT-Fakultät für Chemieingenieurwesen und Verfahrenstechnik des
Karlsruher Instituts für Technologie (KIT)
genehmigte

DISSERTATION

von

Julia Schuler M. Sc.
aus Auenstein

Tag der mündlichen Prüfung: 20.02.2020

Erstgutachter: Prof. Dr.-Ing. Jörg Sauer

Zweitgutachterin: Prof. Dr. Andrea Kruse

FÜR MAPA

Ich will euch zwei Sachen sagen:

1.) Ich, als mündiger, volljähriger Bürger dieses Landes und Mensch, werde mein Zimmer genau dann aufräumen, wenn ich vom Impuls und von der Zeit und vom Bock her das Gefühl habe, dass es jetzt richtig ist.

2.) Ihr seid mein Ursprung, mein Vertrauen, meine Insel und mein Schatz. Mein Mund formt euer Lachen, mein Herz schlägt euren Takt.

Ich bin neun Jahre alt und für mich ist selbstverständlich, ihr seid immer da und Zeit ist unendlich. Ich singe die euch entsprungenen Lieder und was ihr macht, mach ich auch.
Falls ich mich verliere, ihr findet mich wieder und wenn ihr lacht, lach ich auch. Ihr gebt mir Wurzeln in die eine, und Flügel in die andere Hand und einen Kuss auf meine Stirn, der sagt mir: „Ich bin nicht alleine." Dann legt ihr zwischen uns ein Band, sodass wir uns nicht verlieren, sagt ihr. Und dass ich gehen kann, wenn ich will.
Auch wenn ihr mich nicht gefragt habt, gibt es da noch etwas, dass ich euch noch nicht gesagt hab:
Ihr seid mein Ursprung, meine Insel, mein Vertrauen und mein Schatz. Mein Mund formt euer Lachen, mein Herz schlägt euern Takt.

Ihr, ihr seid mein Beweis, dass Liebe mehr als Geld zählt. Seid der Rahmen für mein Weltbild. Alles was für mich als Held gilt. Ihr gebt mir Halt ohne mich festzuhalten, schafft es, wenn ich nicht kann, mich auszuhalten. Würdet nichts tun mich je aufzuhalten, eher bringt ihr mich dorthin. Ich brauch' nichts zeigen und ihr seht mich, brauch' nichts sagen und ihr versteht mich, brauch' nichts haben und ihr nehmt mich, nehmt mich einfach wie ich bin. Und wenn ich Angst hab, seid ihr traurig. Wenn ich weine, weint ihr auch. Dann sagt ihr: „Sei nicht traurig." Und dass ihr immer an mich glaubt und mir kann nichts passieren, weil ich weiß, ihr seid noch hier.

Ich gehör' zu euch und ihr gehört zu mir.
Ihr seid mein Ursprung, mein Vertrauen, meine Insel und mein Schatz. Mein Mund formt euer Lachen, mein Herz schlägt euren Takt.

[Julia Engelmann]

Ohne Euch wäre das alles nichts geworden! Danke für alles was war, ist und kommt! Ich hab euch lieb!

DANKSAGUNG

Für das interessante Themengebiet und die Ermöglichung dieser Arbeit, sowie der fachkundigen Unterstützung während meiner gesamten Tätigkeit möchte ich besonders Herrn Prof. Dr.-Ing. Jörg Sauer danken. Man konnte stets auf ihre Unterstützung in jeglicher Hinsicht zählen, vielen Dank hierfür.

Unter anderem möchte ich Frau Prof. Dr. Andrea Kruse für die Übernahme der Koreferentin danken. Aber natürlich auch für deine tatkräftige Unterstützung und die Möglichkeit alle anfallenden Probleme mit dir besprechen und vor allem viele mit deiner Hilfe lösen zu können!

Chemisch, technisch, organisatorisch, in jeglichem Sinne wurde ich von Herrn Prof. Dr. Nicolaus Dahmen unterstützt, wofür ich mich herzlich bedanken möchte. Danke für viele fachliche und nicht fachliche Diskussionen und für deinen Einsatz mir gegenüber.

Konstante Unterstützung konnte ich durch Fr. Dr. Ursel Hornung erfahren. Danke Uschi, für die freundliche Aufnahme in den Arbeitskreis sowie der Unterstützung bei jeglichen Fragestellungen und der Betreuung der gesamten Arbeit.

Tatkräftige Unterstützung hatte ich durch die Mitarbeit am Projekt von „meinen“ Studenten, die ich in ihren Abschlussarbeiten betreuen durfte. Michael Ernst, Rajaa Jamil Sabri, Marvin Schmitt, Kinza Sha und Armel Mbieul, vielen Dank an euch alle! Michael danke für deine Unterstützung bei den Arbeiten am Kreislaufreaktor und der Erstellung des Modells. Rajaa danke für deine Arbeiten zum Reaktionsmechanismus. Marvin, Kinza und Armel danke für die Unterstützung im Labor.

Hilfe zur Analyse der Lignin Strukturen erfuhr ich von Fr. Dr. Judith Schäfer, Abteilung für Lebensmittelchemie und Phytochemie am KIT. Danke für dein Wissen, deine Messungen und die Diskussionen der Ergebnisse. Für diese Analyse wurden gemeinsame Messungen mit dem Institut für Lebensmittelchemie von Prof. Dr. Bunzel durchgeführt, danke für die Unterstützung.

Immer wieder haben wir gemeinsam gemessen, diskutiert und viel neues versucht, dafür ein großes Danke an dich Dr. Marco Fleckenstein.

Sicherlich wären viele meiner Messungen nichts geworden ohne dich, Birgit Rolli. Danke, dass wir die >1000 Proben zusammen über die Bühne gebracht haben und du das Arbeiten in 134 immer, auch ohne Fenster, angenehm gemacht hast. Danke auch für die Organisation der vielen tollen Feste und die tolle gemeinsame Zeit, die das Arbeiten mit euch allen noch fröhlicher gestaltet haben.

Sonja Habicht, auch an dich geht ein besonderer Dank, danke für die gemeinsame Büro Zeit! Danke für dein offenes Ohr, auf dass man jederzeit zählen kann, sowohl fachlich als auch privat! Auch wenn wir die Oligo Analyse nicht ganz fertigbekommen haben, hast du mir damit sehr weitergeholfen! Wir hatten wirklich schöne Zeiten zusammen!

Herrn Matthias Pagel möchte ich einen besonderen Dank aussprechen; DANKE! Ohne dich wäre das Ganze wirklich in die Hose gegangen. Nur durch dich und dein stets schnelles Handeln konnte ich genügend Messungen machen. Außerdem warst du es nie Leid, wenn ich mal wieder einen Autoklaven kaputt gemacht habe. =)

Immer wieder springst auch du ein und hilfst einem wo du nur kannst; auch ohne dich wäre die Mehrheit meiner Versuche nicht realisiert worden. Dafür ein großes Dankeschön, Thomas Tietz!

Trotz der ganzen anderen Arbeit, die ihr beide habt, helft ihr uns Doktoranden immer wo ihr könnt. Danke an Armin Lautenbach für die Unterstützung bei meinen HPLC Messungen und die gemeinsame Zeit. Danke Alexandra Böhm, dass du dich um so viele Belange innerhalb der Gruppe kümmerst und deine Unterstützung!

Vielfach bedanken möchte ich mich auch bei Hermann Köhler! Ohne Dich wäre meine Biomasse wohl noch immer nicht fertig gemahlen. Dank dir und deiner Kamera kann ich auch in 20 Jahren nochmal die gemeinsame Zeit durchleben.

Allen weiteren Mitgliedern der Arbeitsgruppe „Plattformchemikalien und Materialien aus Biomasse“ vielen Dank für die freundliche Aufnahme, die Unterstützung und die tolle gemeinsame Zeit.

David und Marcus (und Robert 😉) ohne euch wäre meine Zeit hier nicht mal halb so toll gewesen. Ihr habt mich in jeder Situation ertragen und mich immer unterstützt, danke! Ich freue mich wirklich in euch dreien Freunde gefunden zu haben! Ich vermisse unsre Dienstag/Mittwoch/Donnerstag Nachmittage nach vier! Marcus, nochmal danke für die letzten Korrekturen!

Der „Frauengruppe“ des IKFT’s möchte ich auch danken, in euch habe ich Freunde gefunden und ihr habt mein Leben bereichert! Sophia, Chiara und Karla euch ein extra danke für alles und eure Unterstützung und euren fachlichen Input!

Gerd Unkelbach, dem Fraunhofer CBP und ICT danke ich für die Bereitstellung der Organosolv Lignine.

An dieser Stelle möchte ich mich auch bei meiner restlichen Familie bedanken. Ihr habt mich mit zu dem gemacht, was ich heute bin. Ich kann mich sehr glücklich schätzen eine so wundervolle Familie zu haben! Danke auch euch für alles was war, ist und noch so kommt! Ich hab euch alle sehr lieb! (Tanti, Ongele, Bianca und Oma, hier ist der Moment gekommen, wo ihr euch besonders angesprochen fühlen solltet 😉.)

Neben der tollsten Familie der Welt, habe ich natürlich auch die tollsten Freunde der Welt! Danke für alles! Ihr habt jegliche Erläuterungen zu meiner Arbeit immer und immer wieder

ertragen, auch wenn ihr damit eigentlich nichts anfangen könnt. Und seid, so wie es sich für gute Freunde gehört, immer für mich da!
Besonders danken möchte ich mich hier bei dir, Sunny: mal abgesehen von der langen Freundschaft, die uns verbindet, bist du auch in schwierigen Zeiten den Weg mit mir gegangen. Auf dich kann ich mich 1000 prozentig verlassen, ich kann mich unglaublich glücklich schätzen dich als Freundin zu haben! In jeglichen Situationen kann ich auf dich zählen und du hast dann sogar noch deine freie Zeit geopfert, um meine Arbeit zu korrigieren und mir fachlich guten Input zu liefern und meine Arbeit besser zu machen. ♥

Kristian, Du unterstützt mich in allen Lebenslagen und bist immer für mich da. Ohne dich wäre vieles nicht zu bewerkstelligen gewesen! Auch von deiner Seite aus steckt sehr viel Arbeit und Zeit in dieser Arbeit, ob fachlicher Input, Probleme diskutieren und Lösungen zu suchen und glücklicher Weise auch oft zu finden oder den ganzen Korrekturen. Ohne dich hätte ich das und so vieles anderes außerhalb der Promotion nicht geschafft. Danke, dass auch du immer an meiner Seite stehst und ich auf dich zählen kann! ♥

Zum Schluss, weil ich‘s nicht oft genug sagen kann:
Danke MAPA!

This work by Julia Schuler was supported by a grant from the Ministry of Science, Research and the Arts of Baden-Württemberg. Az: 200007 as part of the BBW ForWerts Graduate Program. Thanks to the Ministry of Science for the financial support and to the graduate program for the support and great events!

Erklärung über selbständige Anfertigung der Dissertation:

Hiermit erkläre ich, dass ich die beigefügte Dissertation selbstständig verfasst und keine anderen als die angegebenen Quellen und Hilfsmittel genutzt habe. Alle wörtlich oder inhaltlich übernommenen Stellen habe ich als solche gekennzeichnet und die Satzung des Karlsruher Instituts für Technologie zur Sicherung guter wissenschaftlicher Praxis in der jeweils gültigen Fassung beachtet habe.

Ich versichere außerdem, dass ich die beigefügte Dissertation nur in diesem und keinem anderen Promotionsverfahren eingereicht habe und, dass diesem Promotionsverfahren keine endgültig gescheiterten Promotionsverfahren vorausgegangen sind.

_____

Ort, Datum Unterschrift

Abstract

Currently, the majority of platform chemicals are gained petrochemically. The ecological goal, however, should be the substitution of crude oil with biomass. Lignocellulose plays an essential role as it is the only bio-based source of aromatic compounds. For example, it could be a source of bifunctional aromatic molecules, such as the monocyclic compounds catechol or guaiacol or bifunctional oligomers. Bifunctional components are widely used in the chemical industry as these are reactive and variable as pesticides, precursors for fine chemicals such as perfumes and pharmaceuticals, or as building blocks in organic synthesis. The overall goal of this work is to find a process that provides platform chemicals from lignocellulosic (residues). The different behaviors of different biomasses need to be investigated to understand the reaction and to create such a process. The hydrothermal liquefaction of lignin for the extraction of platform chemicals has great potential since it is possible to recover the aromatic and already functionalized structures directly. In this case, water is used under elevated pressure and at an elevated temperature as solvent and reaction partner. A Kraft lignin, Indulin AT, was selected as a reference and studied in this work, which is integrated into the bioeconomy network. With different biomass sources, different lignin degradation molecules are incorporated into the cleavage reaction, and various end products can be recovered. Therefore, bark and Kraft lignin, both of which are produced in large amounts as waste streams, besides this also lignin from individual processes such as Organosolv process are to be investigated and used as starting materials.

In order for building a process, it is also important to study the influence of different types of reactors. The reactor type influences the reactions of the reactants and the mixing behavior of the reactants. The reactions taking place in the reactor depend on the mixing of the reaction media. A tube, a continuous tank reactor, a loop reactor, and micro batch autoclaves were investigated and compared. The different reactor types show no differences in the yields and the behavior of the reactions so that the internal mixing of the reactor types does not influence the liquefaction process. However, it was expected that external back mixing should positively influence the cleavage reactions. When fresh feed and freshly split unstable products are brought into contact with the product mixture, the monomeric fission products may increase as the unstable products can be stabilized by the other products and repolymerization can be prevented. Similarly, dilution with the back mixing takes place, and this could also help reduce repolymerization. In a cycle reactor, various intermediates between a flow tube and a CSTR can be realized, nevertheless the loop reactor used resulted in carbonation reactions due to the long residence times and unfavorable mixing and therefore was not investigated further. Therefore, tests for external back mixing were additionally carried out. In this case, the pre-split product mixture was mixed with fresh feed. It was only possible to mix the liquid products; the gases and solids were not returned. Since the gas could not be recycled, methanol was added to the feed, because it should be split into carbon dioxide and hydrogen, however in this way, no increase in monomeric products could be achieved. To obtain the different concentration profiles the various degradation reactions and products were investigated at different temperatures (250, 300, 350, 400 and 450 °C) and different reaction times (0.25-24 h) and a homogeneous catalyst (1 wt.-% Potassium hydroxide KOH). The screening experiments were carried out in micro batch autoclaves (10 and 25 ml), as the type of reactor showed no influence on the liquefaction and so the reproducibility could be better recorded. Higher

temperatures, longer reaction time and a larger amount of catalyst drive the reaction towards gasification. Above 350 °C, water has near and supercritical properties and drives the reaction to gasification. At 250 °C, the total cleavage reaction is very slow, and there is hardly any gasification or liquefaction, only after long reaction times the biomass is liquefied. At 450 °C, the reaction is almost wholly on the gasification side, and the catechol yields are close to zero. In summary, the desired liquefaction hardly occurs at 250 °C, while at 450 °C almost complete gasification takes place. One of the preferred products, catechol, arises on the one hand via guaiacol, whereby a methyl group is split off. However, this is just one reaction path to catechol. The highest catechol concentration is currently 350 °C and 0.5 h reaction time. Under the same hydrothermal conditions, bark and Indulin AT provide comparable catechol yields. Other products, such as a higher proportion of syringol by using bark as starting material, suggest that other monomeric units are present in the bark lignin core structure and therefore less guaiacol is present, which explains the lower catechol yield. This could also be confirmed by examining the different lignin structures. The results of the studied Organosolv lignins (beech, poplar, and *Miscanthus*) show similar behavior with temperatures and residence times. However, due to their different monomeric units, the product spectra are different from the Indulin AT spectra. For this reason, different lignin types must be investigated separately, as they generate different product areas. For this, batch micro autoclaves were also used to obtain the concentration profiles, making it possible to obtain more information and show that the reactions are reproducible.

Based on these results, the reaction network was built up from lignins based on coniferyl alcohol. It is now possible to predict the monomeric product mixture for different reaction temperatures and residence times for different biomass. This makes it possible to adapt the downstreaming for each biomass.

These studies allowed to gather information on the key reaction of the monomeric products and to develop a reaction network containing a model describing the degradation of coniferyl-based lignin for various biomass sources. Hydrothermal liquefaction appears as a reasonable conversion technology because functional groups remain in the product molecules. On this basis, a biorefinery could be built. Within this work, the liquefaction process itself could be better understood by studying different reactor systems. Internal standards have been achieved within analytics, and the analysis of oligomer components has been continuously improved.

ZUSAMMENFASSUNG

Aktuell werden Plattformchemikalien hauptsächlich aus fossilen Rohstoffen hergestellt. Langfristig muss jedoch die Rohstoffbasis der chemischen Industrie einen ökologischen Wandel erfahren. Das bisher verwendete Rohöl könnte dabei durch Biomasse ersetzt werden. Lignocellulose, spielt dabei eine wichtige Rolle, da sie als einzige biobasierte Quelle für aromatische Verbindungen dienen kann.

Besonders bifunktionelle Komponenten finden in der chemischen Industrie Einsatz. Sie sind reaktiv und können vielseitig eingesetzt werden. Beispiele wären die Nutzung als Pestizide, Vorstufen für Feinchemikalien wie Parfüms und Pharmazeutika oder als Bausteine in der organischen Synthese. Lignocellulose könnte eine Quelle für bifunktionelle aromatische Moleküle sein, da in seiner Struktur bereits funktionalisierte Seitengruppen vorhanden sind. Das Gesamtziel dieser Arbeit ist es einen Prozess aufzubauen, der Plattformchemikalien aus Lignocellulosen bereitstellt. Um die Reaktionen innerhalb eines solchen Prozesses zu verstehen und einen solchen Prozess zu erarbeiten. müssen die unterschiedlichen Verhaltensweisen verschiedener Biomassen genau untersucht werden.

Die hydrothermale Verflüssigung bietet für die Fragmentierung von Lignocellulose ein großes Potential. Zum einen wird hierbei ein umweltfreundliches Reaktionsmedium genutzt, zum anderen können so funktionelle Seitengruppen besser erhalten bleiben, da die besonderen Eigenschaften von Wasser unter hohen Druck und hohen Temperaturen (350 °C, 250 bar) dies ermöglichen.

Der gesamte Prozess der hydrothermalen Verflüssigung von Lignin zu bifunktionellen Komponenten wurde in dieser Arbeit untersucht.

Aus verschiedenen Biomassequellen können unterschiedliche Endprodukte gewonnen werden, da sich damit sowohl die Grundstruktur des Ligninmoleküls als auch die einzelnen Spaltprodukte in den Reaktionen unterscheiden. Aus diesem Grund werden Rinde und Kraft-Lignin aus der Zellstoffindustrie, die beide als Reststoffströme in großen Mengen anfallen, aber auch Lignine aus speziellen Verfahren wie dem Organosolv-Prozess eingesetzt.

Für die Entwicklung eines solchen Verflüssigungsprozesses ist es entscheidend unterschiedliche Reaktortypen zu untersuchen, damit ein geeignetes System gewählt werden kann.

Der Reaktortyp kann über das Umsatz- und Mischverhalten der Reaktanden Einfluss auf die Reaktionen haben. Um diesen Einfluss zu beurteilen wurde ein Strömungsrohr, ein kontinuierlicher Tankreaktor, ein Kreislaufreaktor und Mikrobatchautoklaven untersucht und miteinander verglichen. Die verschiedenen Reaktortypen zeigen keine Unterschiede in den Ausbeuten und dem Verhalten der Reaktionen, so dass angenommen werden kann, dass die interne Rückvermischung der Reaktortypen keinen Einfluss auf den Verflüssigungsprozess hat.

Um nicht nur internes Mischverhalten zu untersuchen, wurde zusätzlich eine externe Rückvermischung betrachtet. Es wurde erwartet, dass die externe Rückmischung die Spaltungsreaktionen positiv beeinflussen sollte. Wenn unbehandeltes Feed und frisch gespaltene instabile Produkte in Kontakt mit dem Produktgemisch gebracht werden, könnten die monomeren Spaltprodukte zunehmen, da die instabilen Produkte durch die anderen Produkte stabilisiert werden können und eine Repolymerisation verhindert werden kann. Außerdem findet eine Verdünnung durch die Rückmischung statt, was dazu beitragen kann

die Repolymerisation zu verringern. Es wurde vorgespaltenene Produktmischung mit frischem Feed gemischt. Gase und Feststoffe wurden auf Grund technischer Gegebenheiten nicht zurückgeführt. Durch externe Rückvermischung konnte jedoch ebenso keine Zunahme der monomeren Produkte erreicht werden.
Bei Temperaturen von 250-450 °C, Reaktionszeiten von 0,25-24 h und unter Einsatz von 1 Gew.-% Kaliumhydroxid (KOH) als homogenem Katalysator, wurden Konzentrationsprofile ermittelt. Die Experimente wurden in Mikrobatchautoklaven (10 und 25 ml) durchgeführt, da der Reaktortyp keinen Einfluss auf die Verflüssigung zeigte und so die Reproduzierbarkeit besser abgebildet werden konnte. Höhere Temperaturen, eine längere Reaktionszeit und eine größere Menge an Katalysator treiben die Reaktion in Richtung Vergasung. Oberhalb von 350 °C hat Wasser Eigenschaften im nahen und überkritischen Bereich und treibt die Reaktion zur Vergasung hin. Bei 250 °C ist die Gesamtspaltreaktion sehr langsam und es findet kaum Vergasung oder Verflüssigung statt, erst nach langen Reaktionszeiten wird die Biomasse verflüssigt. Bei 450 ºC ist die Reaktion fast vollständig auf der Vergasungsseite und die Catecholausbeuten sind nahezu null. Die höchste Catecholkonzentration liegt bei 350 °C und 0,5 h Reaktionszeit vor. Wie Lignin kann auch Rinde als Edukt verwendet werden. Unter gleichen hydrothermalen Bedingungen liefern Rinde und Indulin AT vergleichbare Catecholausbeuten. Die Ergebnisse der untersuchten Organosolv-Lignine (Buchenholz, Pappelholz und *Miscanthus*) zeigen ein ähnliches Verhalten bei gleichen Temperaturen und Verweilzeiten. Dafür wurden ebenfalls Mikrobatchautoklaven verwendet, um die Konzentrationsprofile zu ermitteln, wodurch es möglich wurde, mehr Informationen zu erhalten und zu zeigen, dass die Reaktionen reproduzierbar sind.
Aus diesen Konzentrationsprofilen konnte das Reaktionsnetzwerk der Spaltreaktionen von Lignin auf Coniferylalkoholbasis aufgebaut werden. Es ist nun möglich, das monomere Produktgemisch für verschiedene Reaktionstemperaturen und Verweilzeiten für verschiedene Lignine vorherzusagen. Dies ermöglicht es Aufarbeitungsprozesse für unterschiedliche Lignine anzupassen was zu einer höheren Wertschöpfung für den Holz- und Papiersektor führen kann. Biomasse bietet ein hohes Potenzial als Rohstoff für die Gewinnung von Plattformchemikalien durch hydrothermale Verflüssigung. Bioökonomisch ebenfalls, da beide Abfallströme in großen Mengen anfallen, welche bisher meist nicht chemisch genutzt werden. Innerhalb der Analytik wurde die Analyse von Oligomerkomponenten kontinuierlich verbessert. Darüber hinaus konnten grundlegende Reaktionen zu bifunktionellen Verbindungen aufgeklärt und modelliert werden

1 Introduction

1.1 Motivation

Fossil resources are a common source for energy production and chemical industry. However, they bring along problems, like their limited availability or the release of CO_2 in the atmosphere while combusting them. On the one hand the substitution of fossil resources with renewable alternatives for the purpose of energy production results in a lack of platform chemicals. This is a result of the fact that the availability of chemical intermediates is coupled to the production of fuels in petroleum refineries. These chemical intermediates produced from fossil fuel, consume around 15 % of crude oil [1]. To ensure the future availability of chemical intermediates, alternative resources should be considered and investigated

On the other hand, the release of carbon dioxide is the predominant cause of the man-made climate change. Especially combustion of fossil resources which have been long term sinks of carbon produce large amounts of carbon dioxide. To prevent affecting the carbon balance every carbon atom must be included in a closed carbon-cycle. Moreover, also a limit of the overall carbon dioxide release into the atmosphere is needed. Carbon dioxide from power generation, industrial processes, and non-food (woody/lignocellulosic) biomass could play a crucial role in the substitution of fossil resources and could deliver renewable carbon. Only non-food biomass should be considered for the production of chemicals because a conflict between food and feed production should be avoided. This is possible by applying lignocellulosic biomass.

The main components of lignocellulosic biomass are hemicellulose, cellulose, and lignin. Lignin is one of the most common organic compounds in the world. It is the only bio-based macromolecule containing large amounts of aromatic structures. Lignin is built and used in plants to be resistant against environmental influences and to give structure. The lignin structure and amount vary depending on the plant and growing conditions [2][3].

On the one handits structure and stability makes the use of lignin for production of chemicals a challenge. Special treatments are necessary that need to be understood well. On the other hand, lignin is a promising renewable resource, available in large quantities.

One process for the chemical use of lignin that is already established is the production of vanillin [4][5]. About 15 % of the vanillin production is performed using woody biomass as a resource. However, even if it is a process applied at an industrial scale the oxidation of lignin to vanillin remains a challenge, because it is still not completely understood [6]. This elucidates the need for a better understanding of lignin as a resource in order to be able to use its whole potential.

Before lignin can be used in a process, it must be separated from the other biomass components. The Kraft process, for example, is the most common process in the pulp and paper industry to gain cellulose, and the main source for lignin today [7]. Currently, most of the directly useable lignin accrues at the paper industry as a byproduct in enormous amounts, more than 50 mio. t/a [5][4]. Most of the gained lignin (~98 %) is combusted directly

by the pulp and paper industry for the production for on-site energy [5][4]. Hardly any of it is used as a raw material to produce chemicals. The large amounts make the Kraft lignin relatively cheap, however there is still a certain amount of sulfur in the lignin due to the biomass cleavage with sodium sulfide. The sodium sulfide can be a problem in lignin applications, e.g., for the usage of a catalyst because sulfur is a catalyst poison for a variety of catalysts, and it is also incriminating the material of the used reactors. Also, the Kraft process is harsh for the lignin structure itself and leads to a certain change of the structure. It means that the possible cleavage reactions and products could be different compared to other lignins gained from other separation processes [8]. There is not one typical lignocellulosic biomass; there are different ones, e.g., hardwood, softwood or straw. Each of them has a different distribution of the monomer units. Softwood (like pine) lignin is mostly obtained of coniferyl alcohol while hardwood (like beech) lignin also has sinapyl alcohol as a building block [9].

Especially the lignin content in the lignocellulosic biomass needs to be utilized; for the sugar fraction various uses are already available and commercially applied, ranging from industrial cellulose to fermentation after separation and saccharification. So, the overall target is to find a process that provides platform chemicals out of lignocellulosic residues, instead of combusting this carbon source.

Bark or Kraft lignin from pulping or lignins gained out of special processes like organosolv lignins shall be investigated and used as starting materials. While the use of bark or Kraft lignin could offer the possibility of gaining additional valuable products from residues of pulp and paper industry, the organosolv process offers an opportunity to use types of biomass which are of non-industrial uses, like *Miscanthus Giganteus*. The perennial grass *Miscanthus Giganteus* could be cultivated on marginal lands, where different types of agricultural use are not economically feasible.

By applying hydrothermal liquefction on lignin already functionalized products could be gained directly. This could be a efficient alternative to other methodes of biomass utilisation that are based on cracking the carbon source into small components like syngas and rebuilding and refunctionalizing it towards bifunctional molecules.

1.2 Objectives

The processes of separating lignocellulosic biomass into hemicellulose, cellulose, and lignin of the pulp and paper industry are well-known, e.g. the Kraft process in contrast to the utilization of lignin itself. Several utilization processes of biomass have been investigated, nevertheless no process is established until now.

Hydrothermal liquefaction could be the method of choice for the utilization of lignin in the future. Using hydrothermal liquefaction of biomass, it is possible to gain platform chemicals. Therefore, the unique properties of water, an environmentally friendly solvent, are used. Moreover, water is not only a solvent, but it is also a reactant and benefits the depolymerization reactions towards highly functionalized platform chemicals. Compared to the use of biomass as a resource, fossil resources get cracked into small unfunctional pieces and put together again later to the wanted products. Lignin and its monomers are

already highly functional molecules built by nature while using fossil resources the functional side chains must be added in additional reaction steps. By using biomass as a resource in hydrothermal liquefaction, it is possible to use the existing functionalized molecules directly. To realize such a process (compare Figure 1), it is necessary to investigate not only the process itself like reactor types, different biomass sources, moreover the come along analysis and different influences on the reaction behavior to clarify some reaction steps. Additionally, a model of the gained product spectra is profitable, to use suitable downstream processing for every used lignin.

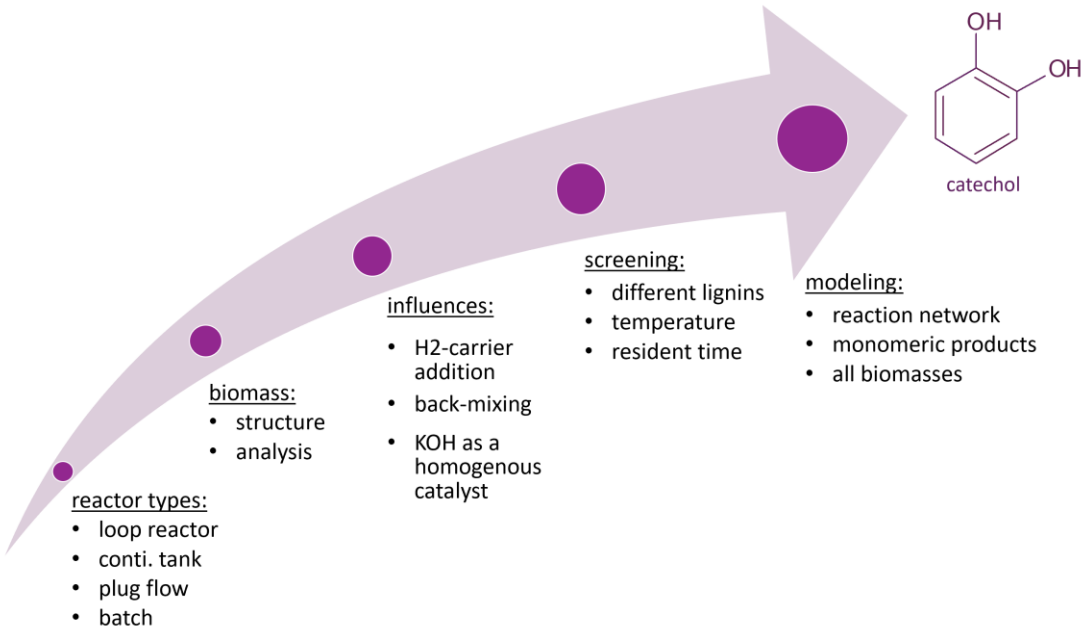

Figure 1: Target scheme of the depicted work; finding a process which provides platform chemicals out of lignocellulosic residues for the production of bifunctional molecules. Including the necessary milestones to fulfill this project.

The challenge of the liquefaction of lignin is to keep the functional groups and to improve selectivity towards bifunctional components like catechol. This work investigates the reaction mechanism for the hydrothermal cleavage of lignin and the reaction pathways via oligomeric intermediates, as well as the direct cleavage to monocyclic compounds. Hence, this leads to a lot of different challenges which need to be solved. Therefore it is necessary to understand the different reaction pathways, which compounds are for example formed by the cleavage of aryl ether bonds. The other question is, what is created by the cleavage of the other bond types and which compounds are created through this. These bonds are much more challenging to cleave and most likely the basis for forming oligomers and tar. Therefore, the repolymerization needs also to be investigated. Freshly cleaved products, which are still reactive, could come in contact with each other and fresh feed and react in repolymerization reactions to oligomeric compounds. For the gain of platform chemicals like catechol the reaction pathway towards this monoaromatic structure needs to be understood. With hydrothermal liquefaction, it could be possible to gain especially bifunctional

components like catechol. The selectivity towards these highly functionalized molecules is higher in hydrothermal liquefaction than, e.g. in solvolysis processes [10]. Bifunctional components have high usage in the chemical industry as intermediates for the production of pesticides, precursors to specialty and fine chemicals such as perfumes and pharmaceuticals.

To develop a procedure for the production of platform chemicals out of different biomass respectively different lignins via hydrothermal liquefaction a suited reactor system must be identified. Classical continuous reactor types were tested in the beginning: a plug flow reactor and a continuous tank reactor (the mixing by flow due to the instrument-based conditions spared external stirring, the flow characteristic showed sufficient mixing).

These two reactor types make it possible to study the influence of the internal back mixing in the reactor on the depolymerization reactions. Also, a continuous system is typically used to perform reaction engineering studies of hydrothermal lignin depolymerization and especially with the target to perform kinetic studies. Additionally, the continuously operated reactor types, a batch reactor was applied. For the investigation of an external back mixing influence and also for gathering kinetic studies, a loop reactor system was used. Additional external back mixing experiments were performed to understand the effect of an external back mixing better. Also, several experiments were performed by using model compounds like a synthesized oligomer, guaiacol or catechol to achieve more insight into cleavage reactions, consecutive reactions and reaction mechanisms.

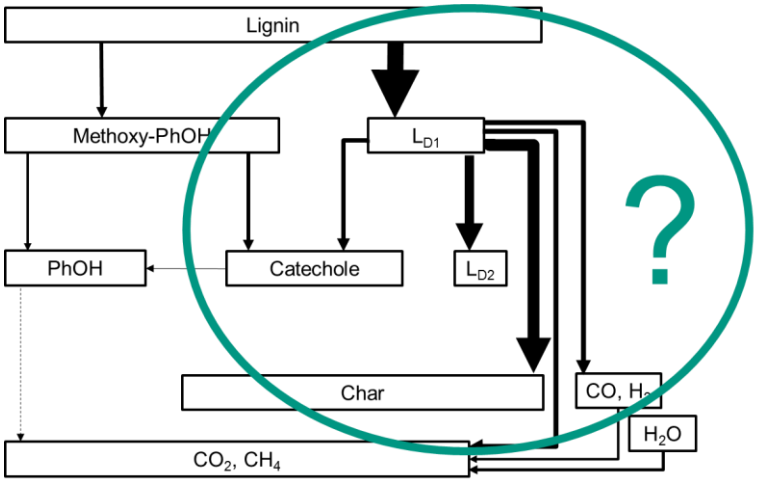

Figure 2: Assumed reaction network based on former studies, including the gap between lignin as a macromolecule and the product gases and solid residues [10].

Lignin of completely different sources was used in investigations to get a procedure and model for different types of lignin source and to close the gap of the reaction network shown in Figure 2. Different lignin sources were investigated because with the wood type the lignin structure differs. With different biomass sources, different lignin degradation molecules get built in the cleavage reaction, and different end products could be gained [11]. For example, leads coniferyl alcohol to guaiacol and guaiacol to catechol as a product, while sinapyl alcohol delivers syringol (Figure 3) [12][13].

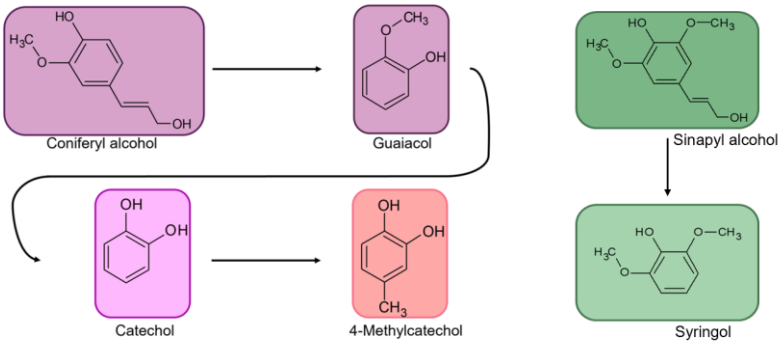

Figure 3: Product examples out of two monomeric units; coniferyl alcohol and sinapyl alcohol.

When there are no sinapyl building blocks in the lignin, no syringol will be gained in the cleavage process [14]. It needs to be minded while the liquefaction process and product spectra are investigated. Therefore, five different lignins, gained by three different procedures were investigated in this work to get to know the cleavage reactions and to understand the influence of temperature and retention time at the hydrothermal liquefaction. The liquefaction with water is supposed to keep the functional sidechains and to improve the selectivity towards bifunctional molecules [15]. For each biomass concentration profiles for the main monomeric products were prepared. This made it possible to gather information about the key reaction of the monomeric products and to develop a reaction network including a model that describes the degradation of coniferyl alcoholic based lignin compounds for different biomass sources. The temperature of the hydrothermal liquefaction ranges from 250 °C up to 450 °C, 0.25 up to 24 h residence times were chosen to get access to concentration profiles, which is the basis in order to enlarge the existing reaction network and to determine the parameters of the rate equations.
The infrastructure of analytic methods which is used during the parameter studies for the hydrothermal liquefaction of lignin has to cover a wide range of molar masses from the polymeric compound lignin to oligomeric intermediates and monomers which are the targeted product of the conversion processes.
Lignin itself is a challenging resource and brings different problems in its handling, especially during analytical investigations of it, which need to be addressed while working with lignin. These challenges are also discussed in this work. Without a general understanding of these problems, no progress in building an economic and ecologic process for the production of bifunctional components out of lignin as a renewable feedstock without the competition to food will be possible. So, an understanding of the whole reaction and the problems which occur with them is a fundamental need.

1.3 Hydrothermal cleavage

The 3D macro molecule lignin can get cleaved in different phenolic compounds. Hydrothermal cleavage is showing promising results, and water is an environmentally friendly solvent and reaction partner.

The properties of water are adjustable via variation of temperature and pressure [16]. This makes it possible to control the selectivity towards specific reactions, which is an advantage compared to other depolymerization processes [10]. Furthermore, biomass contains large amounts of water naturally and with water as a solvent, an energy intensive pre-drying can be avoided [15].

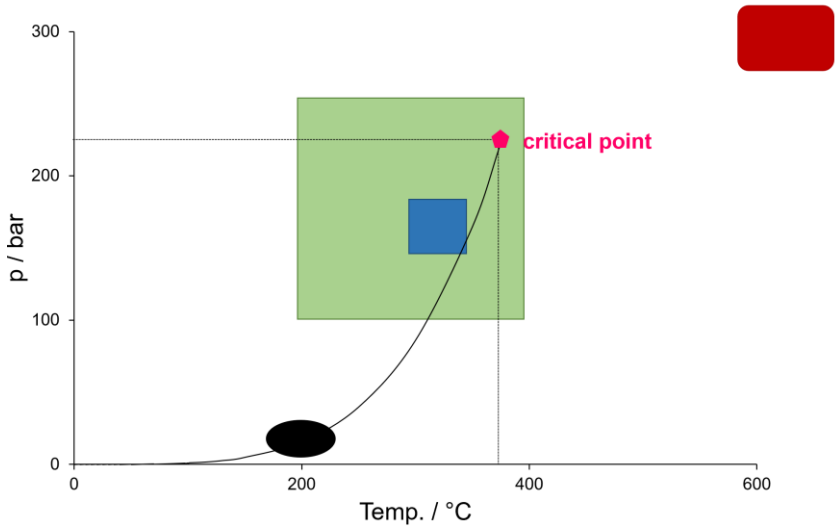

Figure 4: Hydrothermal treatment as a function of the pressure and temperature of water. The blue area marks the conditions of the hydrothermal conversion to platform chemicals. The black box marks the area of the hydrothermal carbonization, the red one the supercritical water gasification while the green one defines the area of the hydrothermal liquefaction [17].

Via hydrothermal liquefaction methods (Figure 4) functional groups can be produced [17]. In the range of 200 °C and the corresponding pressure of water hydrothermal carbonization takes place, above 600 °C supercritical water gasification occurs [18].
For the production of platform chemicals, a temperature range from 150 °C to 400 °C at equilibrium pressures delivers the best results [17]. The desired hydrothermal liquefaction takes place at around 280-380 °C (Figure 4).
In water, the selectivity towards the remaining of functional groups increases, compared to that in ethanol it decreases [19].

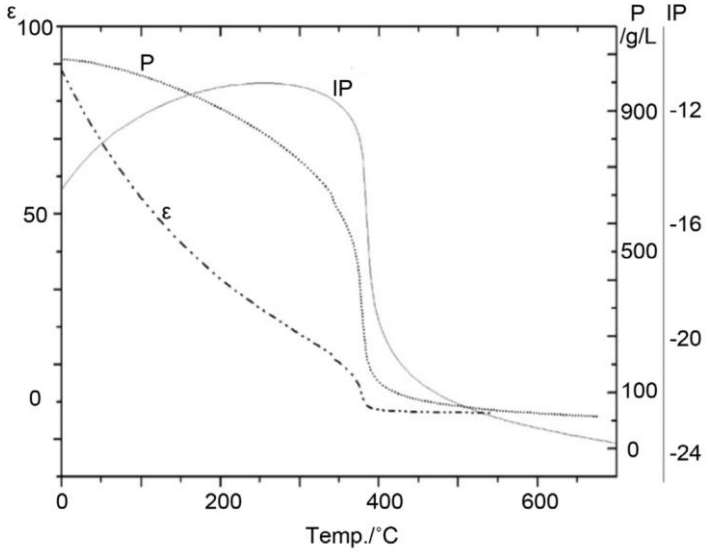

Figure 5: Properties of water as a function of temperature at 25 MPa (density ρ, ion product IP and relative static dielectric constant ε) [17].

The unique properties of water under these conditions see Figure 5, offer special opportunities for gaining bifunctional aromatics [19][17]. Under near- or supercritical conditions of water, its density is changing drastically, which leads to different solubilities for organic substances. These different solubilities of products offer new possibilities and make it possible to degrade a large molecule into smaller pieces under pressure [17]. The decrease of the ion product leads to highly dissociated water molecules, which change the polarity of the solvent enormously [18]. Furthermore, hydrogen is available through the occurring water gas shift reaction, and also the dielectric constant is decreasing [17,20]. In past research on chemical lignin utilization, the main focus was to produce phenol out of the lignin. However, a process for the technical production of phenol is still not established, because the phenol yield stagnates at low values (< 10 wt.% [19,21]) [19]. Also, the complex structure of lignin delivers a complex mixture of phenolic derivates [19] which make the production of phenol not economic.

To understand which bottlenecks, and challenges are arising by lignin usage, various reaction pathways need to be understood to design a procedure for lignin depolymerization while depolymerizing lignin repolymerization reactions of the intermediates occur.

Nevertheless, lignin could be a source for many monomeric and oligomeric compounds with more than one functional group. The gained products depend on different depolymerization methods and used lignins [22]. With these special properties of water, a procedure for lignin depolymerization with containing functional side chains is possible.

1.4 Biomass utilizations

At present there are three main applications of wood [7]:

- Pulp and paper industry
- Construction material (e.g. Furniture)
- Energetic use for production of electricity and heat.

Most of the common pulping processes produce lignin in a certain way, but not as a prior product. The sugar-based parts, cellulose, are the prior products. Individual processes, e.g., the production of biogas, use biomass as a resource, but primarily the sugar-based components. Whereby, the overall goal is energy production [23].
Different approaches like the production of alcohols by fermentation processes are investigated and already realized. Unfortunately, these processes are often associated with a low yield.
Referred to the production of bifunctional aromatic structures the studies need to shift towards the non-sugar-based parts of biomass, the lignin. Pulping technologies that can be a source of lignin like e.g. the Kraft, sulfite or organosolv processes are established. The presented work investigates lignin of the Kraft process as well as from the organosolv process. Kraft lignin was prioritized because of its availability and because of the possibility to gain a high value product from a side product. In addition, organosolv lignin was chosen although it is a prior product and not a residue, since it has a high lignin quality e.g. a low amount of residual pulping chemicals or containing sulfur.

1.4.1 Kraft process

Paper, cart board or related products consist mainly of almost pure cellulose fibers. These fibers are gained out of different pulping processes, In the pulp and paper industry, the Kraft process is the most common process to convert wood. Thereby, almost pure cellulose is gained out of the produced wood pulp. In 1879 Carl F. Dahl conducted a procedure, the soda cook, but used sodium sulfate to degrade the wood structure [7]. This led to a more effective process, the Kraft (“strength”) process. The incoming wood gets peeled so that the bark gets separated from the wood. The wood is chopped to chips of cm-size, these chips are cooked in an aqueous sodium sulfide and sodium hydroxide solution at 140 to 170 °C for 3 to 4 hours. In this step, mostly all of the hemicellulose gets degraded, dissolved and removed. The strongly alkaline solution also dissolve the lignin fraction of the wood (delivering the so-called black liquor). The remaining solid fraction is collected and washed. The exact chemical composition and process parameters depend on the used wood [7].

1.4.2 Organosolv process

This process uses an organic solvent for the lignin solubilization. The chopped wood is heated up in an alcohol-water-mixture under mild pressure. Organosolv pulping delivers high-quality lignin without sulfur contamination. This process uses an organic solvent for the lignin solubilization. The cut wood gets heated up in an alcohol-water-mixture at around 160-200 °C and 20 bar. The alcohol which is most widely used is ethanol [24]. The wood structure gets divided into its three main streams; cellulose, hemicellulose, and lignin, under these conditions. The lignin and hemicellulose are dissolved in the organic-water solvent phase, and the lignin can later be precipitated through the evaporation of the solvent. The hemicellulose is hydrolyzed by the alcohol via interacting with the hydroxy group of the alcohol, which is functioning as a hydrogen-donor, into sugars under these conditions. Different alcohol ratios, heating rates, and reactor systems can be used. After the precipitation, the residue gets filtered and dried [24][25].

The organosolv process is more gentle towards the molecule structure of the lignin, as it is more expensive until now it is only used in first technical scale plants and not widely established in the industry like the Kraft process [24][25]. The organosolv process has like the Kraft process influence on the resulting lignin structure, resulting in different reactions and products in the further lignin liquefaction process with organosolv lignin compared to the Kraft lignin [5][6].

1.5 Lignin structure

In lignin, the three-dimensional macromolecule structure of aromatic rings is linked via different chemical groups and bond types (Figure 6). Until now, the size of these molecular structures in the plant is unknown [27].

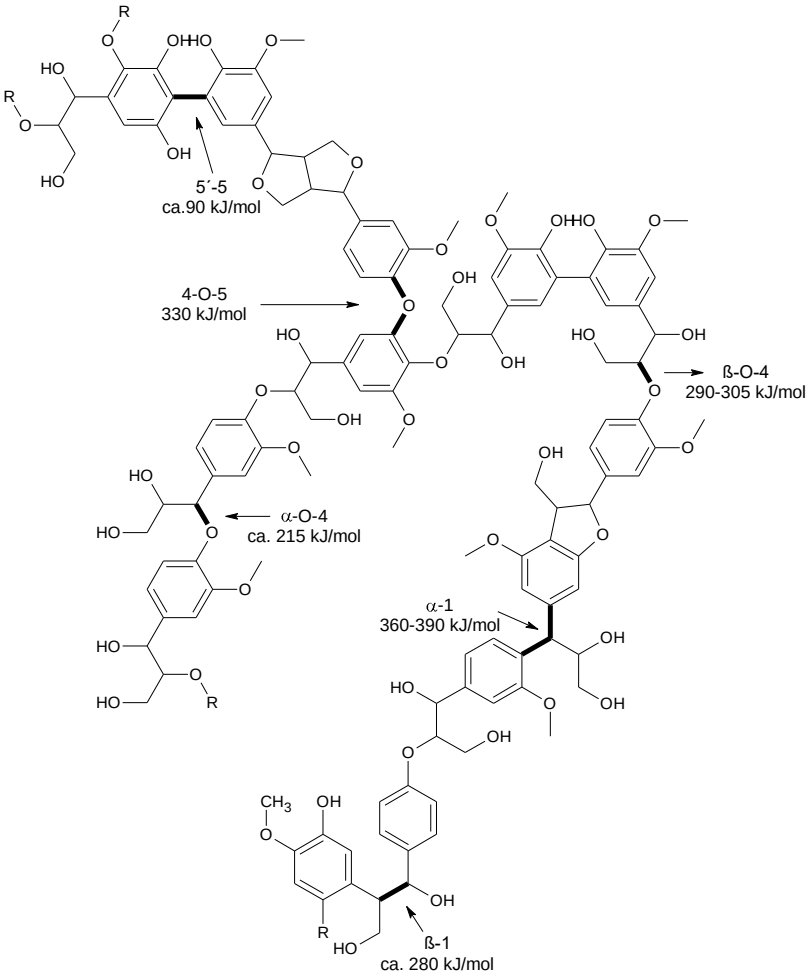

Figure 6: Typical structural elements of lignin with binding energies [27].

Lignin consists of three basic monomeric units of which the distribution depends on the type of plant which produced the lignin (Figure 7) [9]. So every plant delivers lignin with a different composition, besides this, also the separation process has a significant impact on the structure of the obtained lignin [22,26].

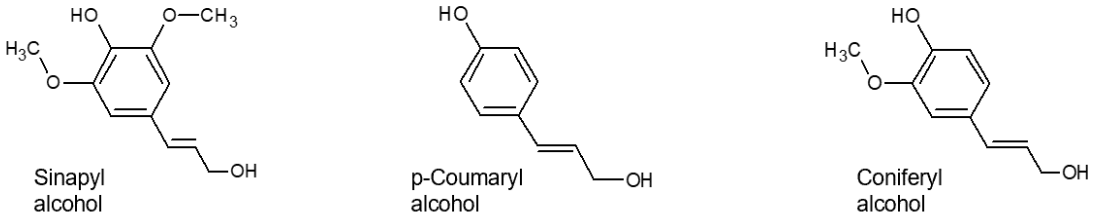

Figure 7: Monomeric building blocks of lignin; sinapyl alcohol, p-cumaryl alcohol, and coniferyl alcohol.

Sinapyl alcohol, p-cumaryl alcohol, and coniferyl alcohol are the basic monomeric units of lignin. Sinapyl alcohol leads to syringol, while coniferyl alcohol leads to guaiacol by hydrothermal treatment. The combustion of lignin forms as products mostly methoxy phenols, however, the occurring products differ depending on the lignin source because of the monomeric building blocks [28]. Different wood delivers different products, of which a lot, however not all, are characterized until today. Softwood like pine (see Figure 8B) has a different structure as hardwood like beech (see Figure 8A) [29].

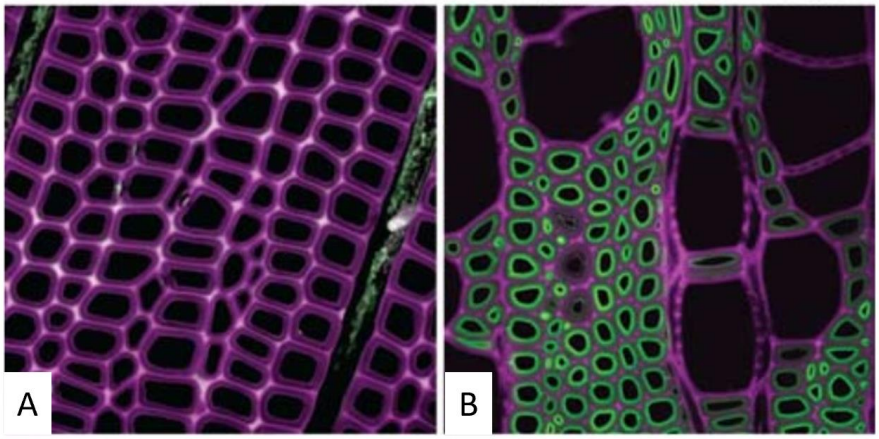

Figure 8: UV-fluorescence images of two different kinds of wood. Different emission spectra are shown in different colors. A: hardwood, pine, the purple regions show guaiacyl-rich lignin. B: softwood, beech, the green regions reflect syringyl-rich lignin [29].

The monomeric units couple between each other via alkyl-ether bonds, phenol-ether bonds, C-C bonds, and diaryl ether bonds, the different bond types are shown in Table 1.

Table 1: Bond types (C-C bonds and ether bonds) common in the lignin molecule.

C-C bonds	ether bonds
5-5	ß-O-4
ß-1	α-O-4
ß-2	4-O-5
ß-5	
ß-ß	

The most common bond in the lignin molecule is the ß-O-4-bond, which has a relatively low binding energy (290-305 kJ/mol) in contrast to, e.g. C-C-bonds (490 kJ/mol) and is hence one of the first bonds which are cleaved during the liquefaction process (Figure 6) [9,29]. Thermogravimetric analysis (TGA) can show the different bond types of biomass. For cellulose and hemicellulose, a characteristic peak can be gained (see Figure 9), while the lignin mass decrease takes place over a broader temperature range. This indicates more different thermally stable bonds in the lignin than in the cellulose [30], which makes it necessary to use harsher conditions to decompose lignin than cellulose.

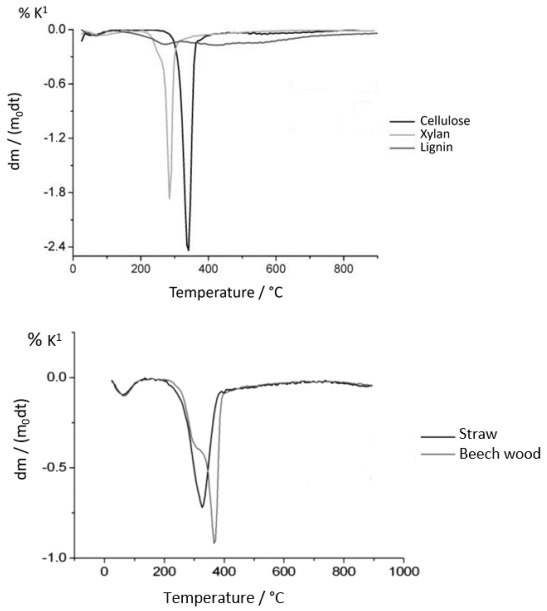

Figure 9: Differentiated TGA diagram of cellulose, xylan (used for hemicellulose) and lignin. Moreover, a differentiated TGA diagram of straw and beech wood [30].

The aromatic part of the lignin molecule is can be a precursor for phenolic monomers or oligomers. The degradation of methoxy groups leads to products like methane or methanol. Water-soluble acids are dehydrated delivering alkene or oxidized delivering alcohol functionalities at these conditions (Figure 10) [20,26].

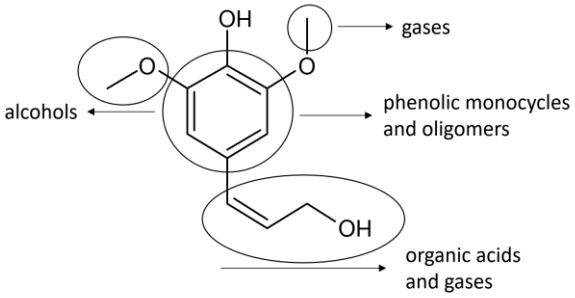

Figure 10: Simplified illustration of the precursors for thermal degradation products of a lignin monomer unit [31].

Besides these phenolic monocycles, oligomers are formed. Liquefaction products with two functional groups, like catechols, are promising molecules for the use as a platform chemical (Figure 11).

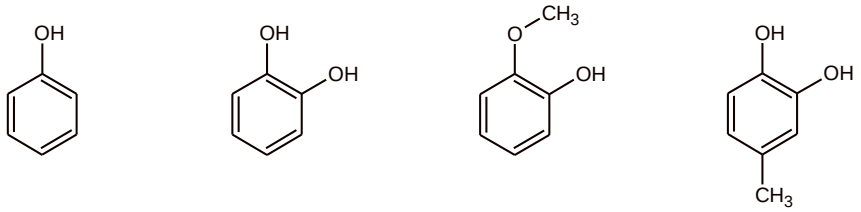

Figure 11: Four of the favored monomeric products of lignin; guaiacol, catechol, and phenol.

Catechol is a product with high potential (Figure 12) [32]. With its two functional groups, it can serve as a starting material for plastics or the production of adipic acid.

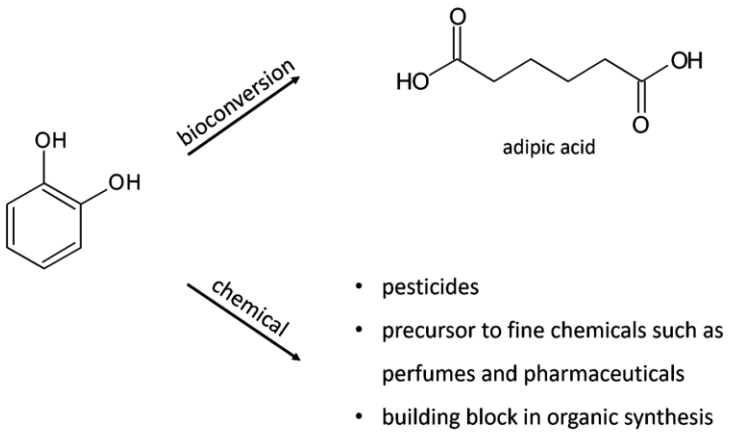

Figure 12: Possible use of one of the gained products; catechol. In a bioconversion towards adipic acid and the chemically use towards pesticides, a precursor to fine chemicals or building blocks.

Catechol can be used as a precursor to fine chemicals such as pharmaceuticals. It is used to produce neuromodulators for the central nervous system and hormones in the blood circulation; dopamine, noradrenaline, and adrenaline (Figure 13) [33].

Figure 13: High-value products, synthesized over catechol as a precursor. Pharmaceuticals like dopamine, noradrenaline or adrenalin are produced over catechol as a precursor [33].

1.6 State of the art

A classic state of the art chapter is barely feasible in this research area, because of the enormous amounts of possibilities in utilizing biomass. In this research field, a lot of fundamental studies on lignin degradation have been performed and there is a lot of fundamental and even advanced prior art of using biomass as a resource. Nevertheless, in light of the fact that there are a few little contrasts in the investigations affect hugely the outcomes and results, the correlation of each work is hardly conceivable. However, each work helps to understand the fundamentals better and improve the whole research field. Lignocellulosic biomass or the lignin itself is hardly used as a resource in the production of platform chemicals. The only established industrial process is producing vanillin out of lignin sulfonate. One main producer of vanillin is by the Norwegian company Borregaard [6]. They produce about 15 % of the worldwide vanillin production [6]. Vanillin out of lignin is obtained over an oxidative lignin degradation under high temperature, pressure, an alkali pH and oxygen [6]. Ultrafiltration with a following ion exchange purification step is used. To gain a pure product several crystallization steps are performed after an ion exchange [34].

In general, procedures using lignocellulosic biomass as a starting material for the production of platform chemicals include:

- Hydrothermal processes:
  - Liquefaction
  - Carbonization
  - Gasification
- Pyrolysis
- Solvothermal processes
- catalytic processes:

- base catalyzed
- acid catalyzed
- metal catalyzed
- oxidative processes

Prior arts, like studies about the different procedures mentioned above, can help to understand several things in the hydrothermal liquefaction process and can be used to gather information about reaction mechanisms or analytics. Pyrolysis is one of the processes which provided already a lot of conclusions, e.g. in regard to analytics.
There are different pyrolysis types divided by operation temperatures and other conditions; with a slow heating range and temperatures of 550-950 °C, the conventional pyrolysis is performed [35]. These conditions lead to carbonization of the biomass and are used in the activated char production. With residence times under five seconds with temperatures of 1050-1300 °C, the third type of pyrolysis is defined. In this process mostly gaseous products are gained [35].
With biomass as a starting material bio oil, next to gases and some char, can be generated in other pyrolysis types, e.g. the flash pyrolysis (short residence times and temperatures around 500 °C) [36][37]. A pilot plant to produce fuels out of biomass is located at the KIT. In the bioliq plant, a so-called biosyncrude is produced out of biomass, which gets gasified to syngas in a second step and then reformed in fuels [37]. Biosyncrude is an energy densified liquid which can be transferred easily to a gasification plant [38].
The gained advantages of these projects, like a better understanding of the gasification, liquefaction or carbonization steps or analytical methods and the determination of pyrolysis products, support other investigations like the hydrothermal liquefaction considered in this work.

Equally, hydrothermal gasification investigations help in general understandings of the use of biomass as a resource. Hydrothermal gasification uses, like the hydrothermal liquefaction process, the special properties of supercritical water. Biomass contains already water, which makes pre-drying unnecessary. Under supercritical conditions, biomass is soluble in water and water also reacts as a reaction partner not only as a solvent [39][40]. Supercritical gasification can be performed with or without a catalyst and is a process intended to generate gaseous products like hydrogen or methane [39][40]. With a catalyst, it is possible to reduce solid residues and to increase the gas yields [39]. The macromolecule lignin, cellulose and hemicellulose get degraded to small molecules, and even the ring structures get cleaved [41]. Reaction mechanisms for this process are expected to happen in certain ways also in the hydrothermal liquefaction process.

In previous work at the IKFT the lignin cleavage of lignin towards phenol under the influence of water and ethanol was investigated; "*Optimization of the reaction parameters of a CSTR and a PFR (Batch) for the recovery of phenol from hydrothermal biomass liquefaction"* of Daniel Forchheim [10]. In this work, the lignin degradation is studied under the influence of different solvents and the influence of a heterogeneous catalyst. The reaction parameters

were optimized in this work towards an economic phenol production out of lignin. Also, the use of Raney nickel was investigated and showed a selective dehydroxigenation of catechol to phenol. Forchheim pointed out that the product spectra decrease in water in contrast to ethanol as a solvent. A reaction network was developed and modeled, which identified the main monomeric phenols and built a base for the analytical methods and preparation methods. This work should be a follow-up investigation in several ways. Therefore, some of the basic treatments were performed like in the work of Daniel Forchheim, to ensure the reproducibility and comparability of this work with prior experimental data, furthermore, new achievements of other studies were considered in this work.
Such as the work of the University of Aarhus. They are working on the field of hydrothermal liquefaction of biomass also. Instead of heterogenous catalysts a homogenous base catalyst (potassium carbonate) is utilized [42]. This is intended to decrease the coke formation with the disadvantage that a saponification with lipid-rich biomass might occur [43][44]. The focus of the Aarhus work is on fuel production, so elimination of oxygen was preferred. It was also tried to recycle the water in the process, however, this led to an increase of the oxygen content [42], also the potassium carbonate seems to increase the oxygen content of the gained bio-crude. Some lignins of different biomass sources are more soluble in alkaline solvents.
Moreover, it is also known that strong bases like potassium or sodium hydroxide enhance lignin degradation towards smaller molecule sizes [14]. The effect of the base to the cleavage reaction is higher for potassium hydroxide than sodium hydroxide [45]. The University of Aarhus built a technical plant in an extended lab-scale, nevertheless, no industrial process of the hydrothermal liquefaction of lignin has been established by now. Other researchers like Beauchet et al. investigated the influence of sodium hydroxide on the lignin cleavage [46]. They showed a higher yield of monomeric products and a high depolymerization grade of the lignin under the influence of sodium hydroxide. With the use of a homogeneous base catalyst, the hydrogen production increases and the water gas shift reaction under hydrothermal conditions gets promoted, and the carbon dioxide content gets reduced by potassium and sodium hydroxide [47]. Acid-catalyzed lignin cleavage reactions lead to deoxy- and demethoxygenation, which convert catechol for example towards phenol [48]. Acids could increase the catechol yields but do not influence the guaiacol yields at the beginning of the cleavage reactions, whereas a base catalyst also decreases the guaiacol yield towards catechol [31]. Cheng et al. 2012 also show that water in a co-solvent (alcohol-water) liquefaction increases the degradation of lignin. In pure ethanol, lignin degradation was observed to be lower [49]. They also showed a high dependence of the gained product mixture to the reaction temperatures. Heterogenous metal catalysts like nickel, platinum or ruthenium did not increase the degraded lignin amount but change the structure of the obtained molecules, because of the change in solubility of tetrahydrofuran [49]. Singh et al. investigated methanol as a solvent for the hydrothermal cleavage of lignin [50]. Organic solvents could increase the yield of water-insoluble oily products [51].

Due to the fact that there is no industrially process which uses biomass in a chemical way (except the vanillin production), no classical state of the art is given by now.
All possible variations, e.g:

- in the experimental proceeding
- biomasses sources
- the default of standards (mostly different analytical procedures)
- a lack of understanding of the basic reaction mechanisms happening in biomass degradation processes,

lead to a huge amount of fundamental studies, however, as explained before the comparison of these parameter sets cannot easily be performed. Therefore, as an example is given concerning the oligomeric analysis of Indulin AT (see 2 Methods and Materials; 2.1.1 Indulin AT – Kraft lignin) via size exclusion chromatography (SEC), are also insufficient results observed in the literature. E.g., Shu et al. [52] have performed measurements with SEC, with a polystyrene calibration, which is often used, what can lead to incomparable results when a different method is performed. These main disparities are also shown in M. Azadfar [53] and many other investigations. A detailed study of the natural oligomer products has so far not been considered in detail in the literature. Model substances are often used (as in PJ. Deuss [54] and O. Gordobil et al. [55]), however, only specific parts of the molecules are considered. Consequently, many questions remain open, which, however, need to be considered in order to form an economic and ecological value chain for lignocellulosic materials. Therefore, an optimization of the SEC method and the attempt to create a database is particularly important for the basics of lignin research, which is also part of this work. The literature must be evaluated intensely to compare results and to use perceptions in other studies, to precise the influences of the investigated parameter sets. Only single results, for instance, the product spectra of the pyrolysis and analysis of this, and understandings, like the influence of temperature regarding the gasification reactions, can be used to compare different studies. Comparable to putting together a puzzle; several single puzzle pieces must be put together in small steps to see the overall picture. This makes it possible to build a common ground for the understanding and using biomass as a resource.

2 Methods and Materials

2.1 Applied lignins

To design a process suitable for different biomass and lignin sources of varying structure, it is necessary to investigate more than one lignin. Therefore, five different biomasses were chosen to be examined in this study. Hence, different biomass sources and isolation methods were selected. Two of them are side streams of the pulp and paper industry; three are products from Organosolv pre-treatment (see also chapter 1.4).

- Kraft lignin; waste product out of the pulping industry, trade name “Indulin AT”, the wood source is pine wood (WestRock industries, Atlanta).
- Beechwood bark; also waste of the pulping industry (Fa. Sappi, Stockstadt).
- Organosolv lignin prepared by the Fraunhofer Center for Chemical-Biotechnological Processes CBP in Leuna via the organosolv process with beech as a wood source.
- Organosolv lignin prepared by the Fraunhofer Institute for Chemical Technology in Pfinztal via the organosolv process with *Miscanthus Giganteus* as a lignin source.
- Organosolv lignin prepared by the Fraunhofer Institute for Chemical Technology in Pfinztal via the organosolv process with poplar wood as a lignin source.

The Kraft lignin is available in large amounts on the market, and also the bark is provided by the pulp and paper industry in large amounts, while the organosolv lignins are only produced in small scales (lab and pilot scale). The bark was chosen because it is not chemically pre-treated, and it was and can be used directly. Furthermore, to see the influence of using whole biomass directly without lignin separation first.
If lignin is used as a chemical raw material in the future, Kraft lignin is just one option, also purer lignins without sulfur residues would be needed. Therefore, the organosolv process could be used as a separation method. In a lignocellulosic biorefinery, the sugars of lignocellulosic biomass separation would be used fermentatively and the lignin for chemical purposes [56]. *Miscanthus* and poplar can be grown in short rotation plantations and integrated in the biorefinery.

2.1.1 Indulin AT – Kraft lignin

Indulin AT is lignin gained by the Kraft process (see chapter 1.4.1). Kraft lignin is a residue of the pulp and paper industry. The biomass source is pine wood. It is purchased from WestRock industries (Atlanta, USA). It is commercially available and also used as reference lignin in the Bioeconomy cluster of Baden-Württemberg. It contains sulfur, because of the isolation process, which is poison to many catalysts (e.g., Pt, Pd or Ni-containing catalysts).

2.1.2 Organosolv lignin out of beech wood

A pilot plant at the Fraunhofer CBP in Leuna produces organosolv lignin out of beech wood. In a 400 l reactor at 200 °C beechwood is separated in a water-ethanol mixture into lignin, cellulose, and hemicellulose. Purchasing small amounts is possible. This process shall be commercial with lignin as the main product. Also because of the fact that it is only a pilot scale plant and not a commercial production yet, it is still more expensive than Kraft lignin.

2.1.3 Organosolv lignin out of *Miscanthus Giganteus* and poplar

At Fraunhofer ICT in Pfinztal, two different biomasses were used in an organosolv process to gain lignin. *Miscanthus Giganteus* and poplar wood were treated with an ethanol-water-mixture. The process is an acid-catalyzed reaction. *Miscanthus Giganteus* can be grown on marginal lands and creates no competition with the food supply. Poplar can be grown in short rotation plantations so that it would also be available, and no forest wood will be used.

2.1.4 Beech bark

The layer above the wood of a stem is the so-called bark. It is the outermost layer and consist of inner bark and outer bark. The inner bark is living tissue while the outer bark is dead tissue. The dead part of the bark contains the highest concentrations of lignin. Bark is an essential part of the living plant. It is built to resist physical (e.g., weather, heat) and biological (e.g., animals, funguses, bacteria) environmental influences. It also has an important function as a part of the transport and storage system inside the tree structure [57]. In comparison to wood, bark contains more water, polyphenolics (mainly tannins), ashes and extractives besides the cellulose, hemicellulose and lignin fractions [58]. The fractionation of these different substances is mainly based on the plant type, the age of the plant itself and the climatic conditions of the growing. The lignin structure contained in the bark is mostly depending on the wood of the plant and the growing conditions. Bark is also a byproduct in the pulping industry; its amounts are proportional to the gained lignin. Bark mostly gets combusted to produce energy or put back on landscapes to improve earth quality [7]. Hardwood bark, like beech bark, contains around 30 wt.% of lignin [B][59]. Previous measurements confirm a lignin content of the evaluated beech bark for about 30 wt.% [60].

2.1.5 Synthesized lignin oligomer

To get an intermediate between the raw lignin molecule and the monomeric end products, a synthesized oligomer was investigated [61].
A synthesis of vanillin over ß-O-4 bonds was chosen (Figure 14) because ß-O-4 is the most frequent bond in lignin, especially in the Kraft lignin Indulin AT, which has been used as reference material in this work.

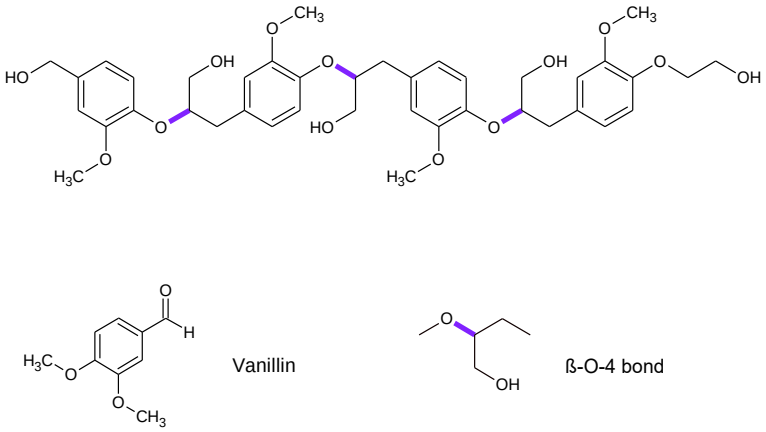

Figure 14: One possible lignin oligomer molecule with four aromatic rings, synthesized after Rui et al. using vanillin as a starting molecule which gets bond over ß-O-4 bonds (marked blue) [61].

It is a three-step synthesis performed after Rui et al. (see Figure 15) [61]. Chemicals were used as described in the work of Rui et al., vanillin is first functionalized to allow an oligomerization afterward.

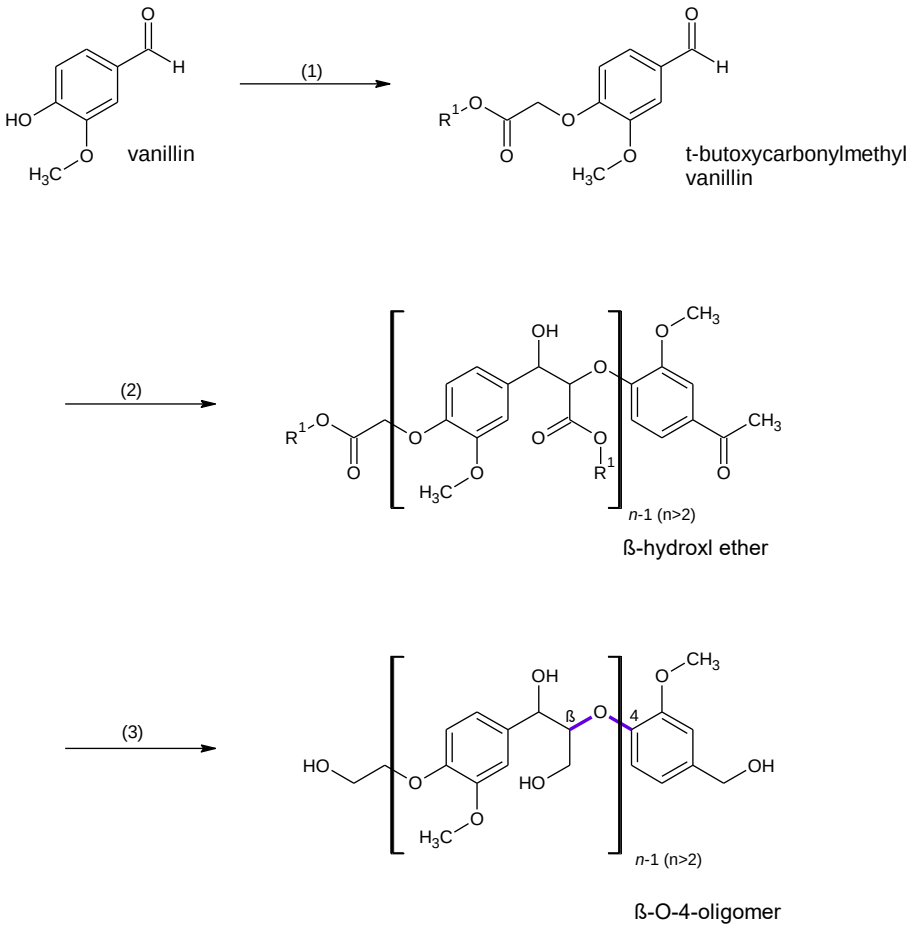

Figure 15: Three step synthesis after Rui et al. [61]. (1) first step: functionalization of the vanillin molecule to t-butoxycarbonylmethyl vanillin. (2) Second step: the oligomerization to the ß-hydroxyl ether. (3) Third step: defunctionalization towards the ß-O-4-oligomer (ß-O-4 bonds marked blue). (after [61])

Therefore, t-butoxycarbonylmethyl vanillin (1) is synthesized via a reaction with butyl-2-bromoacetate. The gained yellow solid is washed several times to decrease starting material residues. To ensure the necessary product is gained, ^{1}H-NMR and ^{13}C-NMR measurements, as described, were performed. In a second step, the oligomerization of the produced monomer is induced by lithium diisopropylamide (LDA) in tetrahydrofuran (THF) solution. Molecules with minimum of two t-butoxycarbonylmethyl vanillin units are produced, and this light-yellow solid (ß-hydroxyl ether (2)) is also measured via the described ^{1}H-NMR and ^{13}C-NMR methods. As the last step the functional groups of the oligomers which allowed the oligomerization must be removed again. They get reduced to hydroxy groups with lithium aluminum hydride. The gained lightly yellow syrup is also checked vis the described NMR measurements. The synthesized oligomer links its units via ß-O-4 bonds (4). Figure 15 shows the synthesized molecules.

2.2 Analytical Methods

Different analytical methods were used in this work to analyze the lignins themselves, solid residues, gaseous products, and liquid products of the hydrothermal degradation. Next, to the mainly used methods, an overview is shown in Table 2, some other methods like HPLC or elementary analysis were used, anyway no further information could have been gained by those methods, so these are not further discussed.

Table 2: Mainly performed analytical methods with their measured components, accuracy and limits.

Method	Measured Components	Limits
NMR	Lignin Structures and solid residues	Structure complexity leads to a interference of signals
Chromatography		
Gas chromatography with gas sampling	Main gaseous products of the degradation process	Only suitable for gaseous products
Gas chromatography with liquid sampling	Main monomeric phenolic structures of the degradation process	No aqueous samples, different concentrations of the single components lead to different qualities
Size exclusion	Oligomeric residues of the degradation process	No standard method is known and no suitable calibration components available

2.2.1 NMR measurements

The lignin structure is highly complex and versatile depending on its source and isolation method [29][62]. The lignin structures were investigated by 2D NMR measurements. To get information about the lignin structures and the influence of the applied isolation processes, heteronuclear single quantum coherence (HSQC) measurements (after [63][64]) on the different lignins were performed. In contrary to 1D-NMR measurements, couplings between individual nuclei can be seen in 2D NMR experiments. Indirect couplings are present via bonds as well as directly across space [65]. Thus, information about the spatial structure of the molecules under consideration of the different biomass sources and isolation methods can be obtained. The investigated lignins were extracted prior to the NMR measurements for 24 h with ethyl acetate to separate the extractives and different residues from the lignins. With a ball-milling procedure, the samples get powdered. Grinding jars with 10 mm balls were used, and the samples get milled for 50 min. For the NMR measurement about 30 mg of the powder gets transferred into the NMR tube directly. To get a homogenous gel consistency, about 500 µl of the solvent mixture is added slowly. The solvent mixture is a

ratio of 4 parts DMSO-d6 and of 1 part pyridine-d5 [63][64]. Ralph et al. [63] and Bunzel et al. [66] use a 2D-NMR method without a phosphorylation step and the results gained by their methods could vary from literature, but they are still in the known and expected ranges and get an even better idea about the starting material. Because it is important to mention that in comparison to the above described direct techniques ^{31}P-NMR is commonly used in the available literature to investigate the composition of the lignin. By doing this, the hydroxyl groups in the lignin sample get phosphorylated before the measurement and the resulting phosphor nuclei are analyzed via NMR.
Therefore, most commonly 2-Chlor-1,3,2-dioxaphospholan and 2-Chlor-4,4,5,5-tetramethyl-1,3,2- dioxaphospholan is used as a reagent in a pyridine solution [67]. However, different temperatures, amounts of reagents and reaction times are used in the literature [68][69][70]. This makes it unknown how many of the existing hydroxyl groups are phosphorylated. With different phosphorylation methods, different not completely understood reactions at the main lignin molecule occur, and lead to different results. Furthermore, no attempt for standardization of an NMR method has been undertaken which leads to a non-comparability of the published data.

2.2.2 Chromatography

Gas chromatography was mainly used for analyzing the monomeric components in the product mixture. The investigated separation principle is based on the distribution of components between two phases, gas and solid/liquid [71]. Nevertheless, also, a separation of the products would be the next logical step to get single products. However, the separation of the products cannot just be performed by distillation or extraction. Only parts of similar products can be gained via distillation, which also leads to a interference of the signals in further analytical steps like NMR or chromatography.

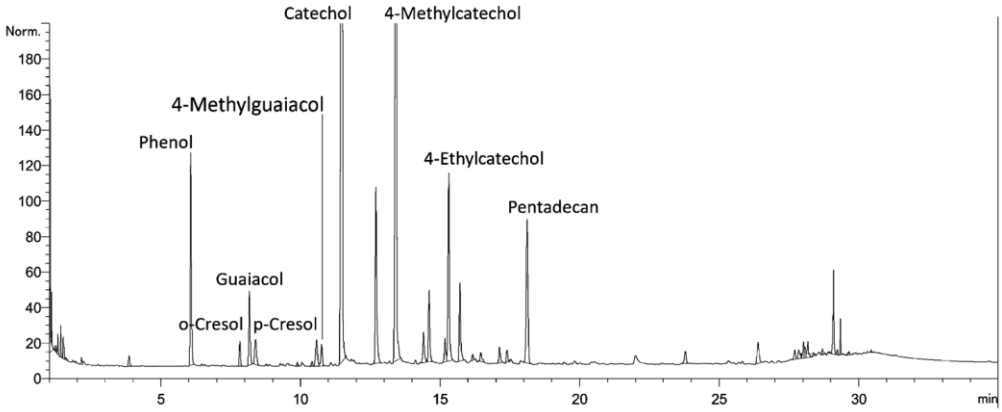

Figure 16: GC-chromatogram of a liquid phase product mixture sample.

Though, more than ten different monomers have been defined and calibrated in the IKFT at KIT. This makes the analytic (qualitative and quantitative) of the main gained monomeric compounds possible (see chapter 2.2.2.2). Besides these, there are still many peaks which

cannot be separated or defined (Figure 16). The signal to noise ratio is also a problem in GC-measurements.

2.2.2.1 Analysis of gaseous samples

The gaseous samples are analyzed by an Agilent 7890 B GC-system with a 2 m Porapak Q column. An Agilent laboratory data system controls the measurement. Manuel injections with a 100 µl syringe are carried out.
For the detection of the compounds a flame ionization detector (FID) is applied. The sample gas is mixed in the detector with air and is injected into a hydrogen flame. The compounds are combusted in the flame and form ions, which are collected at an electrode delivering an electric signal. The advantage of this detection method is it is direct and linear proportionality of the amount of one substance in the sample to the detected signal thereof. The calibration of the measurement method was over a five-point calibration for every one of the sixteen substances.
One more detector used is a thermal conductivity detector (TCD), which measures the change of the thermal conductivity of the gas (mobile) phase against a reference gas flow [71]. (Method described in appendix 8.1.)

2.2.2.2 Analysis of liquid samples

For the quantitative analysis of the liquid products, a Hewlett Packard 5890-II GC system with a Hewlett Packard 5890 autosampler equipped with an FID-detector is used. It is controlled by an HPChem laboratory data system. As a column, a nonpolar 30 m Restek Rtx-1 MS cross bond dimethylpolysiloxane column is used.
As water, which is detrimental for the used GC column, is used as a solvent in the hydrothermal cleavage step, the samples cannot be measured directly, and a sample preparation needs to be applied. Hence, an extraction of the products to an organic solvent is performed before transfer the analysts in an organic matrix which can be analyzed with the described methods.
The performed extraction method has been developed in previous work of D. Forchheim [10], modifications and improvements were necessary for this work to adjust the method to a broader spectrum of lignin. The distribution coefficients were applied as determined by Daniel Forchheim [10] to ensure reproducibility and comparability with prior experimental data. (More details are listed in appendix 8.2 and 8.3.)

2.2.3 Size exclusion chromatography

Gel permeation chromatography (GPC) or size exclusion chromatography (SEC) separate the component mixture based on their size or more precisely on the hydrodynamic volume of it. It is a separation technique solemnly based on the diffusion velocity of the molecules through the column. There are no interactions (neither physical nor chemical) with the solid phase like in other chromatographic techniques [72]. To ensure that there is no or nearly no interaction with the stationary phase for nonpolar molecules a nonpolar solid phase is

needed, and the other way around. With molecules, which have polar and nonpolar regions it is complicated to find a suitable solid phase [73]. Larger molecules cannot enter the pores of the solid phase and hence pass the column fast. Small molecules, however, can diffuse in the pores and have a longer mean way through the column and get eluted later as the bigger molecules. Noteworthy is the fact, that the hydrodynamic volume of a molecule change with the solvent [73].

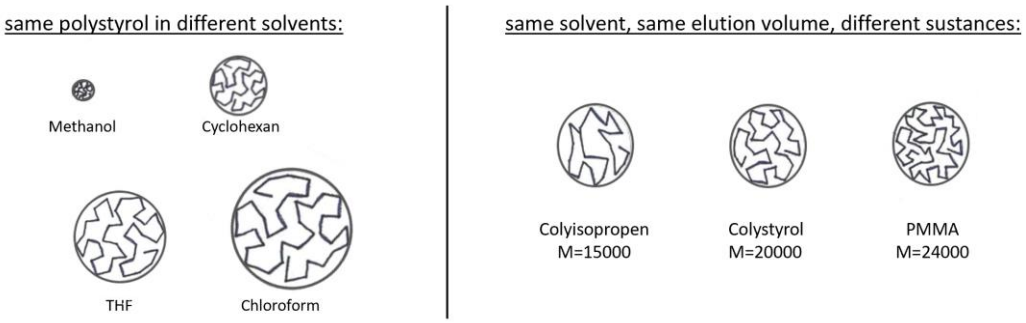

Figure 17: Examples of hydrostatic volumes of the same molecule in different solvents and different molecules in the same solvent [72].

In Figure 17 an example of the behavior of polystyrene in different solvents and different molecules in the same solvent are presented. The polystyrene has a smaller hydrostatic volume in methanol than, e.g. in chloroform; the SEC measurements would show two different molecule sizes for the same molecule. According to Figure 17; it is possible that the hydrostatic volume in the same solvent is the same e.g. polyisoprene and PMMA (Poly(methyl methacrylate)); the SEC results would give one resulting molar mass, even when their molar weight is 15000 or 24000 [73]. Molecules with side chains are also difficult to investigate with SEC because the chemical folding of the molecule can deliver a similar hydrostatic volume to other molecules with no side chains. As lignin is a complex macromolecule with side chains, it is not possible to get all changes in long side chains, if the chemical folding is similar to other cleavage products and consequently this must be considered in the result evaluation.

The biggest challenge is the oligomer analytic; size exclusion chromatography (SEC) seems to be the method of choice, however the lignin structure has nonpolar and polar regions, which makes it very complicated to apply a suitable SEC method, as there should be neither interaction with the polar nor the nonpolar stationary phase (contrary to the HPLC for example). A common method to get a nonpolar product mixture is phosphorylation of the polar hydroxy side chains [74][75]. It would be possible to get an idea of the phosphorylated hydroxy side chains amount by titration, still it is not sure if every hydroxy group is exchanged or if there are any other changes in the structure. By changing the polarity and exchange of the side chains, the molecule has another chemical folding and presumably with this a different hydrostatic volume, which leads to different results in an SEC measurement. Different phosphorylation methods (e.g., reaction time and temperature) deliver different molecules and have a high influence on the results [76][77][78]. So, without

knowing the changes in the hydrostatic volume of the molecules, it is not possible to get a certain molecular weight over SEC measurements. Besides this, no standards for the calibration are commercially available [76][77][78]. In literature, polystyrenes are a common calibration standard of SEC methods. Compared to lignin and lignin degradation products polystyrenes is a different molecule; it consists of a nonpolar chain without any longer sidechains beside the phenyl groups. This delivers no comparable and reliable results [76][77][78][79].

A synthesized oligomer was investigated [61], to gain information about an intermediate between the raw lignin molecule and the monomeric end products. With such components, a more reliable calibration could be possible.

The samples were measured with dimethyl sulfoxide (DMSO) as a solvent, a mixed column and calibrated against pullultants. The mixed column shall help with the polar and nonpolar regions of the oligomers and pullulan is a polysaccharide polymer built of maltotriose units, which also has polar and nonpolar sections. The calibration is done in a range of 100-10,000 g/mol.

Only four samples were selected to start the method development:

- with a reaction time of 30 min and 300 °C reaction temperature,
- with a reaction time of 60 min and 300 °C reaction temperature,
- with a reaction time of 30 min and 400 °C reaction temperature,
- a sample of the synthesized oligomer.

2.2.4 Analytical challenges met during the studies

It is supposed that a lot of radical reactions are taking place depending on the reaction temperature [80]. This results in a variety of different monomeric and oligomeric compounds after the reaction. The product spectra are highly complex with far more than 50 different products and not every product could be identified by now. The analysis and separation of such a complex mixture is also a challenge, which has to be faced while working with lignin as a resource.

2D-HSQC spectra can help, e.g., to identify the molecule structure depending on aromatic or aliphatic structures and also their bond types (shown in chapter 2.2.1 & 3.1). Via NMR measurements it is not easy to get a clear spectrum for the product mixture as against the structural measurements, which makes the structure analysis highly complicated. There is also a superposition of the signals, due to the broad product spectra. Furthermore, different problems occurred with different solvents and measurement techniques.

For instance, aromatic ring signals for the C_2, C_5 and C_6 atoms appear in the lower field (low left corner) of the spectra while their bond types appear in the high field (upper right corner). Figure 18C shows the 2D-HSQC spectra of a product mixture. It shows signals in the aromatic area and not in the aliphatic area. However, there are just signals of the C_5, C_6 C-atoms of the aromatic ring, the signal for the C_2-atom is missing. Which would typically indicate a ring cleavage, however, the lack of the shift to the aliphatic area is contradictory to the ring cleavage. Also, expected signals (upper right corner) for existing bonds were missing. This phenomenon appeared in several measurements and could still now not be

explained. Figure 18 shows four different examples of NMR measurements. A) shows a 1H-NMR of a product mixture in deuterated methanol with a superposition of different signals and a low noise to signal ratio. B) shows the corresponding 13C-NMR to A), with a Bruker Advance 250 MHz. The low noise to signal ratio makes it impossible to analyze a single signal. C) the 2D-HSQC mentioned above.

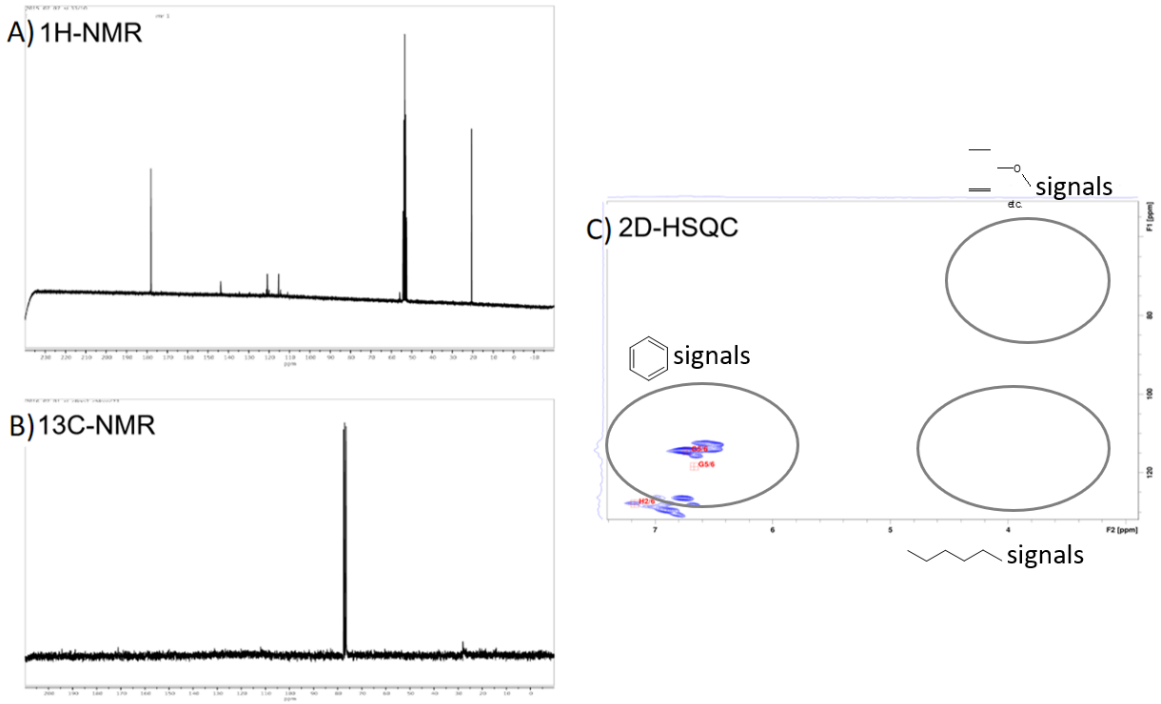

Figure 18: NMR signal of liquefaction product mixtures with different methods and solvents. A) shows a 1H-NMR of a product mixture in deuterated methanol. B) shows the corresponding 13C-NMR to A). C) shows a 2D-NMR spectrum with aromatic signals and the areas of aliphatic and bond signals.

These examples show how difficult it is to get information about the product spectra out of NMR measurements.
Furthermore, with the different reaction parameters the amounts of the single products vary significantly, so to get each component in the right range of the calibration requires numerous measurements in different dilutions [81].
In this work, several limitations of common analytical methods occurred and have been discussed. Further improvements of analytical methods are necessarily requiring comparatively high efforts and costs since no commonly agreed protocols and standards are in place today. A better understanding of biomass and an improvement of analytical standards in this field could be achieved by the met challenges in this work [82].

The lignin molecule itself should be analyzed in the beginning. Only information about the monomeric units and bonds can be achieved, besides this, it is hardly possible to get information about the single molecules (size, structure, side chains, and so on). Without the

knowledge on how precisely the starting molecule is built up, it is not simply to understand the complete reaction pathway towards monomeric phenols. Also, many intermediates are still unknown, because the analysis of the oligomers is highly challenging. Different degradation products are produced in the different cleavage reactions, depending on the lignin source, the process of product isolation and the parameters of the liquefaction process (compare 4.1). To circumvent the unknowingness of the starting molecule model compounds were investigated in this work, to begin with, to get a better understanding of the reaction pathways, intermediates, and the product spectra.

Therefore, a synthesized lignin oligomer and monomeric model compounds were investigated. Guaiacol is used as a starting monomeric model compound. However, also, with a known starting structure, the hydrothermal liquefaction results in a diverse product spectrum (e.g., 4-ethylphenol, 4-methylguaiacol, catechol, 4-methylcatechol, 4-ethylguaiacol). The experimental procedure has to take into account that guaiacol is hardly soluble in water, which complicates the product analysis; therefore, the experimental error is relatively high using guaiacol as a starting material.

Moreover, the broadness of the product spectra aggravates the analysis and the understanding of the reactions. Nevertheless, 4-methylcatechol was also built by using only guaiacol as a starting material, which made it clear that it is a reaction product out of guaiacol and catechol.

To get a closer look at the oligomeric products a lignin oligomer was synthesized. Though the product spectra also got highly variated, and the analytics complicated further.

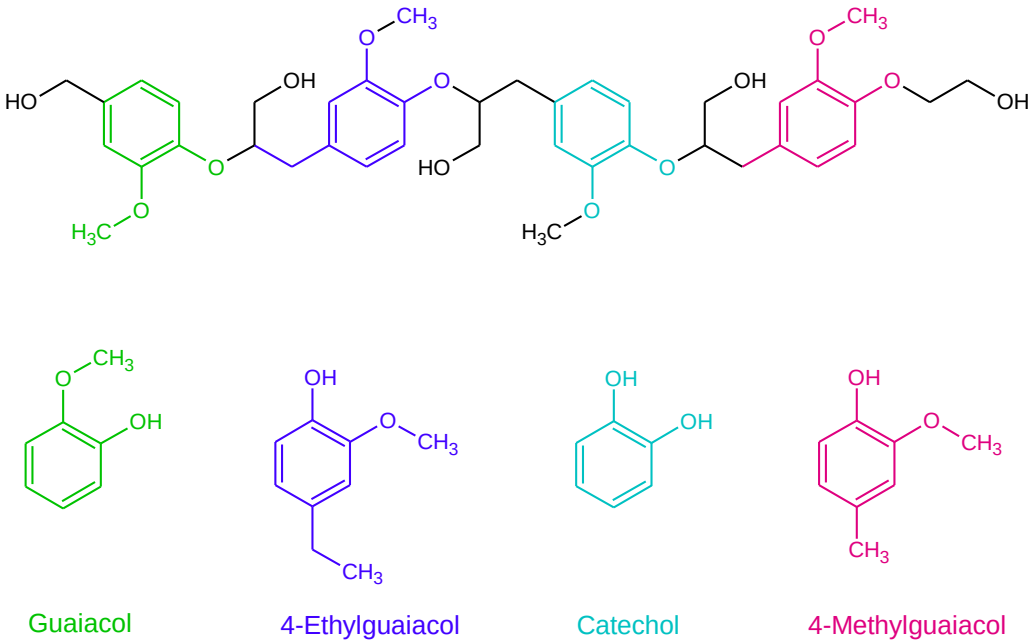

Figure 19: One possible oligomer as a model compound for the cleavage of lignin, synthesized after Rui et al. [61] (above chain) and some of the products out of the hydrothermal liquefaction process. The gained monomeric products (e.g., guaiacol (green), 4-ethylguaiacol (dark blue), catechol (light blue) and 4-methylcatechol (pink)) could be cleaved directly of the oligomeric structure. The colors indicate their formerly position in the oligomer.

Some of the cleavage products are directly formed out of the oligomeric chain (see Figure 19). Still, several intermediates could not be analyzed because of the different reasons mentioned in this chapter. However, also like in the experiments with guaiacol as a starting material it became clear that 4-methylcatechol is a consecutive product and not built directly. The gained monomers are similar in their structure; an aromatic ring with OH, OCH_3 or CH_3 sidechains. This is the main reason why lignin analysis is highly complex because often superpositions of the signals occur. Because of their complex variety and similarity of products formed regarding molecular weight and functionality, it is hard to analyze the individual products, even with GC. Calibration of the used GC method is work-intensive because there is no standard method or database available and some of the components are not separable and hard to get usable peaks out of the measurements. Even the met challenges in this work led to a better understanding of biomass and to an improvement of analytical standards in this field, which improved the understanding of lignin itself and its behavior as a feedstock in HTL.

2.3 Reactor types

2.3.1 Loop reactor

Previous work indicated an influence on the liquefaction reaction results if back-mixing of the reaction mixture to the reactor is performed via recycling with a pump (Figure 20) [10].

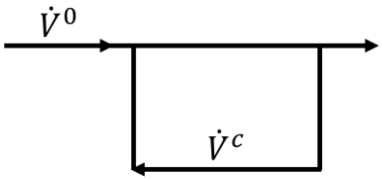

Figure 20: Scheme of loop reactor flows; $\dot{V}^0$ is the volume flow of the feed, $\dot{V}^c$ the volume flow of the circulation.

In a continuous reactor with back-mixing, the products can interact with the unreacted feed and intermediately formed products [83,84][85]. To get optimal conditions for kinetic measurements in a loop reactor a back-mixing ratio (Equ. 5.1 [85]) of >10 even >20 is recommended, to decrease influences of heat and mass transfer processes [85].

$$\boldsymbol{R = \frac{\dot{V}^c}{\dot{V}^0}} \qquad (5.1)$$

R	back-mixing ratio
$\dot{V}^c$	volume flow of the circulation stream
$\dot{V}^0$	volume flow of the feed stream

High flow velocities can be reached with low concentrations of the feedstock in a large quantity of solvent; this allows the investigation of complex reactions [86]. Three different operation modes can be performed with a loop reactor; an ideal continuous stirred tank reactor, a continuous plug flow reactor and any combination of both characteristics.

The reactor setup should allow the investigation of the dependence of the reaction kinetics on the back-mixing ratio. This would e.g. affect the yields of products, which may be interesting for the production of intermediates. Parameters like back-mixing and number of cycles could increase the influence on the reaction pathways. With this continuous system, the identification of critical key components and their kinetics should be possible.

It is assumed that repolymerization reactions may be influenced through the back-mixing, leading to a higher amount of bifunctional monomers. Furthermore, bifunctional oligomers

may be accessible through a novel process design which requires the design of the reactor set-up (Figure 21) for lignin depolymerization.

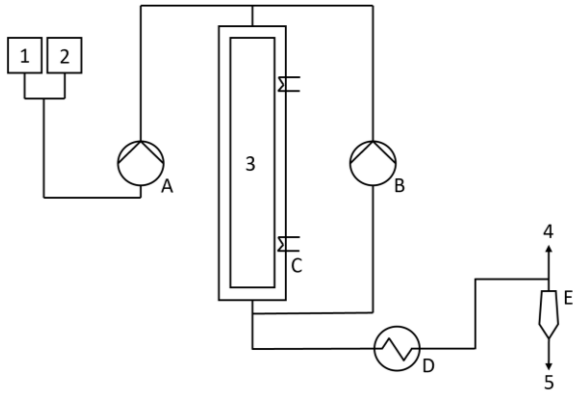

Figure 21: Scheme of the loop reactor; 1 & 2: Feed; 4: gas products; 5: liquid products; A & B: pumps; 3: reactor (1 l); C: heating system; D: heat exchanger; E: phase separator.

2.3.1.1 Characterization of the loop reactor

The loop reactor was designed for long reaction times >40 min and the chosen pumps have a maximum rate of feed pump of 0.8 l/h and the loop pump of 2.6 l/h.
Two different methods to determine the residence times experimentally were applied; step tracer and pulse injection. The reactor was filled with water and heated up. For the step tracer experiment, a displacement of the water with the tracer solution (KOH 1wt.% and phenol dilution) is performed. The reactor feed inlet changes suddenly by switching the feed solution and so does the concentration of the tracer from 0 to the prepared concentration. The concentration at the outlet of the reactor is measured. For the cumulative distribution function F(t) a sudden leap from 0 to one is expected for an ideal reactor. For a nonideal reactor, there is a shift in that leap [87]. For the plug flow mode of the loop reactor a cumulative distribution function F(t) like in Figure 22, with a more direct displacement of the reactor volume with the tracer was expected.

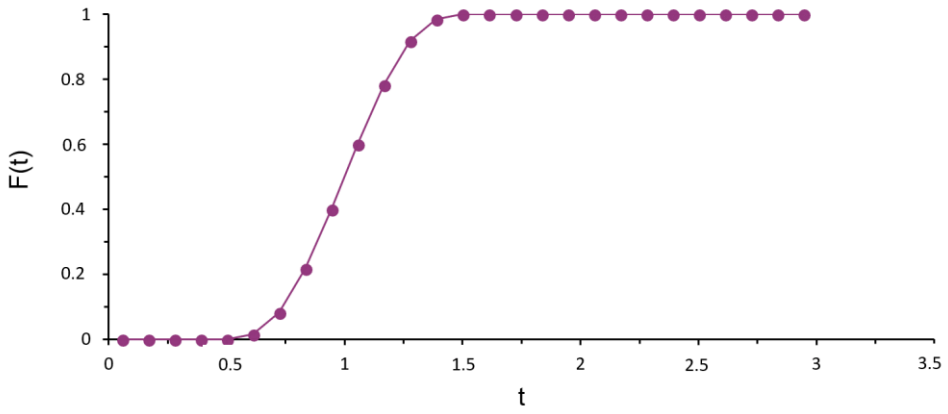

Figure 22: Concentration / time course of the tracer: cumulative distribution function F(t). At time t = 0, a constant amount of tracer is continuously added to the inflowing fluid, so the tracer concentration jumps from 0 to $c_{T,0}$ and then remains at that level — expected cumulative distribution function F(t) of the plug flow mode of the loop reactor, where a volume element passes the reactor.

For these experiments, it is crucial that the applied tracers be stable at the investigated reaction conditions. Phenol and potassium hydroxide were chosen as these are stable tracing components. Phenol is a stable component under the hydrothermal conditions and a product of the target reaction. Potassium hydroxide (KOH) is also a stable component and the applied homogenous catalyst in all experiments [88][89].
For the CSTR a cumulative distribution function F(t) like Figure 23 was expected, with a slower displacement than in the plug flow reactor.

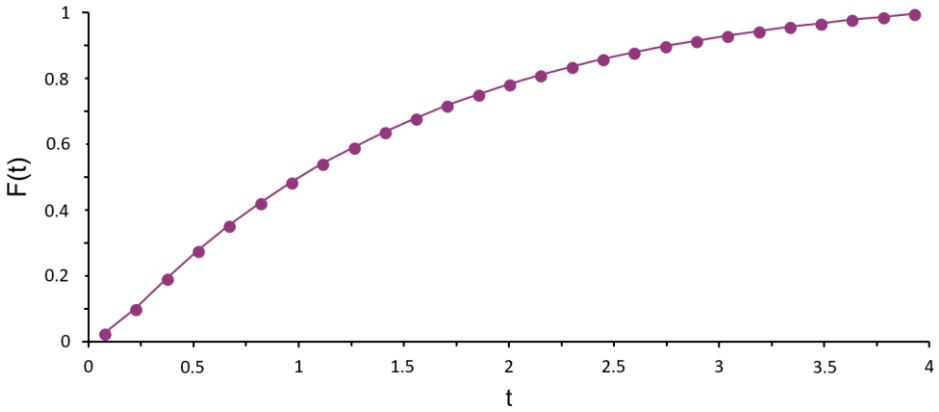

Figure 23: Concentration / time course of the tracer: cumulative distribution function F(t). At time t = 0, a constant amount of tracer is continuously added to the inflowing fluid, so the tracer concentration jumps from 0 to $c_{T,0}$ and then remains at that level — expected cumulative distribution function F(t) of the CSTR mode of the loop reactor, where a volume element gets mixed into the whole reactor volume.

With a pulse injection of the tracer, a small volume of the tracer gets injected, and it gets measured when this volume leaves the reactor. For an ideal reactor the injected volume would pass the reactor as it was injected, however, in a real reactor, a certain back-mixing is happening [85][87].
Nevertheless, residence time measurements showed that the loop reactor as it has been constructed shows the characteristics of a CSTR (Figure 24 and Figure 25).

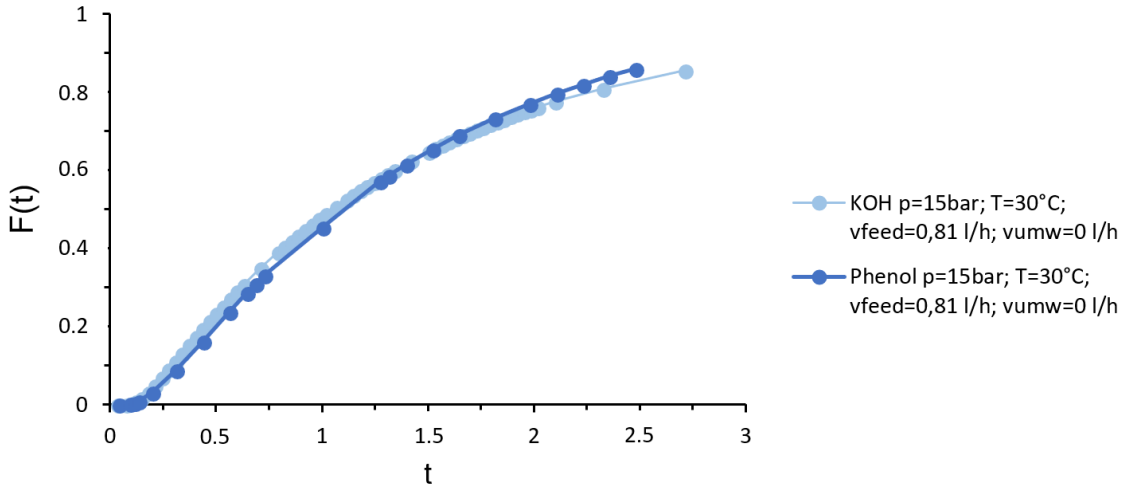

Figure 24: Cumulative distribution function F(t) of the loop reactor with plug flow mode (circulation pump 0 l/h, feed pump maximum of 0.8 l/h). Measured with phenol (dark blue) and KOH (light blue).

Even without the circulation pump, the velocity is too slow to develop a plug flow behavior within the tubular reactor section of the loop reactor. This leads to a high internal back-mixing and indicates that the feed pump capacity is too small to achieve a plug flow behavior. The set up cannot be influenced enough by the pumps which were available in the set-up to achieve different flow behaviors. Even with the fulfilled requirement for plug flow reactor design of a length to diameter ratio (l/d=180) > 50 [90].

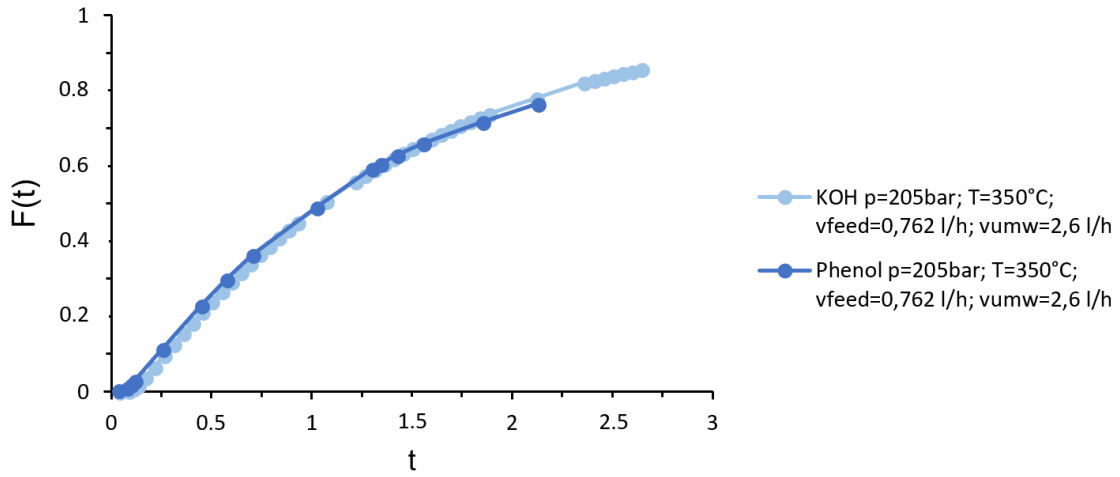

Figure 25: Cumulative distribution function F(t) of the loop reactor with the maximum back-mixing ratio (circulation pump maximum 2.6 l/h, feed pump maximum of 0.8 l/h). Measured with phenol (dark blue) and KOH (light blue).

Different parameters were investigated at different temperatures (250, 300 and 350 °C, different pressures and different circulation pump capacities (back-mixing ratios). And all of the performed experiments show that the given set up is not optimal for the hydrothermal liquefaction process.

2.3.2 Plug flow and tank reactor

To show the influence of the internal back-mixing two microreactor systems were built up to represent both extremes of a loop reactor: the continuous stirred tank reactor and the plug flow (Figure 26).

Figure 26: Lab-scale tube and tank reactor used for the experiments with Indulin AT lignin and a volume of ~40 ml each.

A lab scale of these two reactor types, were built up in the institute workshop out of stainless steel (1.4571) (max. 500 °C, max. 300 bar); a plug flow reactor and a non-stirred continuous

tank reactor, dimensions are shown in Table 3. In this work, only unstirred autoclaves were used, nevertheless, a complete mixing is presumed because of the reaction parameters, and the behavior of water at these conditions and the small volume of the reactor.

Table 3: Dimensions (volume, length and inner diameter) of the two lab scale reactors; a plug flow reactor and a non-stirred continuous tank reactor.

Reactor	Volume	Length	Inner diameter
Plug flow	~40 ml	2.1 m	5 mm
Conti. tank	~40 ml	0.04 m	40 mm

As a feed pump (max. 5 ml/min), an HPLC-pump was used and also the length to diameter ratio increased compared to the tube reactor (l/d=250), to get a good flow profile.
The whole set up for the two lab-scale continuous reactors is shown in Figure 27:

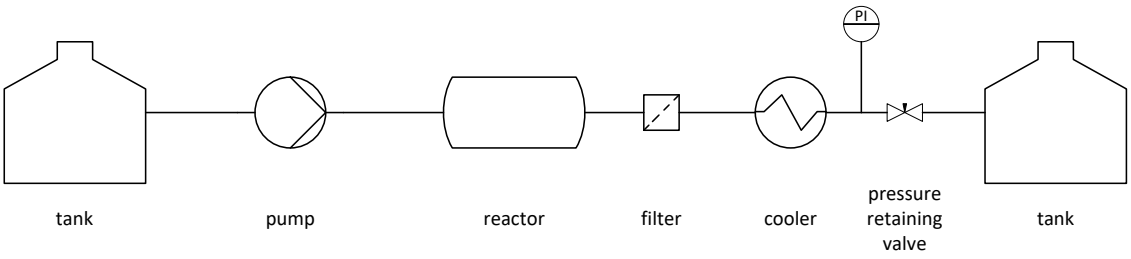

Figure 27: Flowchart of the tube/tank reactor; the reaction media gets stored and advanced in a tank, an HPLC pump serves as the feed pump and pumps the media into the reactor (tank and plug flow), a pressure retaining valve ensures pressure in the reactor, before that valve a filter and water-cooled cooler are installed.

To ensure continuous availability of medium, the reaction media gets stored and advanced in a tank with an HPLC pump the media gets pumped into the reactor (tank/plug flow). To ensure a pressure higher than the vapor pressure of water, a pressure retaining valve is used. A filter is installed after the reactor to prevent clogging of the valve. To stop the reaction immediately after the reactor, a cold-water cooler (~15 °C) is also installed.
Residence time measurements were performed with NaCl and a conductivity electrode. Residence times of 8, 15 and 30 min could be realized in the reactor systems. These measurements showed a decent internal mixing at the investigated conditions for the tank reactor which makes stirring unnecessary.

2.3.3 Batch autoclaves

Stainless steel (1.4571) micro batch reactors (10-25 ml, max. 500 °C, max. 280 bar) were built up in the institute workshop (see Figure 28).

Figure 28: 10 ml batch autoclaves used for all screening experiments for all investigated biomasses.

Different volumes were built: 10 ml and 24.5 ml. However, their behavior during heat up and cool down is the same. With all autoclaves, it is possible to get gaseous samples. The proceeding is further explained in chapter 2.4.1 and 2.4.2.

2.4 Proceeding of the experiments

2.4.1 General proceedings

For the heating unit, a GC oven with a heating rate of 40 K/min is used in all experiments. After the target temperature is reached and additional 15 min heating up have passed, measured for all reaction temperatures in a reference autoclave, the reaction time is started. For the continuous reactors, biomass solution is fed into the reactor after the reaction temperature is reached and a minimum of three retention times have passed to reach steady conditions. After the reaction, the autoclaves are taken out of the oven and put under cold water to cool down and to stop the reaction, while a cooler stops the reaction in the continuous set up (see chapter 2.3.1)
The applied biomass to solvent ratios were used as described in equation (2.1) and (2.2).

$$\frac{m_{\text{KOH solution}}}{m_{\text{biomass}}} = 7.53 \quad (2.1)$$

$$\frac{m_{\text{KOH solution}}}{m_{\text{biomass}}} = 15.06 \quad (2.2)$$

Continuous experiments were performed with a ratio of 15.06, to ensure a wholly solved feed solution. As a solvent a one wt.% KOH (in water) solution is used, just for the catalyst influence experiments the KOH ratio was varied. Samples are taken according to a

procedure described in Figure 29 and analyzed by different methods (see chapter 2.2 Analytical Methods), for continuous and discontinuous experiments.
If different influences, like the addition of a hydrogen carrier, were investigated the additional compound is added to the starting lignin solution. A concentration of 0.5 wt.% (referred to the used mass of lignin) of each hydrogen carrier (methanol and glucose) was chosen.

2.4.2 Experiments in the micro batch autoclaves

Lignin and the potassium hydroxide solution are placed in stainless steel (1.4571) microreactor (10-25 ml, max. 500 °C, max. 280 bar). Figure 29 shows a scheme of the proceeding of the experiment and the analysis of the different sample types.

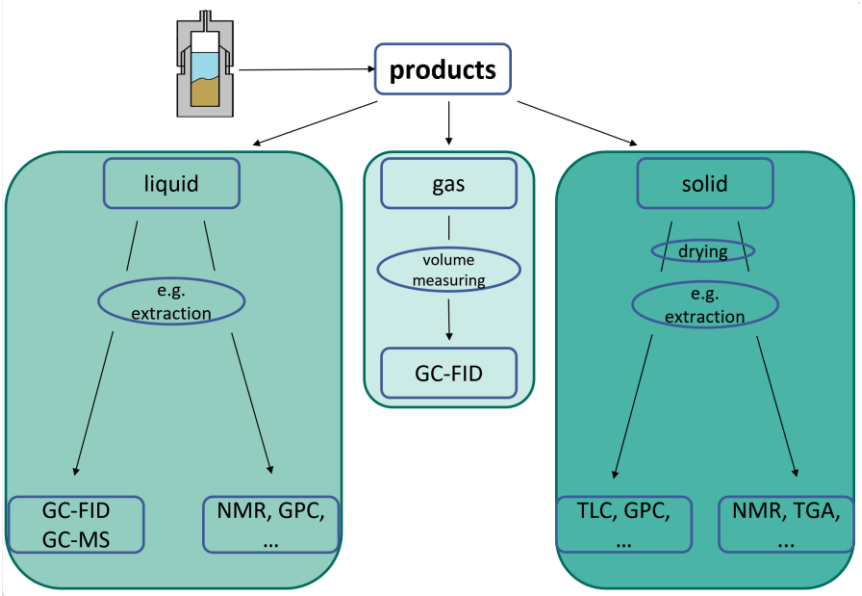

Figure 29: Possible proceedings of the experiments with the batch micro autoclaves and analytical methods used on the gained product phases.

The microreactors (10.0 ml & 24.5 ml volume) are filled with the lignin-base-suspension and sealed before they get heated up in the oven.

2.4.3 Continuous flow experiments in the Plug flow and tank reactor

The reactor is filled with water and preheated until the target temperature is reached, then the feed stream is changed to a lignin solution. A 6 wt.% lignin solution was used, to ensure that a solution and not a suspension is fed in the reactors and therefore to minimize the solid phase in the beginning. The experimental set up is described in chapter 2.3.2.

2.4.4 Continuous flow experiments in the Plug flow and tank reactor with external pre-back mixing

Furthermore, different experiments were performed to check the influence of the external back-mixing of the phenolic monomers and precursors for hydrogen, like in the loop reactor (chapter 2.3.1). To investigate the effect of contact between already reacted/cleaved molecules and fresh feed wanted to be investigated, a pre-cleavage was performed. The pre-cleaved product mixture gets mixed with fresh lignin solution and cleaved together (compare Figure 30).

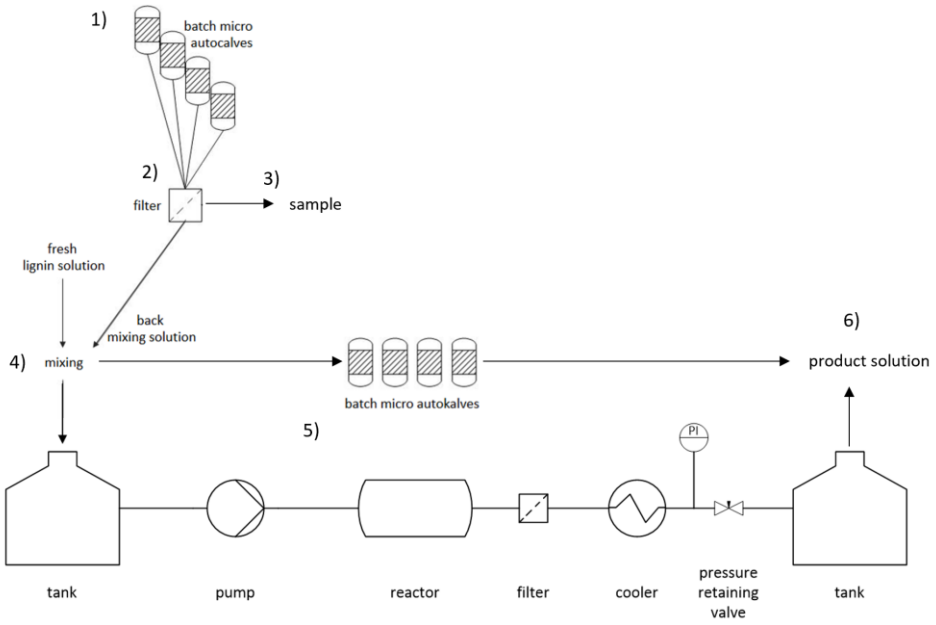

Figure 30: Flowchart of the proceeding and set up of the back-mixing experiments:
1) The pre-cleavage is performed in micro autoclaves.
2) The pre-cleaved solution got filtered.
3) A sample of the pre-cleaved solution is taken and analyzed.
4) Fresh lignin solution and the pre-cleaved solution get mixed.
5) The same set up as in the other continuous experiments is used. Parallel to the back-mixing experiments in the continuous tank micro autoclaves were used.

The pre-cleavage is performed in batch micro autoclaves under the same conditions as the back-mixing experiment later. Before the mixing, the pre-cleaved product mixture gets filtered to prevent clogging in the feed pump. These experiments were performed in the tank reactor and parallel to that in micro batch autoclaves. Three different cases with two different back-mixing ratios were probed:

- A 6 wt.% pre-cleaved Indulin AT mixed with a 6 wt.% fresh Indulin AT solution.
- A 6 wt.% pre-cleaved Indulin AT mixed with a 12 wt.% fresh Indulin AT solution.
- A 6 wt.% pre-cleaved Indulin AT mixed with a 12 wt.% fresh Indulin AT solution with 0.5 wt.% methanol or glucose.

The chosen back-mixing ratios were R = 1 and R = 10. Like described in chapter 2.3.1 a back-mixing ratio of 20 or bigger should be chosen. A back-mixing ratio of 20 would lead to only 0.5 ml fresh feed solution in the investigated set up. This would lead to small product concentrations, and the influence would not be observable anymore. To compare the results of the reactor screening experiments with the back-mixing experiments a starting concentration of 6 wt.% was chosen. Also, a starting concentration of 12 wt.%, like in the other batch experiments, were investigated to see if there is an enlargement of the monomeric products in a higher concentrated starting solution.
In the loop reactor not only, monomeric compounds get back mixed, also gases and solids. To compensate for this absence of produced gas methanol and glucose were added and serve as a hydrogen carrier.

2.4.5 Data analysis of experimental data

The key parameter of the data evaluation of the experiments has been the yield of monomeric compounds in relation to lignin fed to the reactor. The yield of the gaseous products was also measured, however, has not been discussed to further detail. The applied analytical methods are described further in chapter 2.2. High catechol amounts are preferred because of the potential of this molecule.

For the back-mixing experiments, a correction of the measured monomeric concentrations needs to be performed. By recirculating monomeric compounds, not $c_{i,0}$ must be used for the yield calculation but rather ($c_{i,0}$+$c_{i,R}$) as a starting concentration.
Because, e.g., a certain amount of guaiacol, catechol and 4-methylcatechol are already added to the reaction medium in the beginning. To investigate the influence of the back-mixing on the freshly built monomeric units, this already added amount must be subtracted. Therefore the following equations were used to correct the starting concentration and to refer the yield to the used lignin concentration:

$$c_{total} = c_{i,0} + c_{i,R} \tag{2.3}$$

$$c_{fresh} = \frac{c_{total}}{c_{lignin}} \cdot (R+1) - \frac{c_{i,R}}{c_{lignin}} \cdot R \tag{2.4}$$

R	back-mixing ratio
c_{total}	concentration of the sample after the experiment mg/l
$c_{i,0}$	part of the concentration of the freshly used lignin mg/l
$c_{i,R}$	part of the concentration of the back mixed sample mg/l
c_{lignin}	used starting lignin concentration g/l

With this equation, it is possible to suggest the influence of the back-mixing and to suggest if there is a positive impact on the yields of the monomeric compounds. Including the back-mixing ratio in the equation compensates the dilutions of the volume ratios of fresh and pre-cleaved media.

3 Experimental Results

3.1 NMR

For an optimization of the hydrothermal liquefaction process, an understanding of the basics is obligatory. Therefore, different focus areas must be set and determined to lay the foundations for such a process. To begin with, it is necessary to have a look at the analytic of the lignins and the cleavage products, the structure of the used lignin, the reactivity of the different biomass, the possible repolymerization and how this information can be used to get a model, with which the monomeric product mixture can be predicted. Therefore, a reaction network must be built, and screening experiments must be performed. To get a process to produce platform chemicals for every biomass source different lignins must be considered.

3.1.1 Lignin structure - Results

Different lignins were analyzed in respect to their monomeric basic units and bonds, even though the lignin molecule sizes cannot be measured by now in detail.

3.1.1.1 Distribution of the monomeric building blocks

The distribution of the three monomeric building blocks (sinapyl-, coniferyl-, p-cumaryl-alcohol) was analyzed as described in chapter 2.2.1 for the five investigated lignins. The Indulin AT structure contains mostly coniferyl alcohol 97.5 wt.%, with a content of p-cumaryl alcohol around 2.5 wt.% and no detectable sinapyl alcohol units content (Figure 31 and Figure 32).

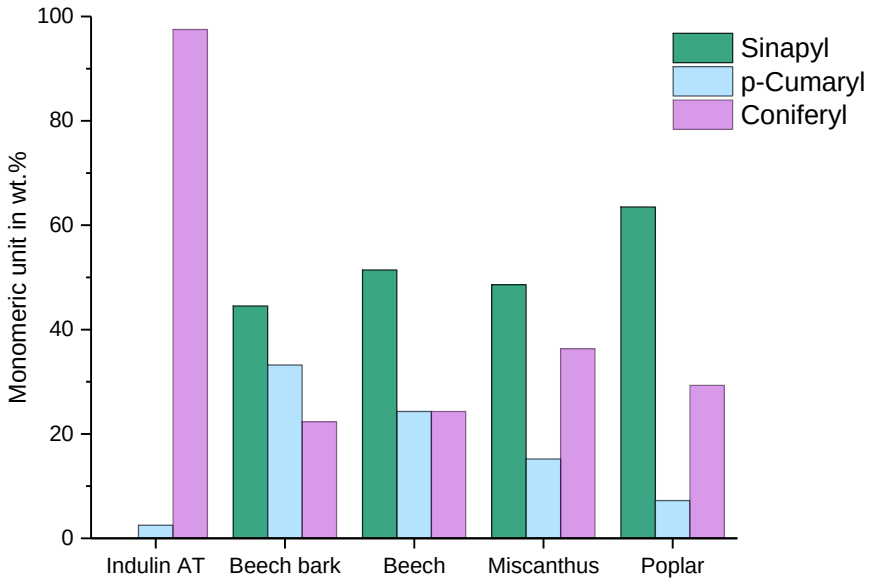

Figure 31: Monomer units in wt.% of Indulin AT, beech bark, Organosolv of beech wood of the FhG CBP, Organosolv of *Miscanthus* of the FhG ICT and Organosolv of poplar wood of the FhG ICT measured by 2D-NMR.[A]

The composition of beech bark and the organosolv beech lignin are comparable (Figure 31). Organosolv *Miscanthus* lignin has a sinapyl alcohol - p-cumaryl alcohol - coniferyl alcohol distribution of 48.6 - 15.2 - 36.3 wt.%, while poplar organosolv lignin shows a distribution of 63.5 - 7.2 - 29.3 wt.% (Figure 31 and Table 20 appendix).

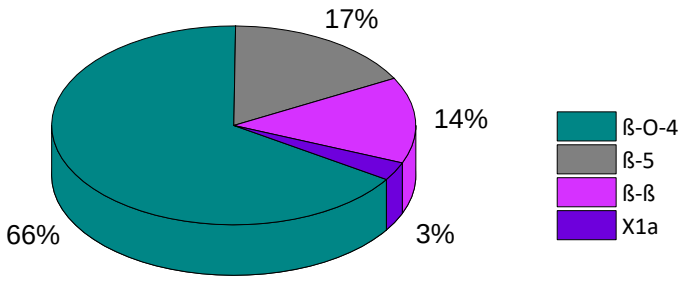

Figure 32: Different bond types of Indulin AT in % measured by 2D-NMR; ß-O-4, ß-5, ß-ß bonds, and X1a cinnamyl alcohol ending group. [A]

Indulin AT mostly contains ß-O-4 bonds (about 66 %), followed by ß-5 bonds (about 17 %), about 14 % of ß-ß-bonds and has about 3 % cinnamyl alcohol end groups (Figure 32).
Beech bark and beech wood lignin contain similar rates of each bond type. Beech bark contains ~77 % of ß-O-4 bonds while the wood lignin contains ~68 %. ß-ß bonds exist in an amount of about 13 % in the bark lignin and 21 % in the wood lignin.

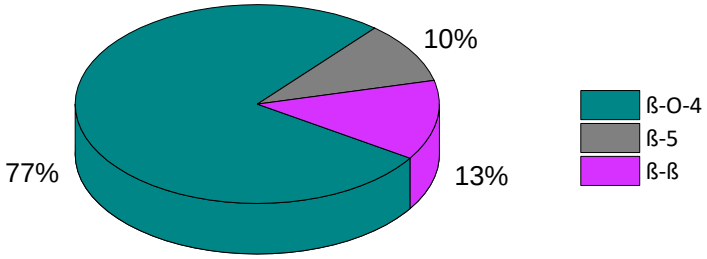

Figure 33: Distribution of bond types of beech bark lignin in % measured by 2D-NMR; ß-O-4, ß-ß and ß-5 bonds. [A]

In the bark lignin are around 10 % ß-5 bonds and in the beech wood lignin around 11 % (Figure 33 and Figure 34).

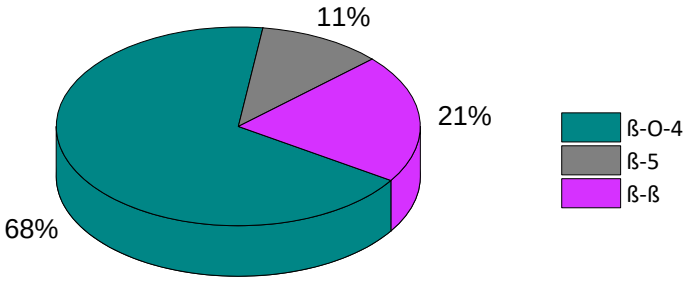

Figure 34: Distribution of bond types of beech wood organosolv lignin in % measured by 2D-NMR; ß-O-4, ß-ß and ß-5 bonds. [A]

Miscanthus Giganteus organosolv lignin shows a distribution of the different bond types of a ~45 % ß-O-4 bonds, ~49 % of ß-5 bonds and ~6 % of ß-ß bonds (Figure 35).

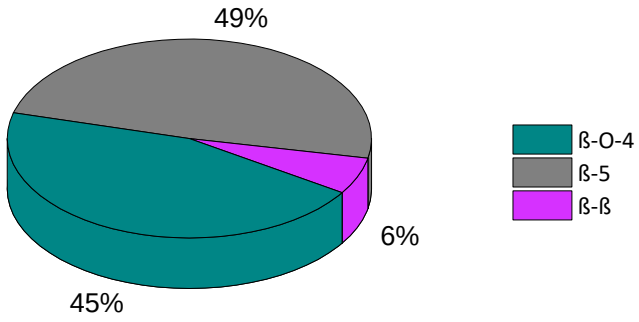

Figure 35: Distribution of bond types of *Miscanthus Giganteus* organosolv lignin in % measured by 2D-NMR; ß-O-4, ß-ß and ß-5 bonds. [A].

Organosolv lignin of poplar wood shows a distribution of the different bond types of a ~69 % ß-O-4 bonds, ~18 % of ß-5 bonds and ~13 % of ß-ß bonds (Figure 36).

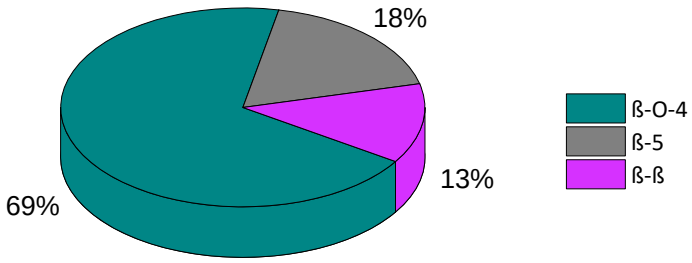

Figure 36: Distribution of bond types of poplar organosolv lignin in % measured by 2D-NMR; ß-O-4, ß-ß and ß-5 bonds. [A]

3.2 Chromatography

For the analysis of the liquefaction products a separation of the product mixture, instead of investigating the whole mixture, would be a logical step to get clearer results. Nevertheless, the separation of the products cannot just be performed by distillation or extraction. Only parts of similar products can be gained via distillation, which also leads to a superposition of the signals in further analytical steps like NMR or chromatography. Also, with thin layer chromatography, a separation of the single molecules is not entirely possible, respectively the molecules are too similar to achieve a clear separation. Different solvents and mixing ratios were used, with non-complete separation could be achieved (Figure 37).

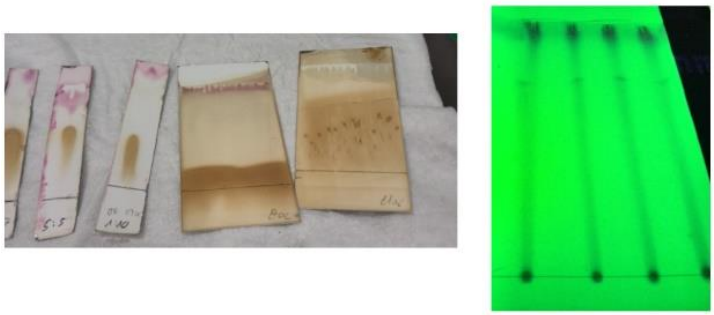

Figure 37: TLC plates with different solvents, mixtures, and ratios of the liquefaction product mixtures.

Instead of the expected single component dots on the thin layer chromatography plate, just lines get visible, which indicate that the separation is not completed.

3.2.1 Size exclusion chromatography

Measurements of the cleavage products were performed via gel permeation chromatography using the newly developed method (see chapter 2.2.3). For the design of experiments in the method trail product mixtures of Indulin AT cleavage reactions were chosen:

- with a reaction time of 30 min and 300 °C reaction temperature,

- with a reaction time of 60 min and 300 °C reaction temperature,
- with a reaction time of 30 min and 400 °C reaction temperature,
- a sample of the synthesized oligomer.

A shift towards smaller molecules with a higher reaction temperature was expected, also with longer reaction time. It was assumed to see different chain length of the synthesized lignin oligomer. That is why these three cleavage product mixtures were chosen for the trial measurements to find a suitable method and setup for the SEC measurements. Figure 38 shows all measurement results of the used RI (refractive index) detector.

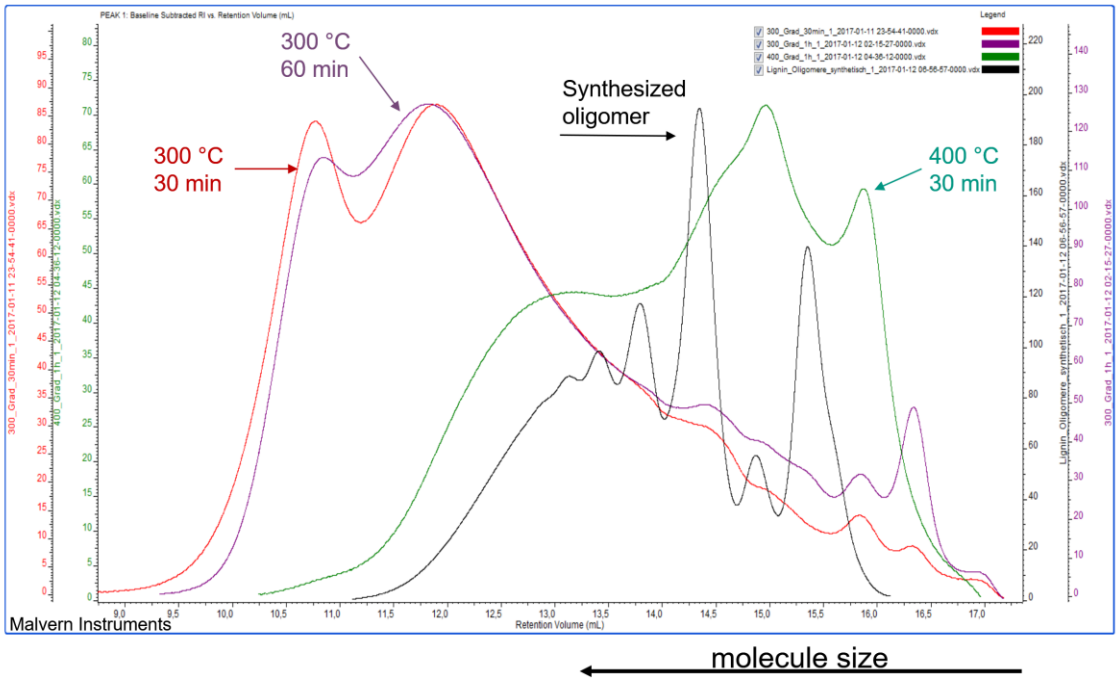

Figure 38: Overlaid RI diagrams of an SEC measurement with DMSO as a solvent. Red is Indulin AT after a reaction at 300 °C and 30 min reaction time; violet is Indulin AT after a reaction at 300 °C and 60 min reaction time, is Indulin AT after a reaction at 400 °C and 60 min reaction time and black is the synthesized oligomer (done by [91]).

Figure 38 shows an SEC chromatogram plotted in a retention volume respectively time, as described above large molecules leave the column first because smaller ones are retained in the pores of the solid phase. The peak area can be integrated and is equivalent to the amount of the single molecule. Wide peaks indicate a wide spectrum of molar masses, for which a separation in individual compounds is not possible with the method applied. With a longer reaction time at 300 °C, the separation of the main peaks is less distinct (see in Figure 38 at ~ 11 ml retention volume). This means that the molecule variety increases. However, the separation of the molecules in this size region is not complete. This is another problem of the SEC with lignin-based samples: the range of molecule sizes is too big, which makes it complicated to cover it all. With 400 °C and 30 min reaction time, the chromatogram shows a shift to the right side, which means that the molecules become smaller than those

obtained at 300 °C. The synthesized lignin oligomer delivers the clearest chromatogram as expected. With higher temperatures and longer reaction time, the product molecules become smaller (shift to a larger retention volume, to the left in Figure 38).
The SEC results reflect the assumptions of a higher degradation grade with higher reaction temperatures and longer reaction times. The done measurements confirmed the expected differences between the chosen samples and have shown a good matching with the synthesized oligomeric chains.

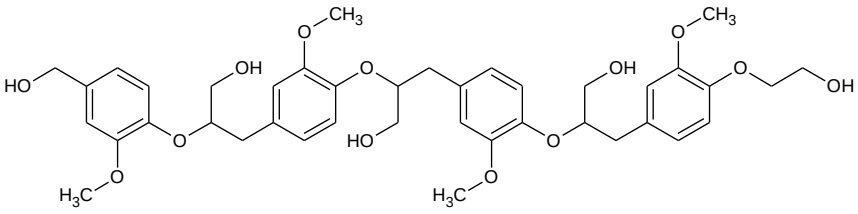

Figure 39: Synthesized lignin oligomer with the smallest chain length of four rings [61] which should be the last peak of Figure 20.

The synthesized lignin oligomers (Figure 39, method described in chapter 2.1.5) deliver the clearest chromatogram (also shown in Figure 38 (black peaks)). In Figure 40 the detailed measurement of the synthesized oligomer can be seen.

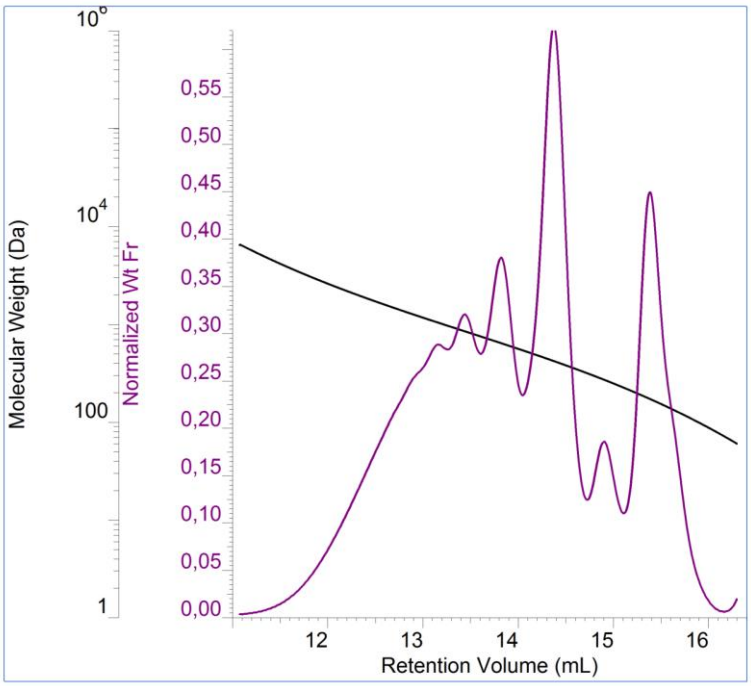

Figure 40: SEC chromatogram (purple) of the synthesized lignin oligomers with the results calibration curve (black) (done by [91]).

Figure 40 shows the chromatogram of the synthesized oligomer. It shows chain lengths of four (15.5 ml retention time) up to eight monomeric units (13.3 ml retention time), and the

results of the synthesized oligomer could get included in the calibration. The different chain lengths from four aromatic rings up to eight rings can be separated and measured. With the synthesized oligomers, the pullulan calibration can be extended. Moreover, more reliable results could be gained. Still, it is not possible to get all changes in long side chains, because the pullulan and the synthesized lignin oligomer show no long side chains. If the chemical folding is comparable to straight chains and consequently the hydrostatic volume is similar, it is not possible to separate these molecules and getting absolute results out of SEC measurements.
The differentiation between different chain lengths of the synthesized oligomer seems to be possible, but to compare measurements of different groups and discuss the different results it is necessary to establish a common system of lignin oligomeric molecules measurements, with a typical column, solvent, and calibration [76][77][78].

3.3 Loop reactor

The residence time is 40 min +/- 8 min. (Table 4). The volume flow rate of the circulation pump the reactor temperature and the pressure have no influence on the residence time. It is expected that under hydrothermal conditions the turbulence and the back-mixing inside the reactor are extremely high because water is near to its critical point [92]. There is no plug flow inside the reactor tube given through the small feed pump capacity, and also no change in the residence times (compare Table 4).

Table 4: Mean residence times of the loop reactor under different parameters; different back-mixing ratios R=0, 1, 2.2, 3.5, different temperatures 250, 300 and 350 °C, and different pressures 50, 95, 120 and 205 bar.

R	250 °C_50 bar	300 °C_95/120 bar	350 °C_205 bar
0	43	40	-
1	32	-	-
2.2	42	40	-
3.5	43	44	45

A flow simulation with Star CCM+ (Figure 41 and Figure 42) of the reactor, with water at 20 °C and the maximum flow rate, also showed, that the flow inside of the tube is slow even with the maximum capacity of the feed pump. A plug flow characteristic cannot be achieved with the existing set-up. Even with the maximum flow rate, areas of stagnating flow exist in the reactor.

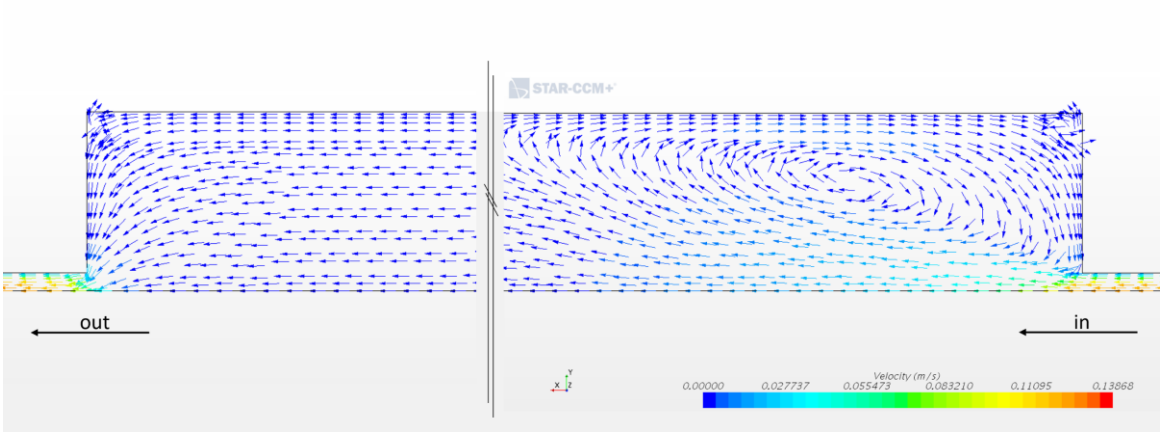

Figure 41: Flow field simulation with Star CCM+ of the flow into and out of the reactor at 20 °C and the maximum feed pump capacity. Dark blue marks the slowest velocity, red the fastest [93].

Figure 41 shows slow velocities in the reactor entrance and outlet, which allows the formation and settling of solid residues. Eddies also increase residence time (locally) and allow the increased formation of solids by repolymerization.
Another depiction illustrates the streamlines in the middle of the reactor. These show the flow velocity with a laminar character. Also, at the reactor wall dominates a slow velocity, just in the middle fast flows are happening (Figure 42), this promotes a settling of the solid parts as well as the dead zones of the reactors entrance and outlet.

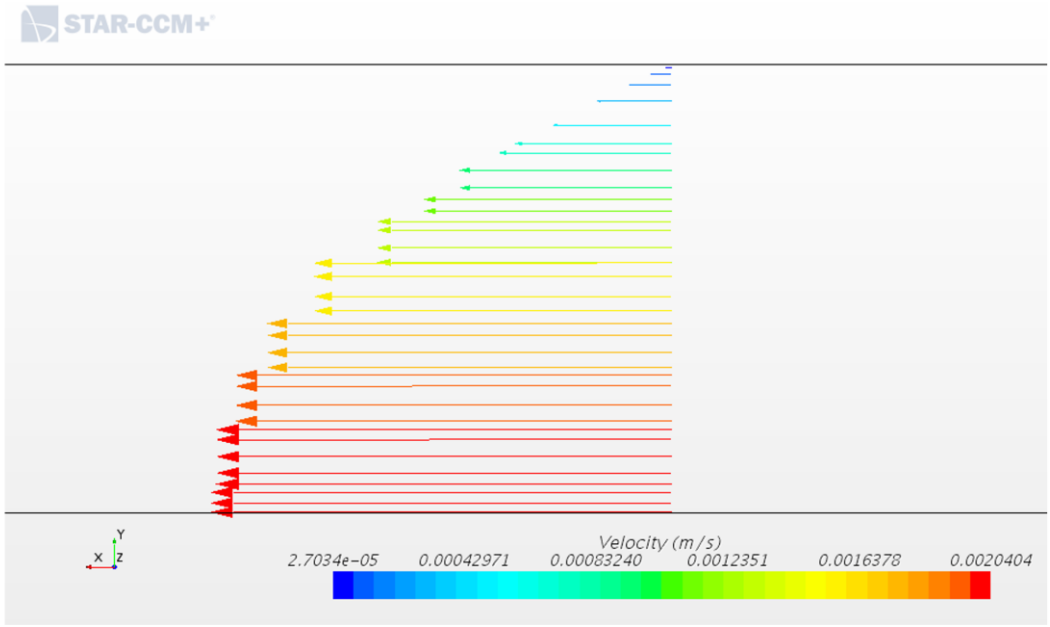

Figure 42: Simple simulation of the flow in the upper half of the reactor tube at 20 °C and the maximum feed pump capacity. Dark blue marks the slowest velocity, red the fastest [93].

The Reynolds number calculated with water at 20 °C and atmospheric pressure also indicates a non-turbulent flow.

$$Re = \frac{v_m \cdot d}{\nu} = 8.76 \tag{3.1}$$

Re	Reynolds number
v_m	velocity
ν	kinematic viscosity
d	characteristic linear dimension: inner diameter

The solid residue was analyzed by scanning electron microscope (SEM) and thermogravimetric analysis (TGA).

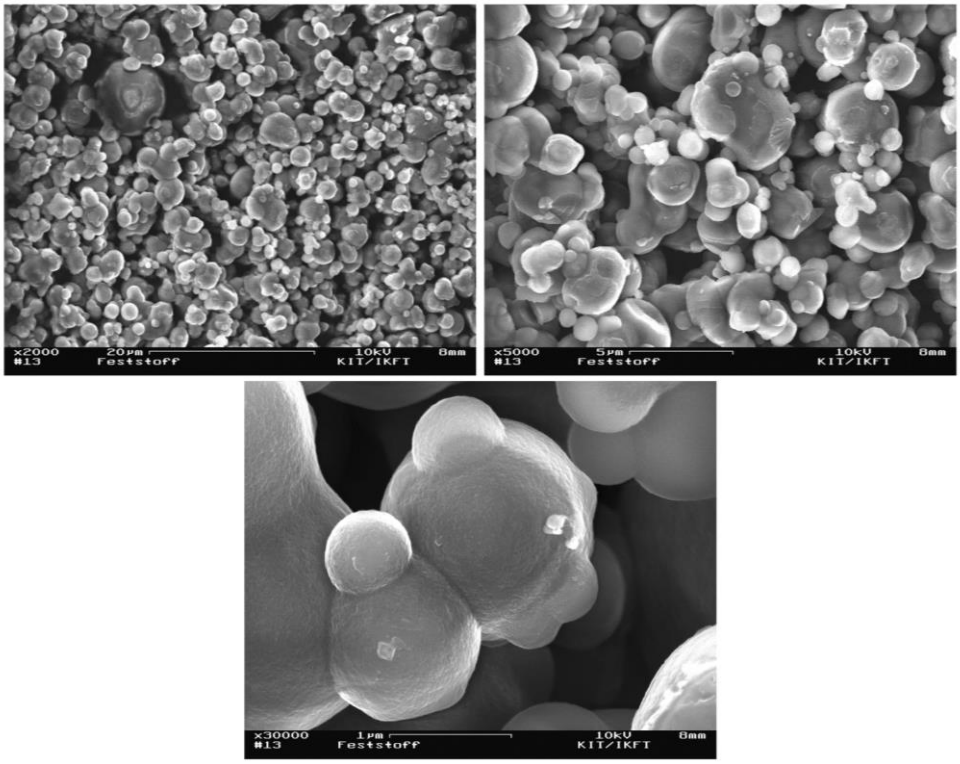

Figure 43: SEM pictures (20 µm, 5 µm, and 1 µm) of the solid residue inside of the reactor after the reaction (300 °C, 1 wt.% KOH, 6 wt.% Indulin AT and a residence time of around 40 min.).

The gained SEM pictures (Figure 43) indicates hydrothermal carbonization without a repolymerization [94]. Which indicates long residence times without liquefaction reactions.

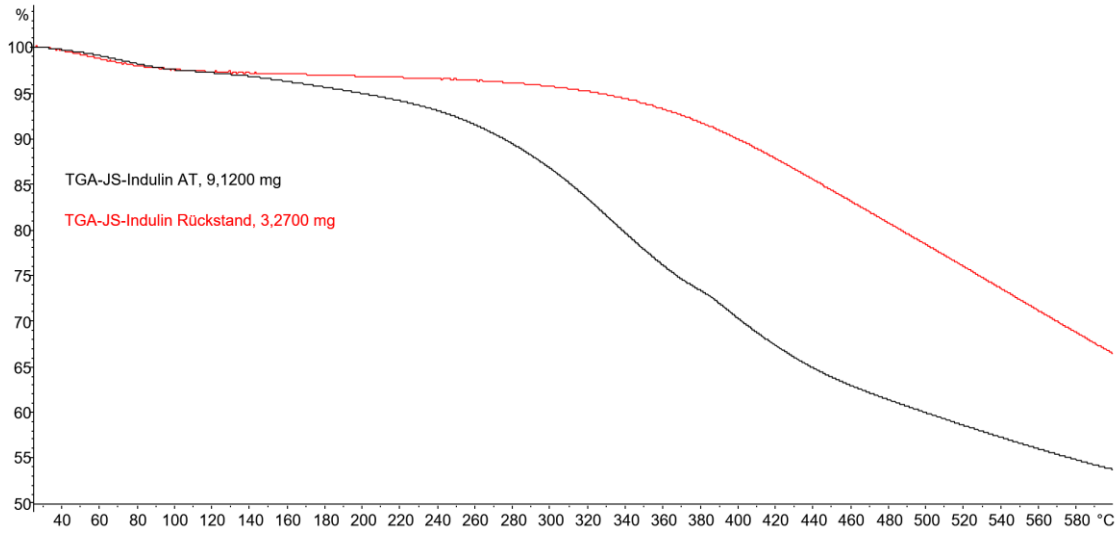

Figure 44: TGA results of the used Indulin AT (black) and the solid residue (red).

The results of the TGA measurements (Figure 44l) show that the Indulin AT gets degraded at around 130 °C and the solid residue at around 280 °C.

3.4 Comparison of reactor types

The influence of the internal back-mixing was tested by using different reactor types; a continuous tank reactor, a continuous tube reactor, and batch reactors. The results for all three reactor types with a starting concentration of 6 wt.% Indulin AT in a 1 wt.% KOH solution with a reaction temperature of 350 °C are shown in Figure 45.

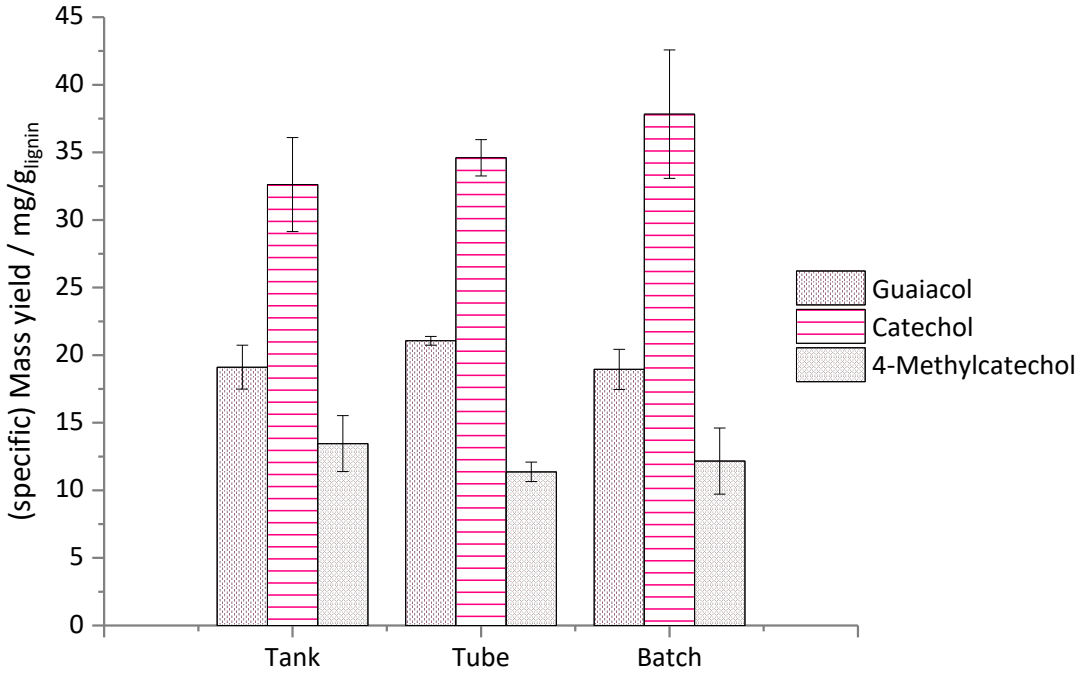

Figure 45: Comparison of the guaiacol, catechol and 4-methylcatechol mass yields in mg per used g lignin in three different reactors; tank, tube, and micro batch autoclaves with 8 min residence time, 350 °C, 6 wt.% Indulin AT in 1 wt.% KOH.

Between the three reactor types are no considerable differences in the monomeric compounds concentrations per gram used lignin for a residence time of 8 min. For longer residence times the results showed that the internal mixing behavior of the tank reactor is not as good as tested with tracer experiments, likewise the tracer experiments with the loop reactor (see chapter 2.3.1).

At the walls of the tank reactor, sublimation of the formed solid residues is occurring, which influence the residence times. With these agglomerations, residence times of only 8 min are feasible. Figure 46 shows the comparison between the produced monomeric amounts of the tube reactor and the batch reactors for 15 and 30 min.

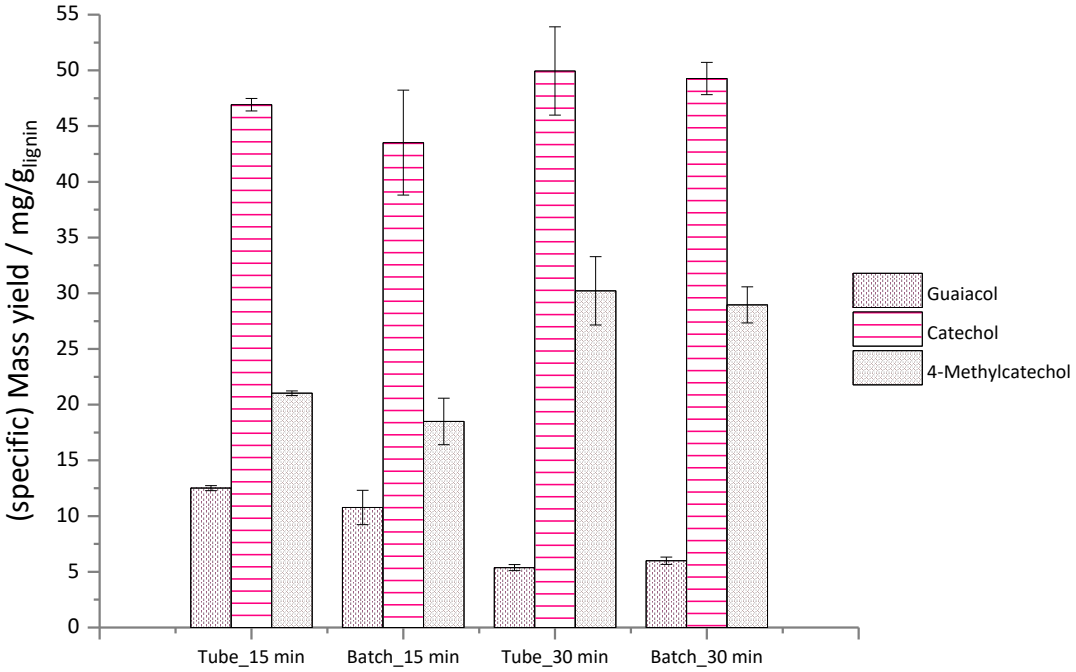

Figure 46: Comparison of the guaiacol, catechol and 4-methylcatechol mass yields in mg per used g lignin in two different reactors; tube and micro batch autoclaves with 15 and 30 min residence time, 350 °C, 6 wt.% Indulin AT in 1 wt.% KOH.

Hence, there is no influence of the reactor type for the hydrothermal liquefaction regarding this work. All continuous reactor types show clogging after a certain time on stream. More than 30 min could not be realized which means that the reactor did not reach steady state operation. In addition to these experiments, the reactor types were compared when methanol was added as a hydrogen carrier (Figure 47), to check if this has an influence regarding the reactor type besides the influence on the reactions happening.

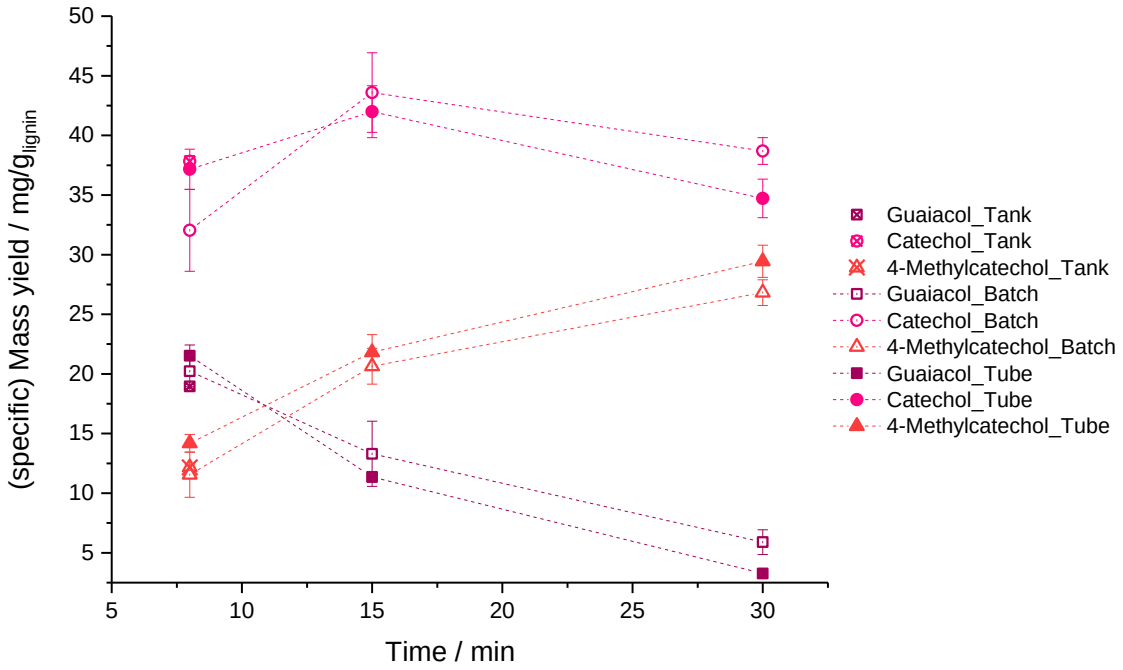

Figure 47: Comparison of the guaiacol, catechol and 4-methylcatechol mass yield in mg per used g lignin in different reactors; tank (crossed symbols), tube (filled symbols) and micro batch autoclaves (empty symbols) with 8, 15 and 30 min residence time and 0.5 wt.% MeOH, 350 °C, 6 wt.% Indulin AT in 1 wt.% KOH.

Even under the addition of methanol as a potential gas phase inducer, the different reactor types showed no considerable variations in the amounts of obtained monomeric compounds. The influence of a hydrogen carrier regarding the reaction network is shown in the following chapter.

3.5 Addition of a hydrogen carrier

To provide more hydrogen, hydrogen carriers were added to the starting solution and to reduce the reactions towards solid products. Therefore, methanol (MeOH) and glucose (Glu) were chosen. A concentration of 0.5 wt.% (referred to the used mass of lignin) of each carrier was set to study the influence of it, without changing the main reactions to much. Because of the similarity of the different reactor types, batch micro autoclaves were used for these screening experiments. The tank reactor was utilized for 8 min residence time, and these experiments gave the same results than those from the micro batch autoclaves. Just like before, longer residence times could not be performed with the tank reactor.

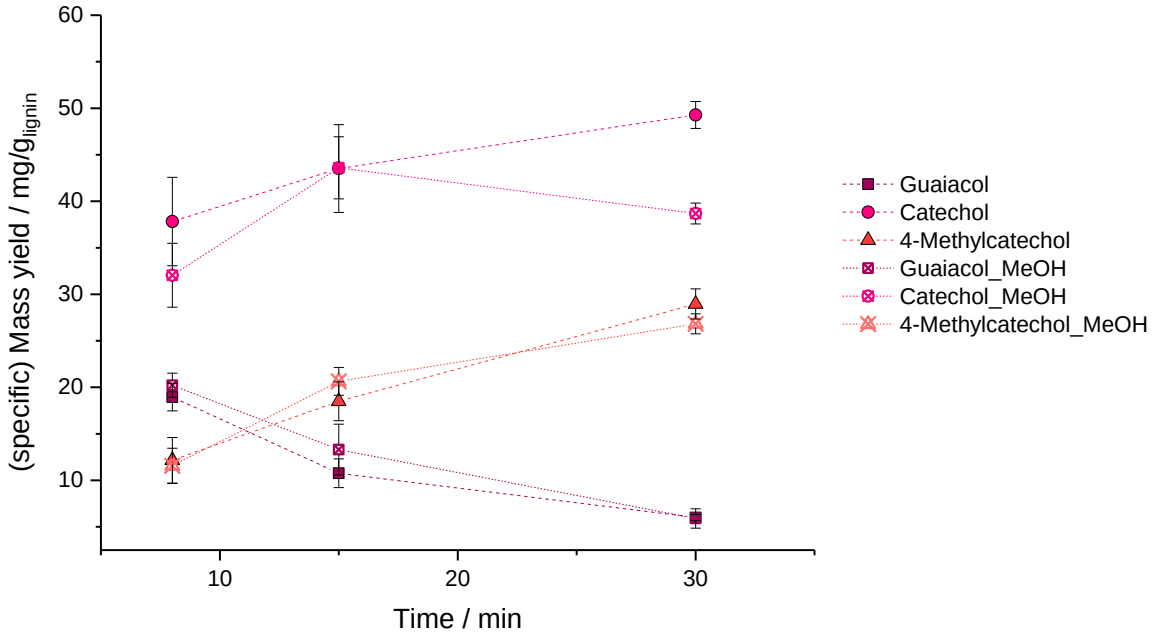

Figure 48: Comparison of the guaiacol, catechol and 4-methylcatechol mass yields in mg per used g lignin in micro batch autoclaves with 8, 15 and 30 min residence time, 350 °C, 6 wt.% Indulin AT in 1 wt.% KOH and 0.5 wt.% MeOH.

Comparing the catechol, guaiacol and 4-methylcatechol concentrations per applied gram Indulin AT showed no increase by adding methanol as hydrogen carrier (Figure 48). Especially for guaiacol and 4-methylcatechol no enhancement could be observed. For catechol, there is no clear trend to observe. The catechol yields decrease with a longer residence time by about 18 %.

With glucose as a hydrogen carrier, the yield of the monomeric compounds could be increased by about 12 % points (see Figure 49).

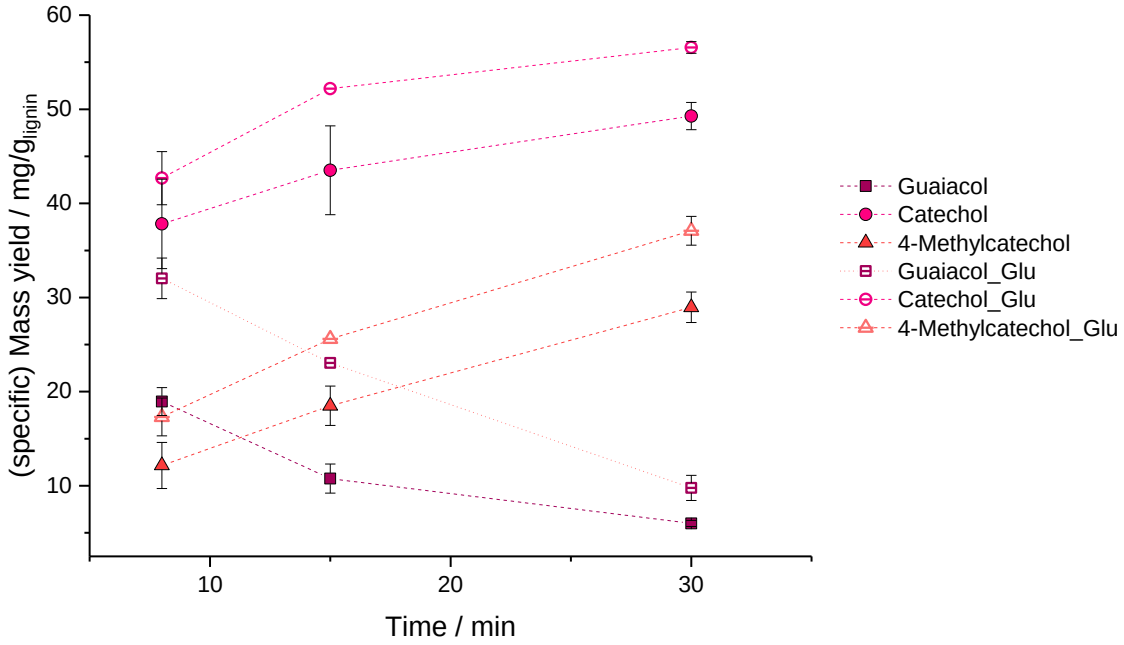

Figure 49: Comparison of the guaiacol, catechol and 4-methylcatechol mass yields in mg per g used lignin in micro batch autoclaves with 8, 15 and 30 min residence time, 350 °C, 6 wt.% Indulin AT in 1 wt.% KOH and 0.5 wt.% glucose.

Glucose increased the yields of catechol, guaiacol, and 4-methylcatechol significantly, while methanol shows almost no influence on the obtained yields.
The aim of adding two hydrogen carriers, like methanol, and glucose, was to investigate whereby the influence on the yields of monomeric compounds and on preventing/delaying clogging. The amount of the solid residue after the reactions was always 50 wt.% of the applied Indulin AT mass in the beginning. Neither methanol nor glucose showed a reduction of the solid residues and clogging cloud not be prevented.

3.6 Influence of Back-mixing

For getting an idea about the influence of the back-mixing external back-mixing experiments were performed. Experiments with pre-cleaved lignin product solutions were done (see chapter 2.3.1 Figure 30). The correction of the measured results is described in chapter 2.4.5 & 2.4.4.
The results are hard to describe because most measured products are consecution products of others. That is why only results of 8 min residence time are shown. There the consecution reactions are not as much progressed as in longer reaction times. In Figure 50 the differential amount of guaiacol, catechol, and 4-methylcatechol in mg per used g lignin with 8 min residence time, 350 °C, 6 wt.% Indulin AT in 1 wt.% KOH and R=10 are plotted.

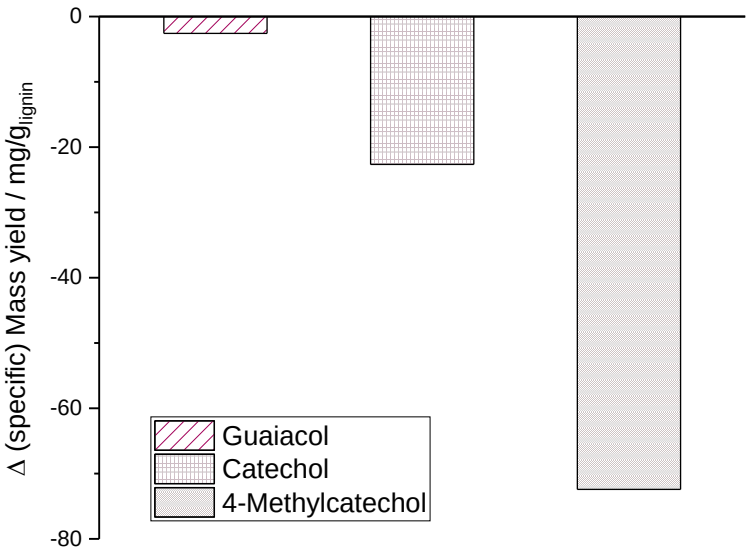

Figure 50: Difference in specific mass yield of guaiacol, catechol and 4-methylcatechol mass yields in mg per used g lignin in micro batch autoclaves with 8 min residence time, 350 °C, 6 wt.% Indulin AT in 1 wt.% KOH and R=10.

The negative differential amounts show that an external back-mixing of only the liquid phase has no positive influence on the obtained monomeric bifunctional component yields. The back-mixed amounts are higher than the gained amounts out of the fresh used Indulin AT. While a higher back-mixing ratio was supposed to increase the positive effect, the opposite was observed, (compare Table 5).

Table 5: Differential specific mass yields of guaiacol, catechol, and 4-methylcatechol in mg per used g lignin in micro batch autoclaves with 8 min residence time, 350 °C, 1 wt.% KOH and different back-mixing conditions, compared to different back mixing volumes and additional hydrogen carrier. Calculated with equation (2.4) in chapter 2.4.5.

mg/g$_{lignin}$	Guaiacol	Catechol	4-Methylcatechol
6%	15.2	29.1	8.9
12 %	11.9	20.8	6.7
6/6 % & R=1	18.8	13.1	-0.9
6/6 % & R=10	-2.6	-22.6	-72.4
6/12 % & R=1	17.3	15.5	2.0
6/12 % & 0.5 % MeOH & R=1	13.9	20.3	5.3
6 /12 % & R=10	29.5	-12.8	-20.1
6/12 % & 0.5 % MeOH & R=10	22.7	-5.6	-14.4

The measured solid amount of each experiment is also not reduced through the back-mixing of liquid products. Clogging was still a problem in all experiments. The measured amounts of gaseous products were not increased, too.

3.7 Lignin screening experiments

To understand the challenges (reaction pathways, analytic, and so on) of lignin better, it is essential to have a look at different lignins and lignin sources, so to see if the behavior of lignin under varying conditions are the same, and whether with each lignin similar difficulties are coming [95]. Therefore, different lignins were used, e.g., a Kraft lignin, organosolv lignins, and bark directly. The influences of different reaction conditions must be investigated to understand the reactions. With different reaction temperatures, reaction times and concentrations of the homogeneous catalyst potassium hydroxide (KOH), the level of gasification and further reactions of lignin are changing and vice versa the concentrations of the bifunctional components like catechol are shifting. The screening experiments were performed in batch microreactors (10 ml – 25 ml) (see chapter 2.4).

3.7.1 KOH influence

Lignin is hardly soluble in water and other solvents with a neutral pH. However, the solubility is better in basic solvents, because of the salt formation. . The cleavage reactions happen faster in a basic environment, therefore KOH is used [96]. KOH shows good performance as a homogenous catalyst, better than NaOH or $Ca(OH)_2$, especially in gaining monomeric compounds like catechol [97][98]. Table 6 shows the influence of the KOH concentration of the yields of catechol and the gaseous compounds H2 and methane

Table 6: Catechol, hydrogen and methane amounts of the gained gaseous phase over different potassium hydroxide concentrations of 1, 3, 5, 6 and 10 wt.% at the same reaction temperature and time of Indulin AT at 300 °C, the resulting pressure and 30 min resident time.

KOH wt.%	catechol g/g_{bark}	H_2 / methane vol.%
1 %	1.42	8.8 / 1.6
3 %	0.89	13.3 / 1.4
5 %	0.76	26.8 / 1.9
6 %	0.28	-
10 %	0.15	48.7 / 3.0

With a higher KOH concentration, the catechol yield decreases while the methane and hydrogen amounts in the gaseous phase increase (Table 6). At 6 wt.% of KOH, no gas measurements were possible due to technical problems. For further experiments, a KOH

concentration of 1 wt.% was chosen to get a higher yield of phenolic monomers and to prevent the enlargement of product gases.

3.7.2 Different lignins

Plants built lignin in different compositions in their wood. This changes the monomeric unit and bond distributions of each lignin. Depending on the origin of Lignin the ratio of coniferyl alcohol, sinapyl alcohol, and p-cumaryl alcohol varies [9], and also the products vary. Through analyzing these products, it is possible to infer the monomer units of the used lignin (Table 7). Syringol is a degradation product of sinapyl alcohol and guaiacol of coniferyl alcohol for example [9,26,29,59].

Table 7: Different products of the hydrothermal liquefaction; Syringol and guaiacol at 300 °C, a reaction time of 120 min and a 1 wt.% KOH solution.

300 °C, 120 min	Ind.AT	Bark	Org.solv	*Miscanthus*
Syringol mg/g $_{lignin}$	0.03	3.27	3.88	1.15
Guaiacol mg/g $_{lignin}$	11.2	5.80	8.99	7.73

To gain concentration profiles of the cleavage reactions and products of the different lignins, screening experiments with different temperatures (250, 300, 350, 400 and 450 °C) and different reaction times (0.25-24 h) were performed.

3.7.3 Influence of the reactor material

The phenol yield was found to stagnate at a certain level in other studies [19,21] and also for the investigated Kraft lignin the phenol amount was found to be limited (Figure 51) [19,21].

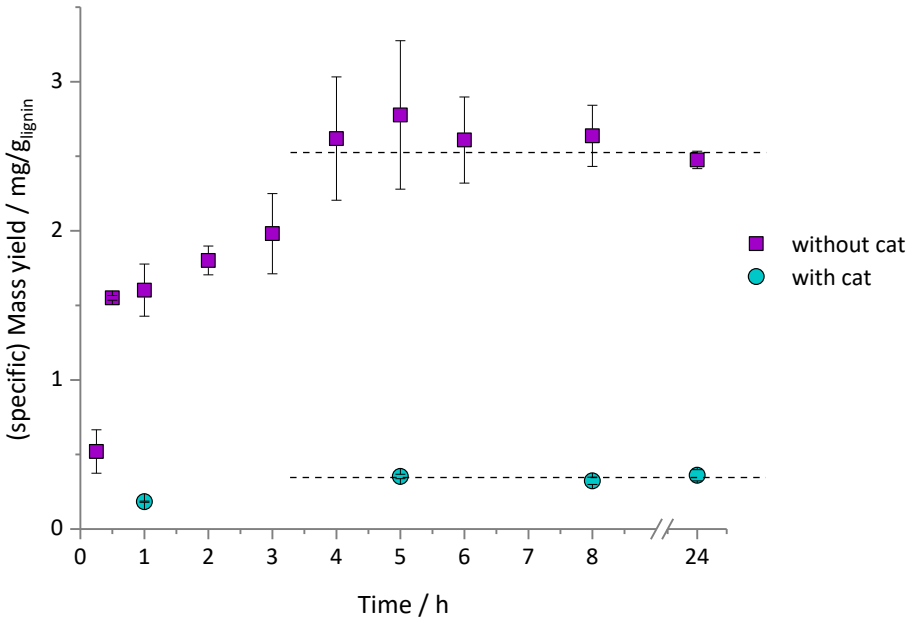

Figure 51: Phenol yields in milligram per gram used lignin at 300 °C, a KOH concentration of 1 wt.% was applied for different reaction times (0.25-24 h). The dark purple squares show the yield obtained without a Ni-catalyst while the light blue dots were performed using Nickel as a catalyst.

The material of construction of the reactor comprises Ni in large quantities. Figure 51 shows that the catalytical influence of Nickel reduces the Phenol yield compared to experiments without this influence. At the reaction temperature of 300 °C, and a KOH concentration of 1 wt.% of the phenol yield stagnates around 0.3 wt.% after a reaction time of approx. 4 h. With the influence of Nickel as a catalyst, the yields are even lower. This observation can be explained by the catalytic activity of Nickel, which amplifies the gasification reaction of biomass and is therefore often used as a catalyst for these observed gasification reactions [39]. Nevertheless, with the gasification of the biomass as a competing reaction, the amount of the targeted bifunctional products decreases rapidly (compare Figure 52 chapter 3.7.4 or Figure 58 chapter 4.6).

3.7.4 Influence of reaction temperature and residence time

For covering the whole area of the hydrothermal liquefaction, see chapter 1.3 and Figure 4, the following temperatures were investigated: 250, 300, 350, 400 and 450 °C. To get concentration profiles and a better understanding of the influence of the experimental parameters, different residence times (0.25-24 h) were performed for every used lignin.

3.7.4.1 Indulin AT

The catechol concentration profiles of the used Kraft lignin Indulin AT over the different reaction temperatures and times are shown in Figure 52. The standard deviation over at least four experiments was calculated and is shown in all diagrams.

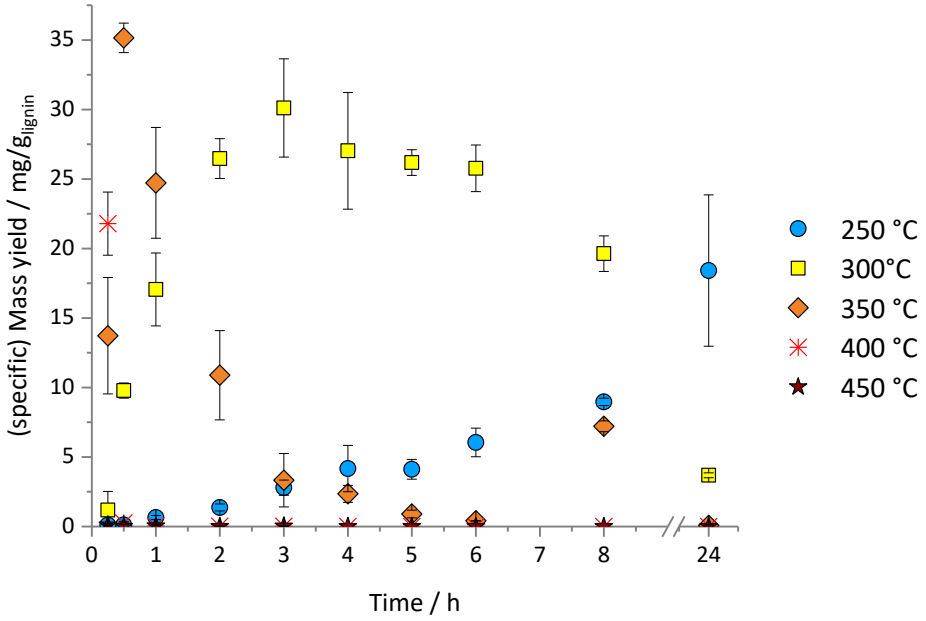

Figure 52: Mass yield of the obtained product catechol in mg per g used lignin (Indulin AT) over the different reaction times (0.25-24 h) and temperatures (250-450 °C) and 1 wt.% KOH. (blue circle - 250 °C, yellow square - 300 °C, orange diamond - 350 °C, red cross – 400 °C, dark red star – 450 °C)

At 400 and 450 °C, the catechol concentrations per gram lignin are lower than 1 mg/g. At a reaction time of 15 min at 400 °C, the amount is about 22 mg/g$_{lignin}$. 250 °C also delivers only small yields below 10 mg/g$_{lignin}$, only with longer residence times the yields increase.
The highest yield of about 35 mg/g$_{lignin}$ catechol is gained at 350 °C and 30 min reaction time. With longer reaction times, the yields decrease directly. With a residence time of 8 h, the yield increases again and decrease with longer residence times than 8 h again.
At 300 °C, the concentration profile shows the forming, the maximum yield and the consecutive reaction in which catechol react forwards.

3.7.4.2 Beech bark

Beech bark was used directly as it was delivered from the pulp and paper industry, just milled and dried for the screening experiments. Figure 53 shows the concentration profiles of beech wood bark, which is used, in the hydrothermal liquefaction with 1 wt.% KOH.

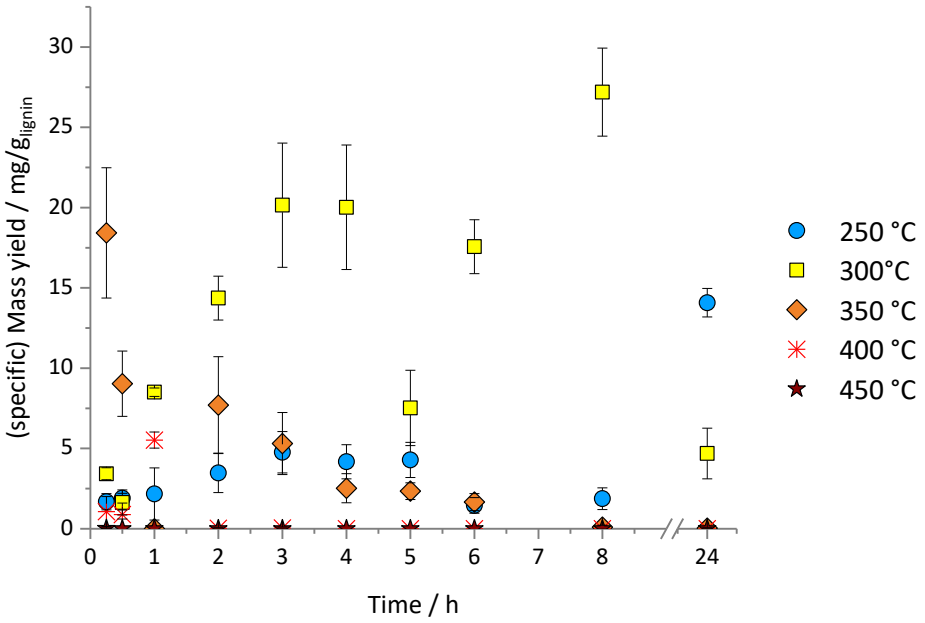

Figure 53: Mass yield of the obtained product catechol in mg per g lignin in the used beech bark over the different reaction times (0.25-24 h) and temperatures (250-450 °C) and 1 wt.% KOH. (blue circle - 250 °C, yellow square - 300 °C, orange diamond - 350 °C, red cross – 400 °C, dark red star – 450 °C)

At 400 and 450 °C, the produced catechol concentrations per gram used lignin are lower than 1 mg/g$_{lignin}$. Just at a reaction time of 60 min at 400 °C, the amount is about 5 mg/g$_{lignin}$. 250 °C also deliver only small yields below 5 mg/g$_{lignin}$. The highest yield at 250 °C is with the longest reaction time of 24 h of about 15 mg/g$_{lignin}$. The highest yield of about 20 mg/g$_{lignin}$ catechol is obtained at 300 °C and 3 h reaction time. At 300 °C, the concentration profile shows the forming, the maximum yield and the consecutive reaction in which catechol reacts forwards. With a reaction time of 8 h, another maximum of about 27 mg/g$_{lignin}$ was reached. At 350 °C and 30 min, the maximum yield of this temperature is reached at around 18 mg/g$_{lignin}$. With longer reaction times, the yields decrease directly.

3.7.4.3 Organosolv lignins

Based on the experiences from the previous results, it was determined that a reaction temperature over 350 °C lead to higher gasification of the used biomass and under 300 °C long reaction times (>5 h) are needed to cleave the lignin into monomeric units. This emerged the two temperatures of 300 and 350 °C as relevant temperatures for the following

screening experiments. Also, the amount of organosolv lignins were limited, which made it necessary to choose only relevant parameters. To verify the relevant temperatures 250 °C experiments were performed for beech wood lignin. However, 250 °C is also not suitable for the hydrothermal liquefaction of lignin gained over the organosolv process. In Figure 54 the concentration profiles of beech wood organosolv lignin are shown.

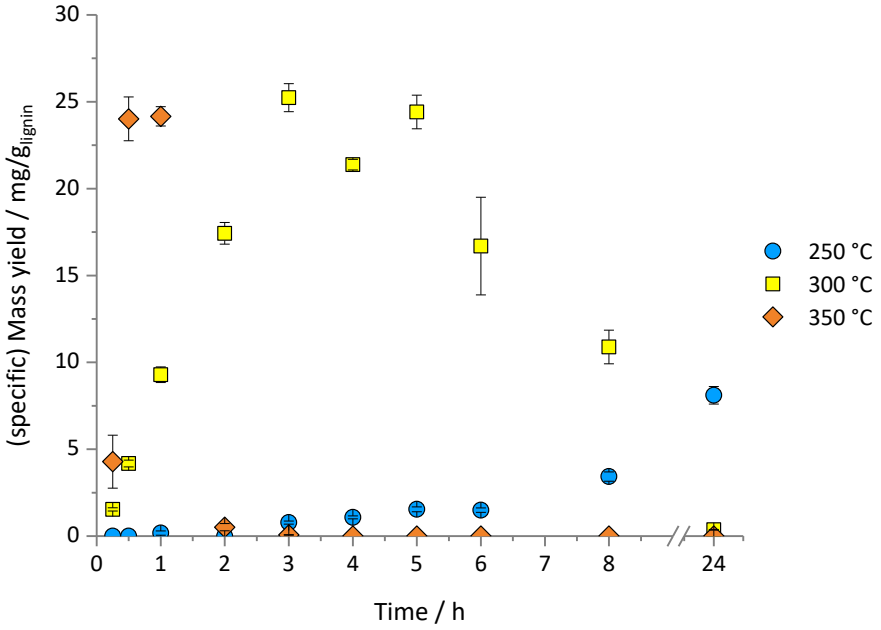

Figure 54: Mass yield of the obtained product catechol in mg per g used lignin (beech wood organosolv) over the different reaction times (0.25-24 h) and temperatures (250-450 °C) and 1 wt.% KOH. (blue circle - 250 °C, yellow square - 300 °C, orange diamond - 350 °C)

250 °C also deliver small yields below 10 mg/g$_{lignin}$. The highest yield at 250 °C could be achieved with the longest reaction time of 24 h. The highest yield of about 25 mg/g$_{lignin}$ catechol is obtained at 300 °C and 3 h reaction time. At 300 °C, the concentration profile shows the forming, the maximum yield and the consecutive reaction in which catechol react forwards. At 350 °C and 30 min and 1 h, the maximum yields of this temperature are reached at around 22 mg/g$_{lignin}$. With longer reaction times, the yields decrease directly. These results led to the assumption that only 300 and 350 °C are suitable temperatures for the investigated process of this work and the other two organosolv lignin screening experiments were just performed for the two temperatures. *Miscanthus Giganteus* concentration profiles are shown in Figure 55.

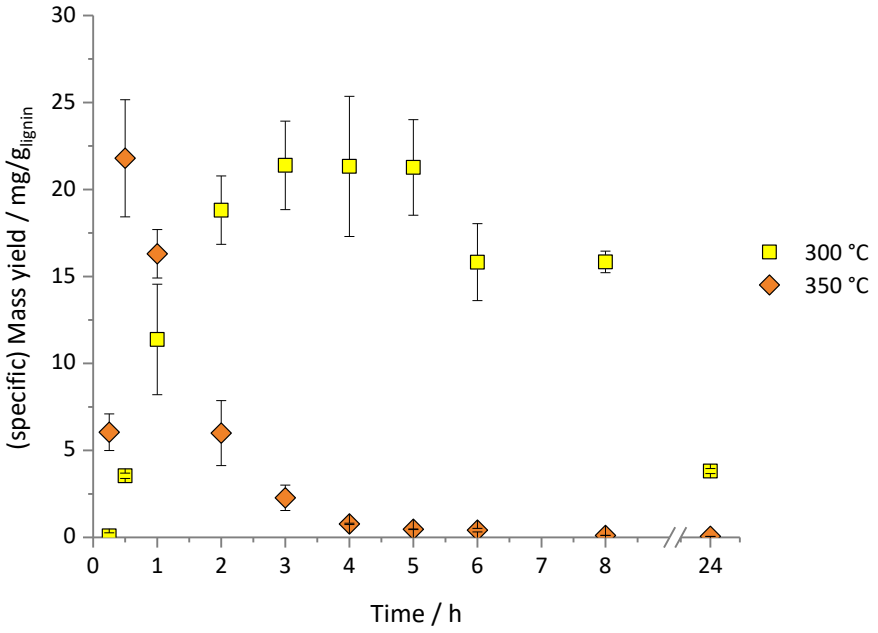

Figure 55: Mass yield of the obtained product catechol in mg per g used lignin (*Miscanthus giganteus* organosolv lignin) over the different reaction times (0.25-24 h) and temperatures (250-450 °C) and 1 wt.% KOH. (yellow square - 300 °C, orange diamond - 350 °C)

The highest yield of 22 mg g_{lignin} catechol is gained at 350 °C and 30 min reaction time. With longer reaction times, the yields decrease drastically. At 300 °C, the concentration profile shows the forming, the maximum yield of about 22 mg/g_{lignin} at 3 h reaction time and the consecutive reaction in which catechol reacts forwards.
Figure 56 shows the concentration profiles of organosolv poplar wood lignin.

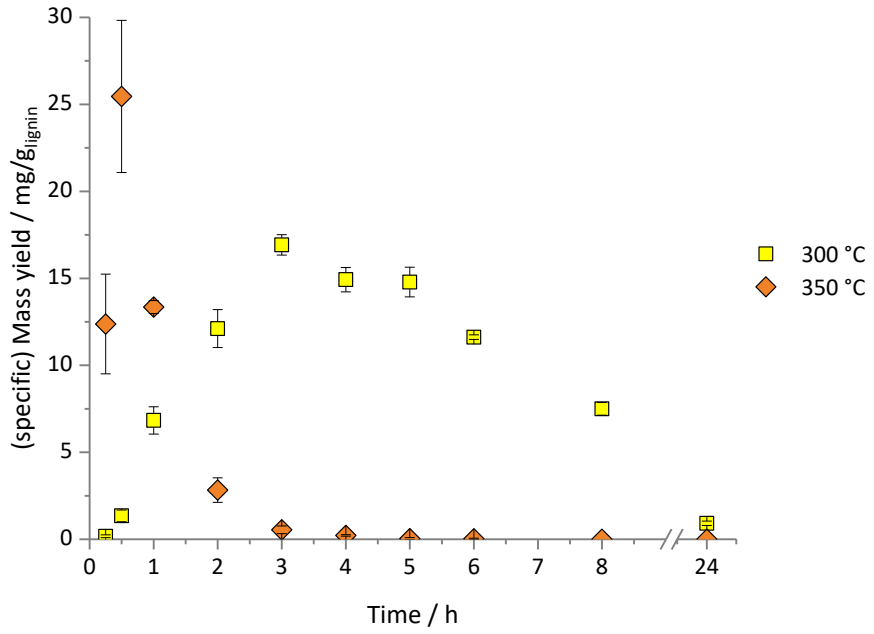

Figure 56: Mass yield of the obtained product catechol in mg per g used lignin (poplar organosolv lignin) over the different reaction times (0.25-24 h) and temperatures (250-450 °C) and 1 wt.% KOH. (yellow square - 300 °C, orange diamond - 350 °C)

The highest yield of about 25 mg/g$_{lignin}$ catechol is gained at 350 °C and 30 min reaction time. With longer reaction times, the yields decrease directly. At 300 °C, the concentration profile shows the forming, the maximum yield of about 17 mg/g$_{lignin}$ at 3 h reaction time and the consecutive reaction in which catechol reacts forwards.

4 Discussion

Reaction engineering of hydrothermal lignin depolymerization needs the consideration of several parameters to be studied, like the influence of temperature (and correspondingly, pressure), residence time or reactor types. Moreover, therefore, the influence of internal and external back-mixing and also, the influence of a hydrogen carrier was investigated. The results of these experiments are shown in previous chapters and discussed in the following ones.

4.1 Lignin structures – Discussion

Five different lignins were applied in these studies: untreated bark, a Kraft lignin and three different organosolv lignins. To get a better knowledge about the used lignins, especially of their molecular structure, 2D-NMR was used to get comparable results. It must be considered that isolation processes influence the lignin structure, e.g., the Kraft-process uses harsh conditions and therefore has an influence on the lignin structure. For example, α-aryl or ß-aryl ether bonds can get cleaved, which increases the phenolic hydroxyl, C-C and C-H side groups [99]. While the organosolv process in comparison is known as a mild process for lignin isolation, in literature it is reported, that even in the same biomass different compositions could have been observed as the results are changing with the applied analytical technique [100].

Despite the harsh isolation conditions of the Kraft lignin, it was shown by HSQC 2D NMR measurements that the reference lignin Indulin AT represents a very native lignin structure. Hence, it is not significantly influenced by the Kraft process [101]. It is assumed that Indulin AT has shorter molecules and chains than organosolv lignin due to the Kraft process.

Based on the structure of the applied lignin type, the cleavage is presumed to deliver mostly guaiacol. Softwood like pine mostly contains guaiacyl rich lignin [29]. Guaiacyl rich (G-unit) lignin means that the main monomeric unit in the lignin is coniferyl alcohol, syringyl rich wood sinapyl alcohol (S-unit) and p-hydroxyphenyl (H-units) p-coumaryl alcohol as a monomeric unit [29]. In contrast, hardwood contains more sinapyl alcohol monomeric units than softwood [29]. Fengel and Wegener [102] wrote an overview of different woods and showed that pine wood lignin, for example, has a G-S-H-unit distribution of 86 % G-units, 2 % S-units and 13 % H-Units. The results show that the pine wood lignin out of the Kraft process of WestRocks is mostly guaiacyl based lignin.

As the investigated bark and one of the organosolv lignins is based on beech wood, a hardwood, it was expected that they are comparable in their structure/composition. Analysis via 2D-NMR proofed this assumption. Beechwood and bark contain guaiacyl and syringyl rich lignin. However, they also show that the variability of the composition in hardwood is much greater than in softwoods (e.g., the syringyl-unit ratio between 20-60 %). They show, like the gained results, that bark softwood typically has a higher G-unit amount, and hardwood bark a higher G- and S-unit amount than the wood of the tree. The difference in the bonding distribution underlies the fact, that bark has a different role in the plant system and is built up differently. Also, the isolation method of the bark lignin was different from the

organosolv process for the wood lignin, which can lead to different results [70]. Poplar is also hardwood and contains as well as beech wood guaiacyl and syringyl rich lignin. [29]. Poplar wood is according to literature also diverse; the lignin composition is even highly diverse between single trees [103] [102]. The ranges of the G-units (8-31 %) and S-units (68-91 %) [103] show that the used lignin is in between (G-units 29.3 %) and S-units. El Khaldi-Hansen et al. investigated beech wood organosolv lignin and compared it with different structural analysis of other literature [104]. Literature also shows that the aryl ether bonds like ß-O-4 are the major bond type (~ 50- 65 %) in beech wood lignin. However, like El Hage et al. [70] discovered these bonds get cleaved first in isolation processes. Also, hydroxyl groups (phenolic and aliphatic) are influenced by the isolation process, and polycondensation can occur. The results of the main monomeric units are varying with the temperature and alcohol ratio of the isolation process. With one isolation method, the distribution of G, S, and H-units were 49 % G-units, 19 % S-units, and 32 % H-units. With the other alcohol amount used in the isolation process the distribution showed 40 % G-units, 17 % S-units, and 43 % H-units [104]. So, the used lignin shows a higher amount of S-units. The organosolv process also uses an acid catalyst, which can lead to different results during subsequent process steps. Moreover, also other literature like Fengel and Wegener [102] show a G-S-H-unit distribution of 56 % G-units, 40 % S-units, and 4 % H-units. Which also shows that the lignins could vary highly in the composition, depending on the age, the location of growth, isolation and measurement method [102].

S. Bauer et al. investigated the lignin composition of *Miscanthus giganteus* with organosolv isolation methods [62]. The results show a range of ß-O-4 bonds of 45 % up to 80 %, depending on the alcohol amount in the isolation process. In comparison to the measurements of the used *Miscanthus giganteus* organosolv lignin with 46 % ß-O-4 bonds, it is on the lower end where less ethanol was used. The major monomer basic building blocks are also in Bauer et al. sinapyl and coniferyl alcohol [62]. El Hage et al. also had a look at the lignin composition of *Miscanthus giganteus* gained with an organosolv isolation. The syringyl-guaiacyl-p-hydroxyphenyl distribution was in this case 44 % S-units, 52 % G-units, and 4 % H-units. The used *Miscanthus giganteus* lignin in this work has lower G- and S-units, instead more H-units with 48.6 % S-units, 36.3 % G-units, and 15.2 % H-units are present. However, El Hage et al. also show that ester bonds, as well as ß-O-4 bonds, get cleaved differently according to the isolation method [70].

The comparison to literature showed the high variety in the lignin structures, depending on the plant itself, the conditions of growth, the isolation method and the analytical method of the structure analysis. This made it important to use one method for this work, which showed similar ranges of the monomeric units and bonds as the literature and fitted the gained cleavage results later on.

4.2 Comparison of the different reactor types

The reactor type has an influence on the conversion by the different mixing and thus retention time characteristics. The reactions taking place in the reactor depend on the perfusion of the reaction media [86][90][105]. In a continuous reactor, different conversion rates

can be obtained than in batch reactors because the concentrations of the reactions are not only affected by the feed and flow rate but also by the internal back-mixing behavior of the reactor type.

4.2.1 Loop reactor

The loop reactor was characterized (see 2.3.1) and tested in several experiments to study the hydrothermal liquefaction behavior of lignin. The characterization showed no typical behavior for a loop reactor, because of the highly laminar flow. Also, the used loop reactor has only a maximum back-mixing ratio of 3.4, this results in a non-ideal behavior of the reactor. The reactor is therefore not applicable to measure reaction kinetics. The first experiments confirmed these expectations, moreover the reactor was blocked by deposits after one hour of operation. Because of the decreasing flow in the rector, the residence time of the solid residue in the loop is higher than the residence time of the liquid, so instead of the hydrothermal liquefaction, hydrothermal carbonization can occur. The gained SEM pictures (Figure 43) confirm the assumption of hydrothermal carbonization without a repolymerization [94], based on the morphology of the particle structure. The results of the TGA measurements (Figure 44) show that the Indulin AT gets degraded at around 130 °C while the solid residue reacts at around 280 °C. If there was mainly repolymerization happening, the degradation of the residue would start earlier than the degradation of the Indulin AT, because the newly combined macromolecules would cleave earlier than the original macromolecules, because the bonds are not as strong as in the original ones [106][107].

The loop reactor needs further developing to be used in hydrothermal liquefaction processes. Due to this principle problem of solids formation, additional experiments had to be conducted to get an understanding of the influences of the reactor types and back-mixing on the reaction. Therefore, additional lab-scale reactors were built and investigated.

4.2.2 Plug flow & tank reactor

Two opposing cases of the internal back-mixing exist: a plug-flow reactor with no internal back-mixing along the reactor and a continuous stirred tank (CSTR) reactor with a complete internal back-mixing when ideal behavior is assumed [105]. For kinetic studies, CSTR is preferred because of the gradient-free behavior [86]. To get information about the reaction parameters and kinetics, the three reactor types (batch, plug-flow, and conti. tank) were utilized and compared. No differences could be identified within the experiments made, which leads to the assumption, that internal back-mixing does not influence the reactants. A batch reactor is a closed system, no continuous in- or output; this leads to a completely mixed media (like in a stirred tank). For the same temperatures and concentrations and stoichiometrically independent reactions are assumed [86][90]. In this work, only unstirred autoclaves were used, but a complete mixing is presumed because of the reaction parameters, and the behavior of water at these conditions and the small volume of the reactor. The outlet of an ideal CSTR has the same composition as the mixture inside of the

reactor. The input gets mixed instantly; just the inlet shows a concentration gradient [105]. With an optimal mixing inside of the reactor of the reactants, at constant temperature and pressure, the reaction rate is also constant [86]. To ensure that steady state is reached several residence times were realized, with sampling to see when the steady-state is reached. In the used tank reactor only, residence times of 8 min could be realized, with smaller flow rates (which should lead to longer residence times) accumulation of solids at the reactor wall is occurring and the effective volume decreases which lead to shorter residence times.

In an ideal plug flow reactor, full radial dispersion of the reactants is provided with the flow direction the reactant concentration changes over the reactor length. There is no radial concentration gradient, but axial. For plug-flow, a constant flow velocity is necessary[86][90]. The temporal progress in an ideally mixed batch reactor is equal with the local progress in the tube, however, normally the reactions are influenced by the internal back-mixing behavior of the reactor type. In an ideal plug flow reactor, no internal back-mixing is occurring [86].

For reactions with a changing reaction volume different internal back-mixing behaviors can provide information about reactions and what is happening inside of the reactor because of the change in the yields, with this the concentrations in the reaction mixture and the gained product mixture compounds [105]. It was expected to get different conversions with the different reactor types, because of the influence of the internal back-mixing behavior [86]. However, no differences in the yields could be observed. The internal back-mixing has no detectable influence on the reactions. The hydrothermal liquefaction of lignin is a complex reaction network with a lot of different intermediates, parallel and consecutive reactions, these reactions interfere with each other and cause a non-ideal behavior. Also, the highly heterogeneous reactions and reaction media result in a non-ideal behavior in the reactor. These effects overlay the influence of the reactor type and lead up to a reaction not influenced by the internal back-mixing in a reactor [108].

Therefore, it appeared useful, applying only the concentration profiles of the batch experiments for further studies on detailed kinetics of the within the complex reaction network as described in sections 3.7.4.

4.3 Addition of hydrogen carriers

To provide additional hydrogen for the liquefaction reactions, hydrogen carriers are added. A hydrogen carrier which is frequently applied in literature is formic acid - while these studies are performed under base conditions to get the lignin solved, it is not possible to use formic acid, because with a decrease of the pH the lignin would not be solved anymore. This would increase the amount of solid compounds in the reactor, and it is assumed based on the experimental results that it would also increase the solid yields. An acid would also change the reaction mechanisms which would make it impossible to compare results and see just the influence of the carrier [109]. Hydrogen is used to saturate double bonds and cleavage reactants, which could increase the monomeric yields in a certain way. It is necessary to produce the hydrogen *in situ* because this way it is more reactive and can interact with the

hydrothermal liquefaction process of lignin [110]. Otherwise, hydrogen gas itself cannot be used in hydrolysis reaction in the lignin cleavage [110].
Therefore, methanol and glucose were chosen. Methanol because of its assumed fast cleavage into carbon dioxide and hydrogen in a hydrothermal gasification step under the used conditions [110][111]. Glucose because it is the monomer of cellulose and cellulose degrade towards glucose directly under the used conditions and cellulose is always part of lignocellulosic biomass. Moreover, glucose reacts forward to hydrogen under the applied conditions [112]. The used concentrations are 0.5 wt.% based on the used lignin mass. Increased methanol feed concentrations influence the reaction mechanism in terms of alkylation reactions, enlarged product spectra and decrease of the yield of catechol [10]. Higher Glucose concentrations promote the carbonization of the biomass [105].
Higher yields of phenolics were expected because the hydrogen should be used in hydrolysis reactions and decrease the consecutive reactions towards oligomers and to decrease the repolymerization. The higher amount of hydrogen available by using glucose leads to higher yields of the investigated monomeric compounds. It could have been observed that the hydrogen is used to hydrate monomeric compounds because the yields of them increase about 12 % points. It is assumed that oligomeric compounds are also hydrated, nevertheless, like in the whole study, it was not possible to measure oligomeric compounds, because the analysis was not enough established at this point of the work. Glucose acts as a reactant in condensation reactions and promotes the hydrolysis [113]. Hydrogen is used to saturate double bonds and cleavage reactants, which could increase the monomeric yields in a certain. Methanol shows no influence on the monomeric yields. It can be assumed that methanol is not able to act as a hydrogen carrier under the investigated conditions. In total with the used conditions, no significant effect could have been observed.

4.4 External back-mixing

Experiments in a plug-flow-, batch-, and a CTR-mode show no differences in the yields and no measurable changes in the reaction network, so the internal back-mixing of the reactor types do not influence the liquefaction process. To verify these results, external back-mixing experiments with different back-mixing ratios were performed in the plug flow reactor (see chapter 2.4.4). With different back-mixing ratios, it is expected to have a positive influence on the cleavage reactions [10]. To put fresh feed and freshly cleaved unstable products in contact with the product mixture could increase the monomeric cleavage products because the unstable products can get stabilized by the other products and repolymerization could be prevented. Likewise, a set dilution is happening with the back-mixing, and this could also help to reduce repolymerization. In a loop reactor, different intermediate conditions between a tube and a CSTR can be realized, the dilution can be set by the back-mixing ratio, and the flow velocity in the reactor can be increased. This improves heat and mass transfer. Additionally, it would be possible to include a monomeric compounds removal set-up in the loop, e.g. polymer inclusion membranes could be used to bind phenolic monomers and prevent future repolymerizations of those [114].

With the used set up, it was only possible to feed the liquid products back in the loop reactor; the gaseous and solid compounds could be not back-mixed due to technical reasons:

- Solids have to be removed in front of the recirculation pump in order to avoid clogging

- Gaseous compounds could not be collected from the batch experiments and the used feed supply only allowed liquid feed

which lead to a decrease of the monomeric product yields. It is assumed that the yields of oligomeric compounds, which are still soluble in the liquid phase like dimers or trimers, were enhanced because of neither the solid residue amount increase nor the gas amount.
To offset the lack of gases methanol was added to the feed (see chapter 4.3), nonetheless, no increase of the monomeric products could be realized that way. A total back-mixing of the whole product spectra, including gases and solids, may have a positive influence on the yields of monomeric compounds because it is assumed that the gases (Table 8) have a higher influence on the repolymerization reactions, e.g. the gained methane yields could degenerate towards active hydrogen [115], which could be used *in situ* (see chapter 4.3) and enlarge the monomeric yields.

Table 8: Gas contribution of a hydrothermal liquefaction experiment of Indulin AT at 350 °C, 30 min residence time, 1 wt.% KOH in mg per used g Indulin AT.

	H_2	CO_2	CH_4	Ethylene	Ethane	Propene	Propane
mg/g_{lignin}	1.3	28.1	4.6	0.01	0.6	0.03	0.07

Solids residues are assumed to consist of ashes, carbonized residues, but also oligomer structures of the original lignin and repolymerized oligomers, with longer reaction times, which would occur with the back-mixing, further cleavage of them could be possible.

4.5 Influence of KOH addition

A base like KOH benefits lignin degradation and makes the lignin soluble in water even at room temperature, which is better for the liquefaction. Nevertheless, at a certain concentration, it could be seen, that the gasification reactions get promoted, which is well described in the literature [16]. This made it necessary to have a look at different KOH concentrations. Experiments under and at 300 °C without KOH showed nearly no monomeric components in the mixture after the reaction while with an increasing KOH concentration the gas yields increased. Lignin degradation without a catalyst starts under hydrothermal conditions above 250 °C [80]. Under 400 °C a base catalyst is necessary to cleave methylene- and aryl-aryl-bonds [80]. Water is, under ambient conditions, a polar solvent, this changes with temperature and pressure. The ion product increases in the beginning with higher temperatures until it decreases drastically at the critical point of water - also, the density and dielectric constant. However, the water molecules themselves are

still polar and can interact with polar species. Water itself acts as an acid/base catalyst because of its dissociation [116]:

$$H_2O \rightleftarrows H^+ + OH^- \tag{4.1}$$

Acids and bases increase the self-ionization constant of water and with this its catalyst function [80]. Temperature shows a high influence on the dissociation of water and with a low dielectric constant the effect of hydrogen bonds decreases and enlarges the single water molecule mobility, but the solubility of salts gets lower. On the one hand till the critical point of water, the KOH dissociation is not as strongly influenced by the temperature as the dissociation of water itself [116]. On the other hand, KOH catalyzes the water gas shift reaction:

$$\begin{gathered} CO + H_2O \rightleftarrows CO_2 + H_2 \\ KOH + CO \rightarrow HCOOK \\ HCOOK + H_2O \rightarrow HKCO_3 + H_2 \end{gathered} \tag{4.2}$$

So with more KOH more active hydrogen is available, which increases the lignin degradation and promotes the gasification of the biomass [116] [14]. Likewise, more of the lignin residues are cleaved under the influence of a base catalyst, and less char is formed. KOH catalyzes the aryl-alkyl-ether cleavage, by ionizing ether bonds by the alkali metal [116][14][117][80]. Small amounts increase the yields of monomeric compounds in the product mixture, while larger amounts benefit the cleavage reaction so much, that gasification is happening. An alkaline solvent solves lignin better than water and promotes degradation also. Still solved oligomers or lignin residues can be precipitated with acidification afterward. With a base catalyst, the solid residue amount decreases, more of the macromolecule gets degraded [80].

4.6 Temperature influence

Higher temperatures, longer reaction time and a higher amount of the catalysts shift the reaction towards the gasification (compare Figure 57). Above 350 °C water is under near or supercritical conditions, which leads to a different behavior then water at ambient conditions and enhances the reaction in the direction towards gasification.

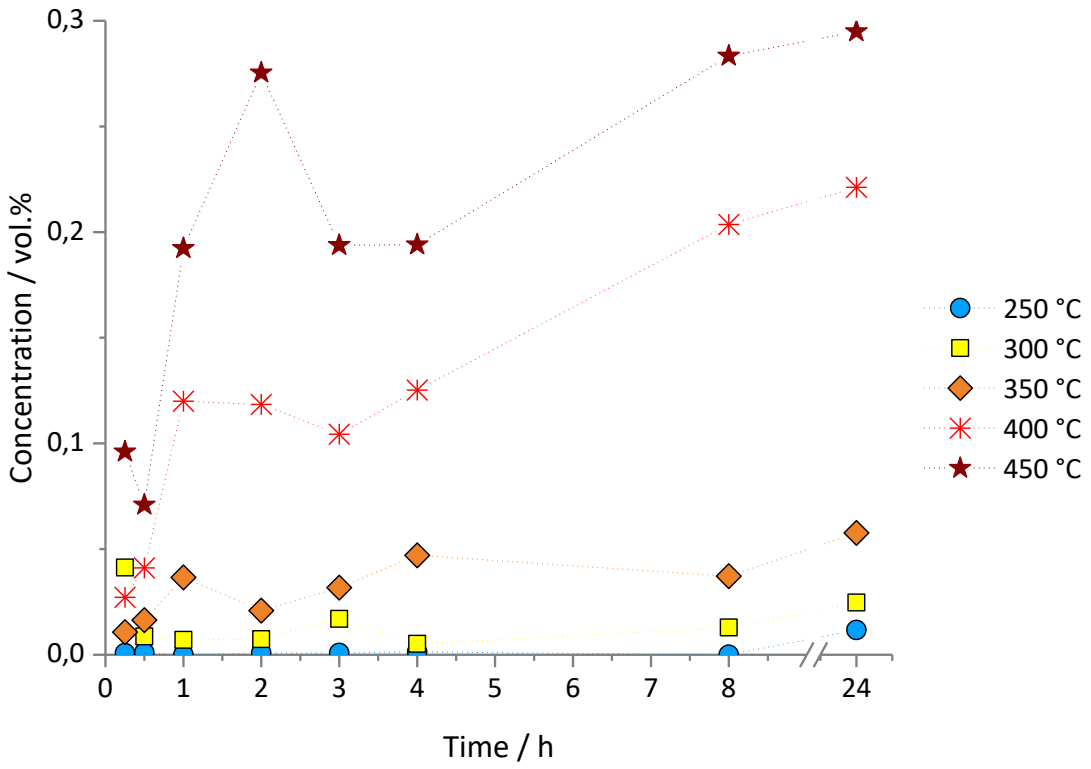

Figure 57: Concentrations of the obtained amount of methane in vol.% over the different reaction times (0.25 - 24 h) at different temperatures (250 - 450 °C) and a KOH concentration of 1 wt.% per biomass (beech bark). (blue circle - 250 °C, yellow square - 300 °C, orange diamond - 350 °C, red cross – 400 °C, dark red star – 450 °C)

The self-ionization constant increases from around 10^{-14} mol^2/kg^2 at room temperature and atmospheric pressure to 10^{-11} mol^2/kg^2 at 300 °C and 100 bar. With this the self-acid/base catalytic behavior of water increases, because of the increase of H^+/OH^- ions [80][118]. With higher temperatures, the resulting pressure enlarges, e.g., from 250 °C with 40 bar to 300 °C with resulting 86 bar. By using biomass as a resource always gases and solid residues get produced. Through the gas products, the resulting pressure increases compared to the equilibrium steam pressure. A higher pressure enlarges the self-ionization constant and with this the catalytic activity of water (see chapter 4.5), which gets also promoted by the used base KOH [80][118]. This promotes gasification reactions [119]. Also, with a lower density (which occurs with temperatures above 350 °C) radical reactions in the degradation get driven towards gasification [80]. At lower temperatures, ionic reaction steps occur, while at higher temperatures radical degradation dominates [120].
At 250 °C the cleavage reactions are slow furthermore gasification reactions are much less occurring. Only after longer reaction times liquefaction occurs (see Figure 58) [21].

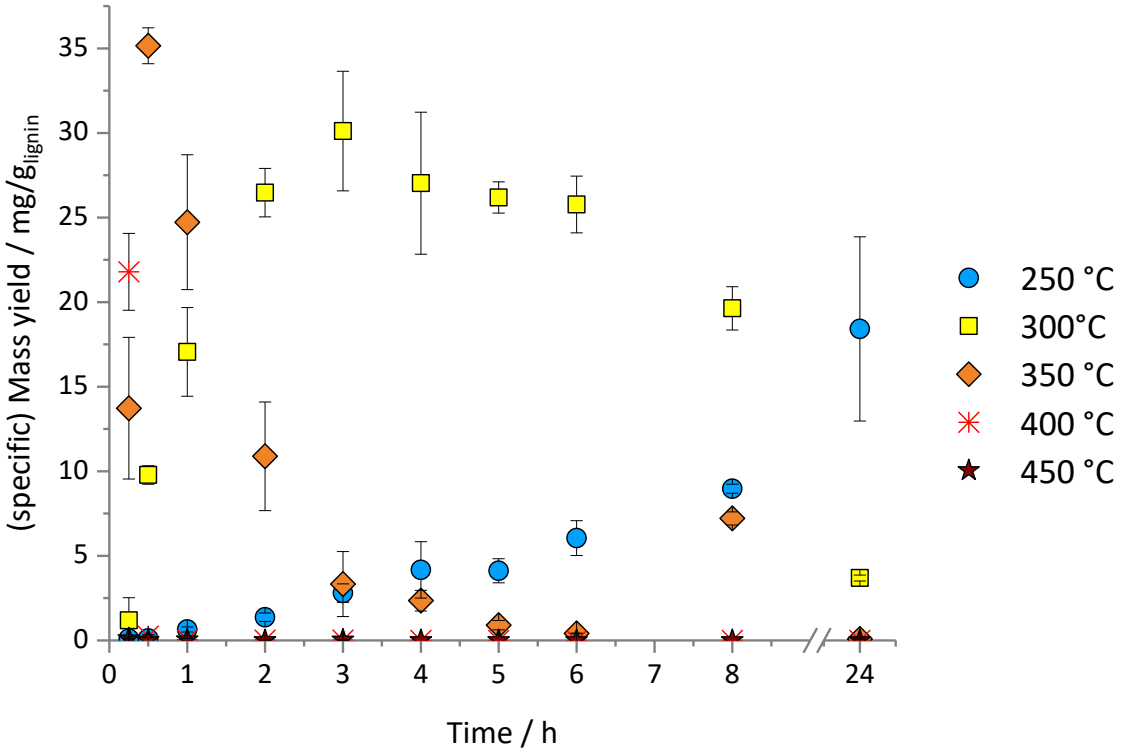

Figure 58: Mass yield of the obtained product catechol in mg per g used lignin (Indulin AT) over the different reaction times (0.25-24 h) and temperatures (250-450 °C) and 1 wt.% KOH. (blue circle - 250 °C, yellow square - 300 °C, orange diamond - 350 °C, red cross – 400 °C, dark red star – 450 °C)

On the contrary at 450 °C, almost the complete reaction is turned towards gasification while the yield of the desired products is found to be nearly zero.
With a lower dielectric constant ε, the number of hydrogen bonds decrease and also their strength. ε is also related to the hydrolysis rate constants, the intermediates of the cleavage are more stable with a higher ε. At temperatures above 350 °C the ε decrease dramatically (Table 9) [121]. While between 250 and 300 °C the change is compared, to the others, small.

Table 9: Dielectric constant ε over the used temperatures [121]

Temperature °C	Pressure bar	~ ε Fm^{-1}
250	50	27
300	200	21
350	200	14
400	200	1.6
450	200	1.4

This effect is supported by observations in literature [17,20,21]. The same can be observed for bark as a starting material and also for the three other organosolv lignins (Figure 60). At 350 °C, the reactions are changing from ionic to radical mechanisms [120], which delivers

more gaseous molecules and less monomeric compounds. Also, more of the original lignin is cleaved, and less solid residue is gained. 350 °C is already near the critical point and so in the transition of the different cleavage mechanisms. With lower temperatures, a longer reaction time is necessary to cleave the macromolecule towards monomeric compounds. It is assumed that the second increasing of the catechol yield at a residence time of 8 h at a reaction temperature of 350 °C is reasoned in a cleavage of repolymerized fractions towards monomeric compounds.

One reaction pathway towards catechol is assumed to proceed via guaiacol (compare Figure 59) [21,83,122]. Figure 59 supports the assumption of a consecutive reaction.

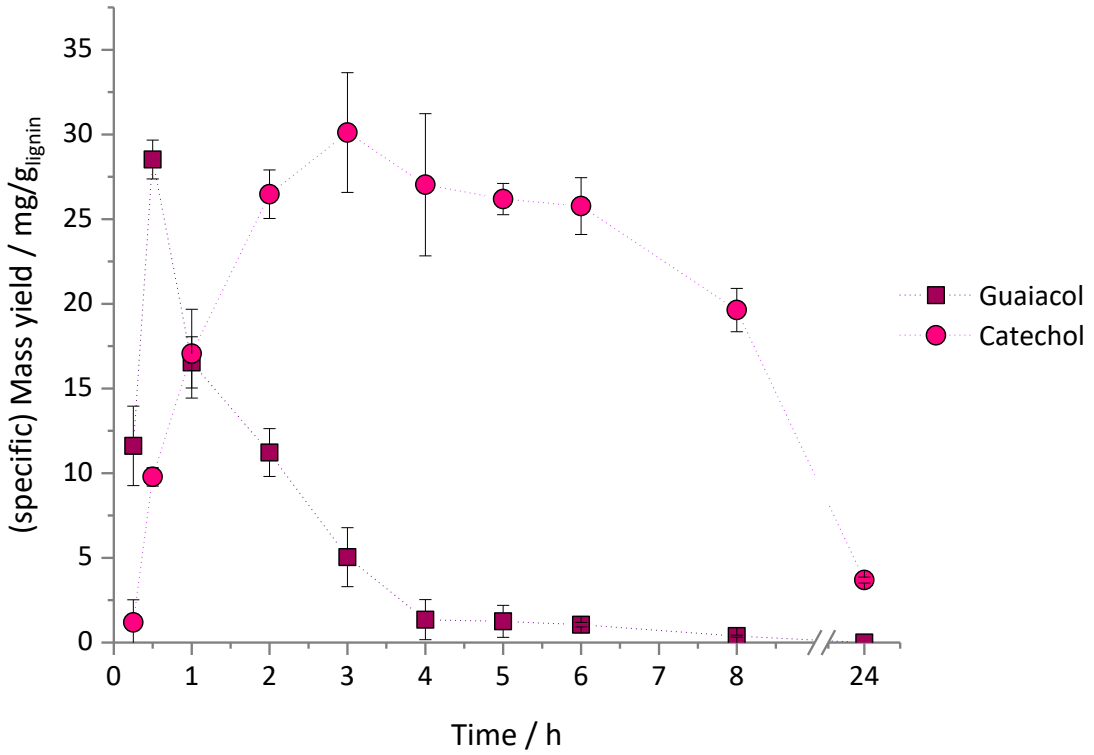

Figure 59: Mass yield of the obtained products guaiacol (dark rose squares) and catechol (pink dots) in mg per g used lignin at the different reaction times (0.25 -24 h) at 300 °C and a KOH concentration of 1 wt.%. (dark pink square – guaiacol, pink circle – catechol)

This is one explenation why the catechol yield is different when bark is used as a starting material. Because of the other degradation products and the NMR measurements (Table 7), it can be concluded that there is less coniferyl alcohol in the bark and more sinapyl alcohol as a monomeric unit, so there are less guaiacol and less catechol as degradation products.

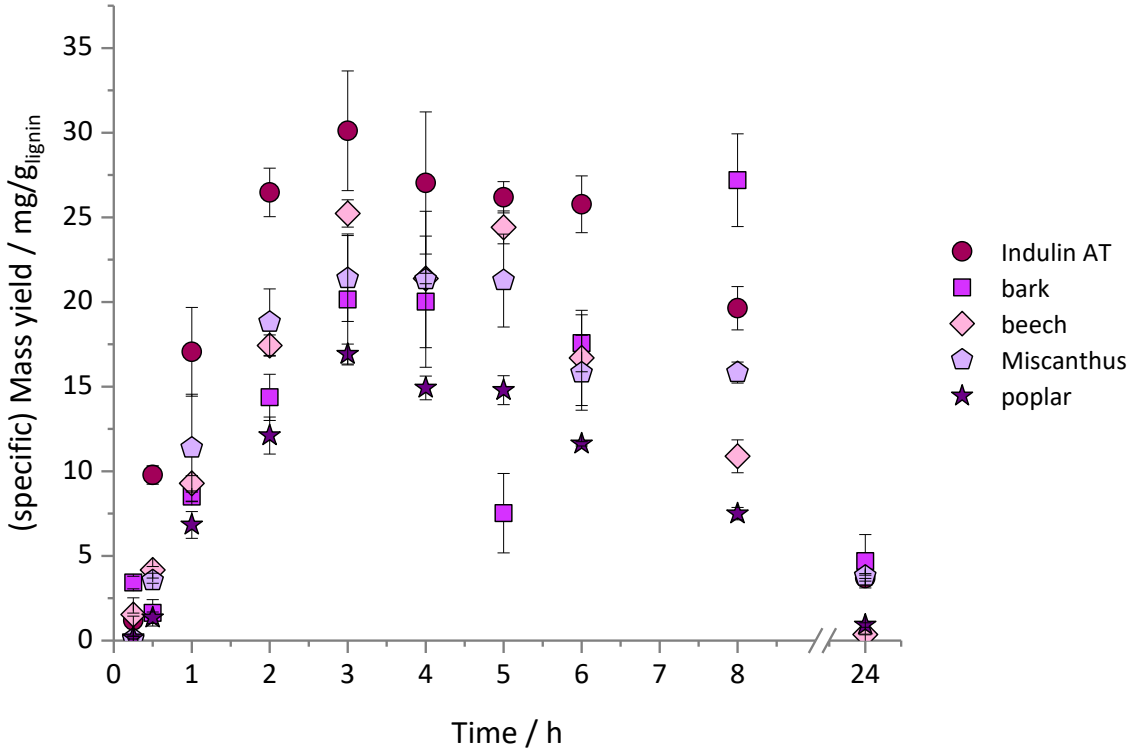

Figure 60: Mass yield of the obtained catechol in mg per g used lignin at the different reaction times (0.25 -24 h) at 300 °C and a KOH concentration of 1 wt.% of five different biomass sources (circle Indulin AT, square beech bark, diamond beech organosolv lignin, five ring *Miscanthus* organosolv lignin and star poplar organosolv lignin).

It is also considered that already degraded lignin-based molecules further react by repolymerization to oligomers, which can get cleaved again, and so the yield of monomeric phenolic compounds decreases. However, still the behavior in dependency of reaction time (Figure 60) and also with temperature is the same during hydrothermal treatment of different materials. Therefore, the reactions are expected to be influenced by the different molecular components present inside of the bark [45]. Taking this into consideration, the observed catechol yield is comparable to the yield observed when using Indulin AT as a starting material. The organosolv lignin of the Fraunhofer CBP also shows the same behavior than the Indulin AT and the used bark (Figure 60). Based on the experiments on the Indulin AT and the amount of organosolv provided by the CBP the parameters were limited. Because of the higher gasification at temperatures above 350 °C just the 250, 300 and 350 °C experiments were performed (see chapter 3.7.4).

Beechwood lignin shows a lower concentration profile over the reaction times compared to Indulin AT, but it is similar to the concentration profile of the bark. Both have the same wood as a lignin source (see chapter 2.1), so this was expectable.

The yields of the other observed products, namely syringol and guaiacol, confirm the NMR results of the monomer basic unit contribution of the different biomass sources because there is more syringol observed in the product mixture of the bark experiments than compared to the experiments with Indulin AT (compare Table 7) [9,26,29,59].

5 Reaction network & model

5.1 Reaction pathways of the lignin liquefaction

Lignin liquefaction delivers three product phases; gaseous, liquid and solid, the share of the phases and their composition depending on the treatment method and the operating conditions (hydrothermal, pyrolysis, acid or base catalyzed, etc.). The main gaseous products of the performed experiments of the hydrothermal liquefaction are mostly carbon dioxide and methane.

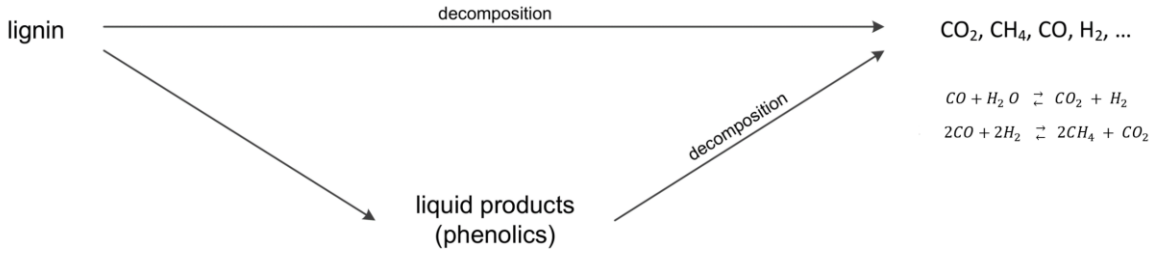

Figure 61: Reaction pathways of lignin towards gaseous products [13].

Gaseous compounds can be formed as primary products of the degradation of the lignin molecule, especially through the split-off of small sidechains methoxy- or hydroxy groups. They can be also formed as secondary products through the degradation of intermediates and the split-off of their side chains (Figure 61) [110][12][13].

The main reactions occurring during the hydrothermal liquefaction are hydrolysis and alkylation reactions by ionic or radical reactions, depending on the conversion temperature. At high temperatures more radicals are formed, which accelerate the cleavage but also the repolymerization reactions [12][13][123]. Through hydrolysis in the presence of water, which acts as a solvent and reaction partner in hydrothermal liquefaction processes, methoxylated benzenes occur as intermediates. Also, via hydrolysis, they react forward to the hydroxylated benzenes, like catechol. The further cleavage of oligomeric intermediates is stopped through saturation with hydrogen and with this, directly out of lignin, stable oligomeric aromatics occur.

Hydrolysis reactions furthermore deliver oxygenated hydrocarbons, which are used in alkylation reactions as reactants [12][13].

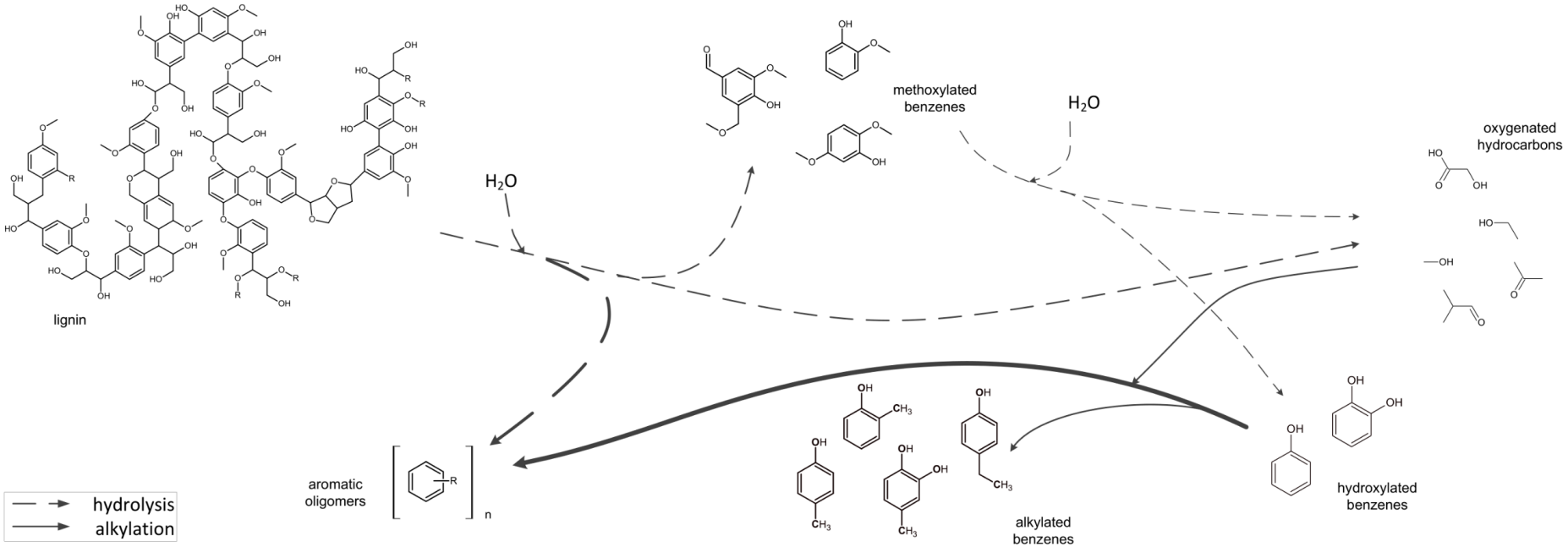

Figure 62: Reaction pathways of lignin towards liquid and solid products [12][13]. Monomeric phenolic compounds with different sidechains (methyl-, alkyl- and hydroxy groups) cleaved out of the oligomer via different reaction mechanisms (hydrolysis/alkylation) under hydrothermal conditions [12][13].

Hydrolysis reactions furthermore deliver oxygenated hydrocarbons, which are used in alkylation reactions as reactants. Via alkylation reactions, alkylated arenes are formed [12][13]. Arenes are also intermediates in reactions to oligomeric compounds. Di- or trimers would be found in the liquid phase (however could not be measured), higher oligomers in the solid phase. A reaction of the monomeric compounds towards di- and trimers could be an explanation for the observation that with an external back-mixing a lower monomeric concentration, but no increased solid amount can be observed. Intermediates with only hydroxy and aliphatic side chains are relatively stable compared to their methoxylated benzene analogs [124].

The reaction pathway towards catechol, for instance, leads through guaiacol (Figure 63) [21,83,122] and then towards 4-methylcatechol. Therefore, the oxygenated hydrocarbons or methoxy radicals out of other cleavage reactions are consumed in an alkylation step.

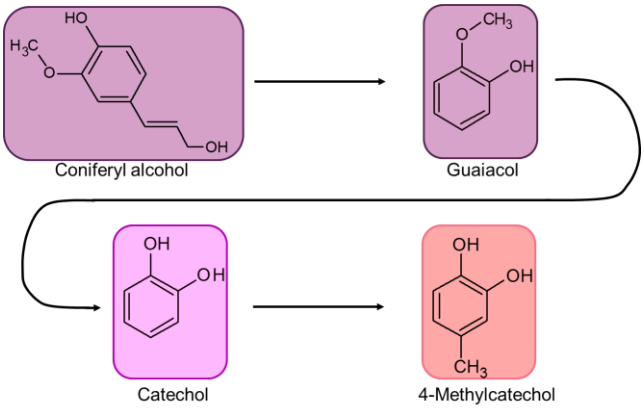

Figure 63: Possible reaction pathways from the basic monomer coniferyl alcohol to guaiacol to catechol and 4-methylcatechol.

Therefore, several reaction pathways towards the catechol can be described, depending on the reaction conditions. In near critical regions, radicals are formed, and radical reactions take place (Figure 64) [123]. The reaction rate is increased this way. This delivers a large number of intermediates and increases side reactions with other molecules.

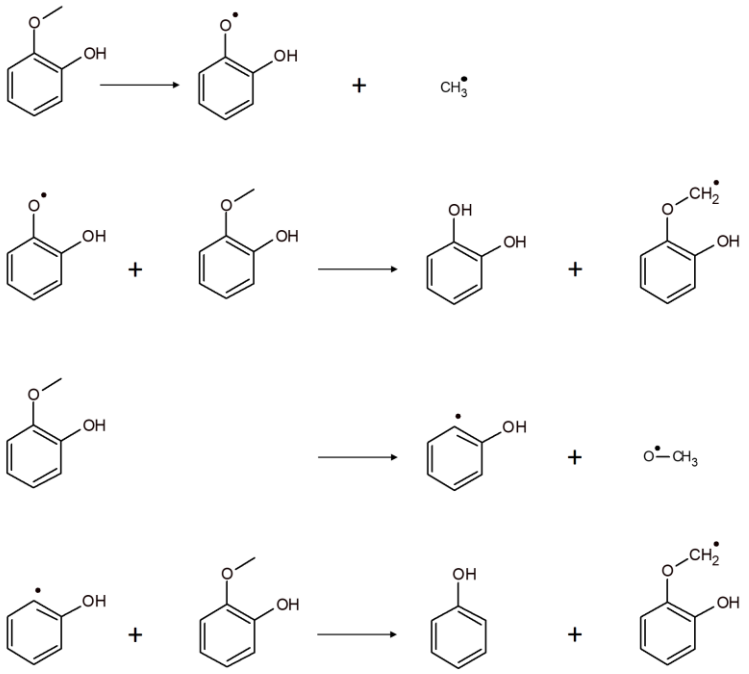

Figure 64: Reaction pathways of guaiacol decomposition under hydrothermal conditions in near critical regions with radical building [123].

Besides this, repolymerization reactions can be promoted by unstable radicals and a large series of reactions. In sub-critical conditions, ionic reactions occur, and the guaiacol molecule gets hydrolyzed with water to catechol (Figure 65).

Figure 65: Reaction pathways of guaiacol decomposition under hydrothermal conditions in subcritical regions as hydrolysis [123].

However, this is assumed to be only one of the different reaction pathways towards catechol (also described in [122]), another might be the direct cleavage out of larger molecules. Guaiacol can also be cleaved directly out of the lignin molecule by the cleavage of ß-o-4-bonds. However, there can be several intermediates and different reactions observed on the way from coniferyl alcohol towards guaiacol and catechol (Figure 66).

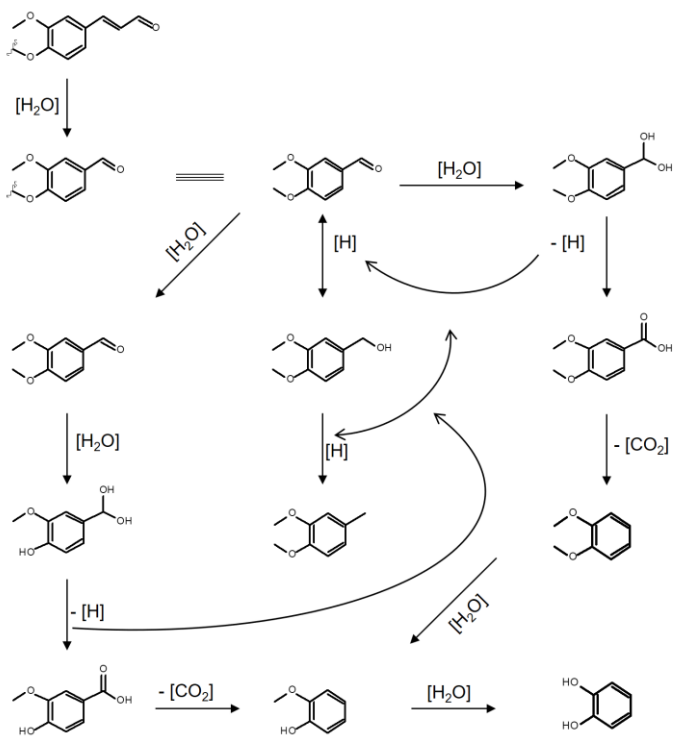

Figure 66: Lignin cleavage with the conversion of coniferyl alcohol and vanillin units, with further reaction steps towards guaiacol and catechol under hydrothermal conditions [125].

Phenol is a stable product in the hydrothermal liquefaction process, which can be observed by the stagnation of its concentrations over time. It arises out of the macromolecule directly, and also as an intermediate in different cleavage reactions (see Figure 64). Small amounts of the formed phenol react forward to cresols, where one way towards the cresols leads over an alkylation step. Therefore, remaining alkyl- and methyl-groups out of other cleavage reactions are used, see Figure 67 [126]. The same can be observed with catechol towards methyl- or, e.g. ethylcatechol. Experiments with only guaiacol show also 4-methylcatechol in the product spectra. Figure 67 shows the reaction pathways towards cresols.

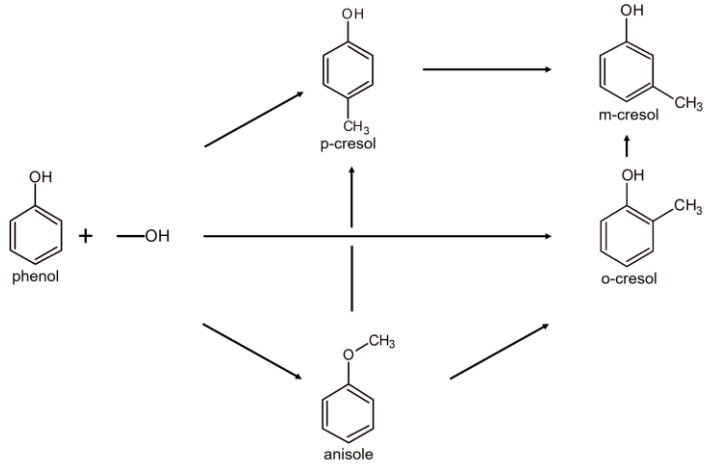

Figure 67: Reaction pathway of phenol towards o-, m- and p-cresol [126].

Depending on the temperature the alkylation step is either radical or of an ionic nature. Oxygenated hydrocarbons out of other degradation steps are used and bond on different positions at the stable aromatic ring again. The increase of functional side chains increases follow, side and repolymerization reactions.
These schemes, described by, e.g. Lui and Sad et al., describe the building of a large number of intermediates [125]. Considering there are more monomeric units' reactions in similar ways and with similar amounts of intermediates, a large number of interactions and new reactions are possible, which makes it very complicated to describe "the" reaction pathways of lignin towards single products. Small changes in the reaction condition and even the mechanisms themselves makes it even more complicated. Also, Lui and Sad et al. used a model compound, which makes it obvious, that lignin is far too complex to be described in one way. Several different reaction mechanisms like alkylation, hydration, dehydration, decarboxylation take place parallel which makes it a challenge to understand or even influence the reactions themselves completely. However, the main reaction pathways are the same for different lignins (compare Figure 81) which makes it possible to build a reaction network.

5.2 Modeling of the monomeric product spectra

The gap of knowledge in the first reaction network (Figure 68), developed by Daniel Forchheim [10], between lignin as a macromolecule and the product gases and solid residues should be investigated in this work. Like in chapter 2.2.4 discussed it is hardly possible to analyze the first lignin oligomer fragments in the cleavage reaction, because of the short reaction times and the lack of oligomeric analytic methods.

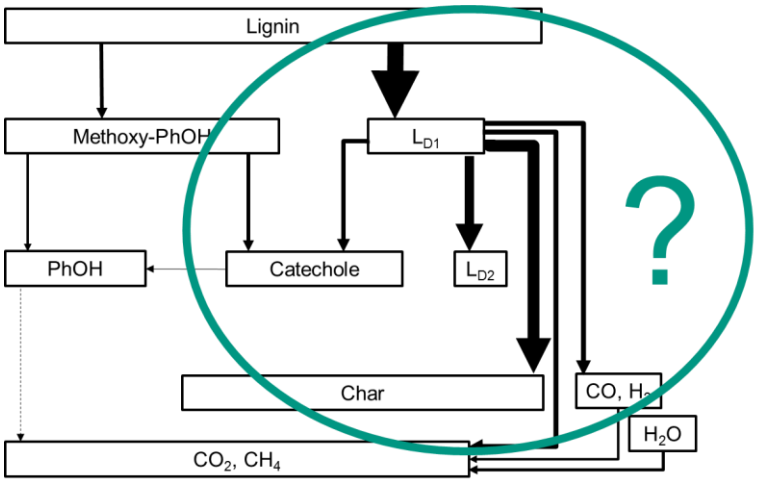

Figure 68: Assumed reaction network based on former studies, including the gap between lignin as a macromolecule and the product gases and solid residues [10].

Out of the gained concentration profiles, different reaction pathways could be identified (like Figure 69). Therefore the results of the batch experiments could be used, because like shown in chapter 4.1 the different reactor types showed no influence on the reactions.

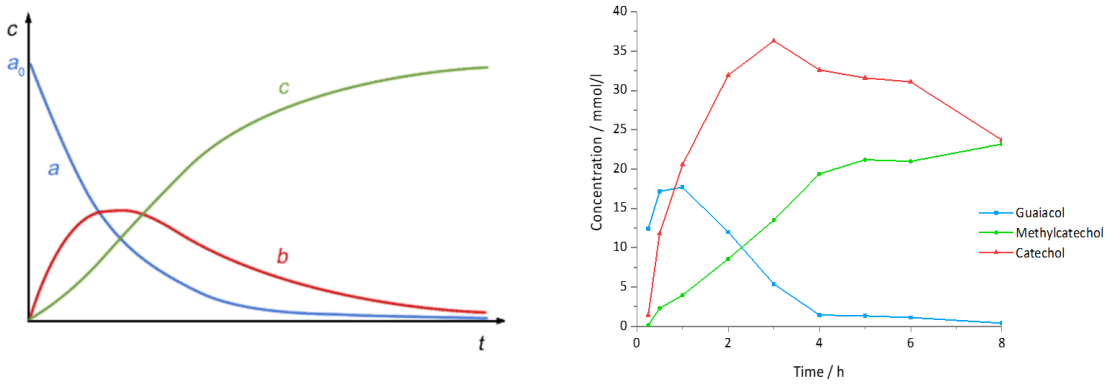

Figure 69: Scheme of the concentrations of three substances in dependency of time in a consecutive reaction: a (blue) → b (red) → c (green) [127]. Compared to the gained concentration profiles of the hydrothermal liquefaction of Indulin AT 300 °C over the time of guaiacol, catechol, and 4-methylcatechol.

To set up a reaction network and the compatible model to predict the product spectra out of different lignin sources, which would help to adjust the whole process especially regarding the downstream processes, it was started with one consecutive reaction:

Coniferyl alcohol → guaiacol + different side products

$$C_{10}H_{12}O_3 \rightarrow C_7H_8O_2 + C_nH_mO_p \quad (5.1)$$

guaiacol → catechol (→ 4-methylcatechol)

$$C_7H_8O_3 + H_2 \rightarrow C_6H_6O_2 + CH_4 \qquad (5.2)$$

$$(H_20 \rightleftarrows H^+ + OH^-)$$

Under the assumption of a reaction under constant volume and a reaction of the first order (n=m=1) these kinetic relations were assumed:

$$r_A = -k_A \cdot c_A^n$$

$$r_B = k_A \cdot c_A^n - k_B \cdot c_B^m \qquad n = 1 \qquad (5.3)$$

$$r_C = k_B \cdot c_B^m$$

k	reaction rate constant 1/s
r	reaction rate mol/Ls
n	reaction order
A	coniferyl alcohol
B	guaiacol
C	catechol

With:

$$r = \frac{dc}{dt} \qquad (5.4)$$

With the obtained information about the reaction constants and parameters, it is possible to quantitatively describe the dependency of the temperature and the reaction rate via the Arrhenius equation and plot (Figure 70), under the assumption of no mass transport limitations.

$$k = A \cdot e^{\frac{-E_A}{RT}} \qquad (5.5)$$

k	reaction rate constant 1/min
A	pre-exponential factor 1/min

E_A activation energy J/mol

R universal gas constant (8.314 J/mol K)

T temperature K

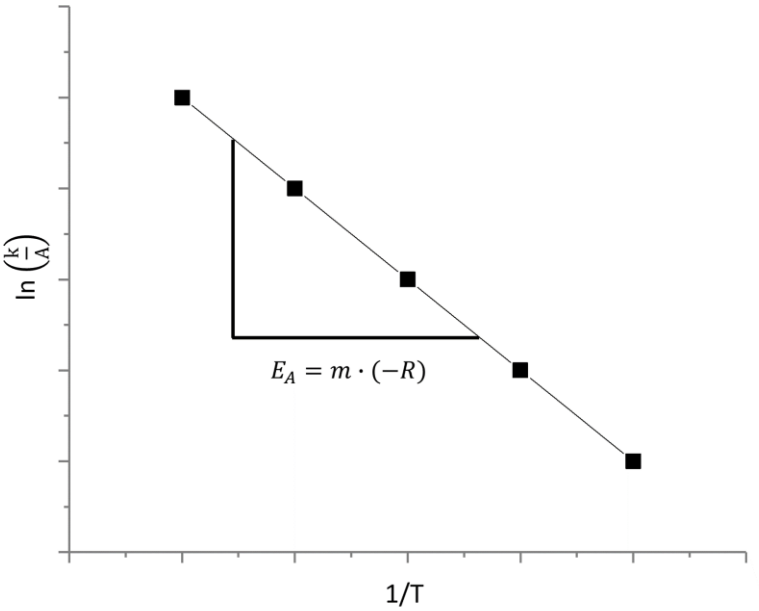

Figure 70: Principle of the Arrhenius plot; natural logarithm of reaction rate constant over the inverse of the corresponding temperature in Kelvin. With the resulting activation energy, out of the slope.

The Indulin AT results were used to build a model of the reactions, because it is mostly built out of one monomeric unit (coniferyl alcohol compare chapter 3.1.1.1). The starting concentration of coniferyl alcohol and the minor amount reacting directly towards catechol is unknown. It was necessary to start backwards and over the molar reaction equations that c_{A0} could be calculated.

The phenol concentration increases with short reaction times fast, like guaiacol and catechol, which leads to the assumption that phenol gets cleaved directly out of lignin (reaction 1. order). With longer reaction times the concentration stagnates at a certain point (compare Figure 51), which indicates a passive product and that there are hardly consecutive reactions. O-cresol and p-cresol are probably these minor follow products out of phenol.

4-ethylcatechol shows similar concentration profiles as 4-methylcatechol, and this suggests the assumption that they are both consecutive products of catechol. While 4-ethylguaiacol and 4-methylguaiacol are follow products of guaiacol.

Based on these assumptions and the extended reaction network (Figure 71) the model could get set up.

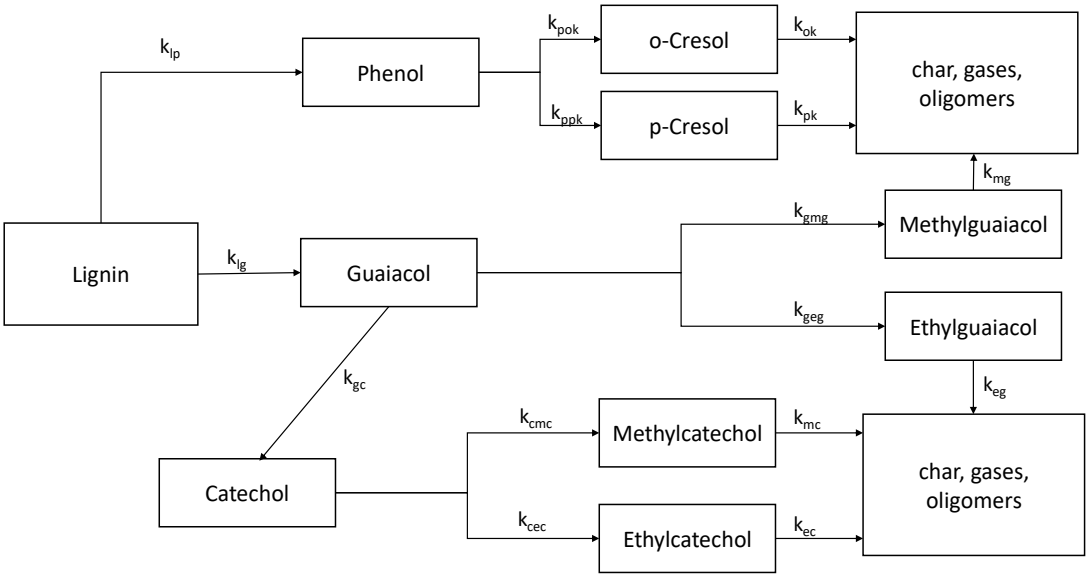

Figure 71: The developed reaction network starting from lignin respectively the coniferyl alcohol amount in the lignin towards different monomeric main reaction products.

The assumption of the coniferyl degradation via a reaction of first order leads to:

$$\frac{dc_{\mathrm{lig}}}{dt} = k_{\mathrm{lig}} * c_{\mathrm{lig}} \tag{5.6}$$

The follow equations are:

$$\frac{dc_{\mathrm{x}}}{dt} = k_{\mathrm{lig}} * c_{\mathrm{lig}} + \sum_{\mathrm{x}} k_{\mathrm{x}} * c_{\mathrm{x}} \tag{5.7}$$

$$k_{\mathrm{lig}} * c_{\mathrm{lig}} = -\sum_{\mathrm{x}} k_{\mathrm{x}} * c_{\mathrm{x}} + \frac{dc_{\mathrm{x}}}{dt} \tag{5.8}$$

This leads to:

$$c_{\mathrm{lig}} = \int k_{\mathrm{lig}} * c_{\mathrm{lig}} * dt = \int \sum_{\mathrm{x}} k_{\mathrm{x}} * c_{\mathrm{x}} - \frac{dc_{\mathrm{x}}}{dt} * dt \tag{5.9}$$

Not all of the lignin/coniferyl alcohol degrades into the assumed pathways and products, just a certain part, hence some of the starting concentrations are calculated, and the gained concentration profiles were described by an exponential function:

$$a * e^{b*t} + c * e^{d*t} \tag{5.10}$$

This fitted function was derived to get the information about the temperature depending on reaction rates.
The model is based on the following differential equations:

$$\frac{dc_{\mathrm{guai}}}{dt} = k_{\mathrm{lc}} * c_{\mathrm{ligCate}} - k_{\mathrm{gc}} * c_{\mathrm{guai}} - k_{\mathrm{geg}} * c_{\mathrm{guai}} - k_{\mathrm{gmg}} * c_{\mathrm{guai}} \tag{5.11}$$

$$\frac{dc_{\mathrm{cate}}}{dt} = k_{\mathrm{gc}} * c_{\mathrm{guai}} + k_{\mathrm{lc}} * c_{\mathrm{ligCate}} - k_{\mathrm{cmc}} * c_{\mathrm{cate}} - k_{\mathrm{cec}} * c_{\mathrm{cate}} \tag{5.12}$$

$$\frac{dc_{\mathrm{metc}}}{dt} = k_{\mathrm{cmc}} * c_{\mathrm{cate}} - k_{\mathrm{mc}} * c_{\mathrm{metc}} \tag{5.13}$$

$$\frac{dc_{\mathrm{etc}}}{dt} = k_{\mathrm{cec}} * c_{\mathrm{cate}} - k_{\mathrm{ec}} * c_{\mathrm{etc}} \tag{5.14}$$

$$\frac{dc_{\mathrm{metg}}}{dt} = k_{guai} * c_{\mathrm{guai}} - k_{\mathrm{mg}} * c_{\mathrm{metg}} \tag{5.15}$$

$$\frac{dc_{\mathrm{etg}}}{dt} = k_{\mathrm{geg}} * c_{\mathrm{guai}} - k_{\mathrm{eg}} * c_{\mathrm{etg}} \tag{5.16}$$

$$\frac{dc_{\mathrm{phen}}}{dt} = k_{\mathrm{lp}} * c_{\mathrm{ligPhen}} - k_{\mathrm{ok}} * c_{\mathrm{okres}} \tag{5.17}$$

$$\frac{dc_{\mathrm{pkres}}}{dt} = k_{\mathrm{ppk}} * c_{\mathrm{phen}} - k_{\mathrm{pk}} * c_{\mathrm{pkres}} \tag{5.18}$$

$$\frac{dc_{\mathrm{okres}}}{dt} = k_{\mathrm{pok}} * c_{\mathrm{phen}} - k_{\mathrm{ok}} * c_{\mathrm{okres}} \tag{5.19}$$

Out of these equations the Arrhenius plot (Figure 72) was evolved.

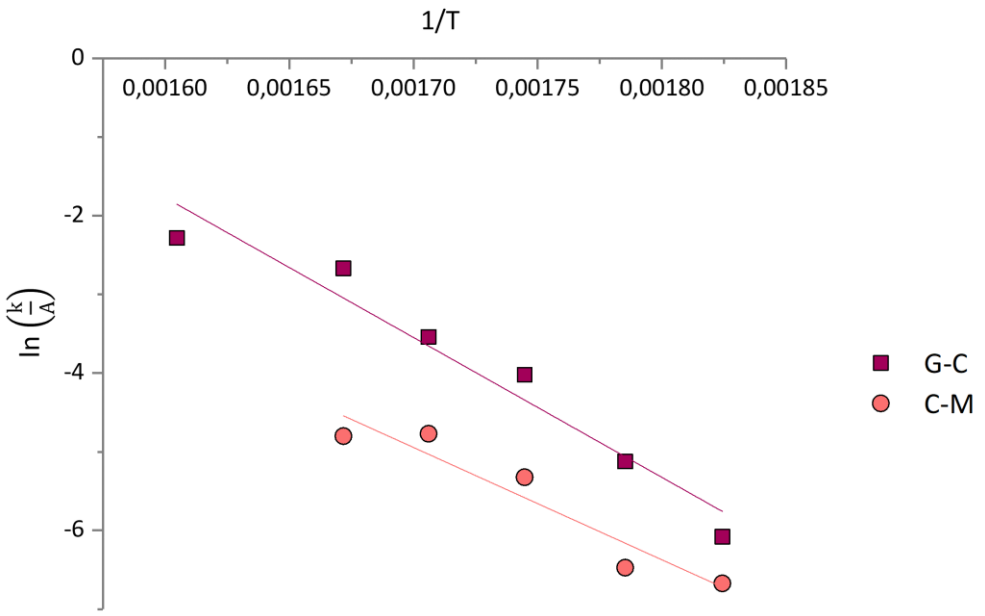

Figure 72: Arrhenius plot for two reactions; Guaiacol to catechol (G-C) and catechol to 4-methylcatechol (C-M). The natural logarithm of the calculated reaction rate constant over the inverse of the corresponding temperature in Kelvin, which delivers the activation energy out of the slope.

And the corresponding activation energies (
Table 10) were calculated out of these.

Table 10: Activation energies in J/mol for the main reactions (coniferyl alcohol to guaiacol “lg”, guaiacol to catechol “gc” and catechol to 4-methylcatechol “cmc”) calculated out of the Arrhenius plots.

E_A	Activation energy J/mol
lg	3.06 E+04
gc	1.48 E+05
cmc	1.19 E+05

Through the Arrhenius plots, the first assumption of three different reaction mechanisms over the investigated temperature range (see chapter 4.6) got reassured. At 250 °C and over 350 °C the lignin degradation behaves different (see chapter 4.6), which was expected because of the change of properties of water with the temperatures and the availability of hydrogen in the reaction. This reasons to a temperature range from 275 to 350 °C for the first model.

5.3 Monomeric product profiles

An expectation of the gained product spectra can be given by the model based on the coniferyl alcohol fraction. For Indulin AT the following concentration profiles at 300 °C were calculated through the built model (Figure 73).

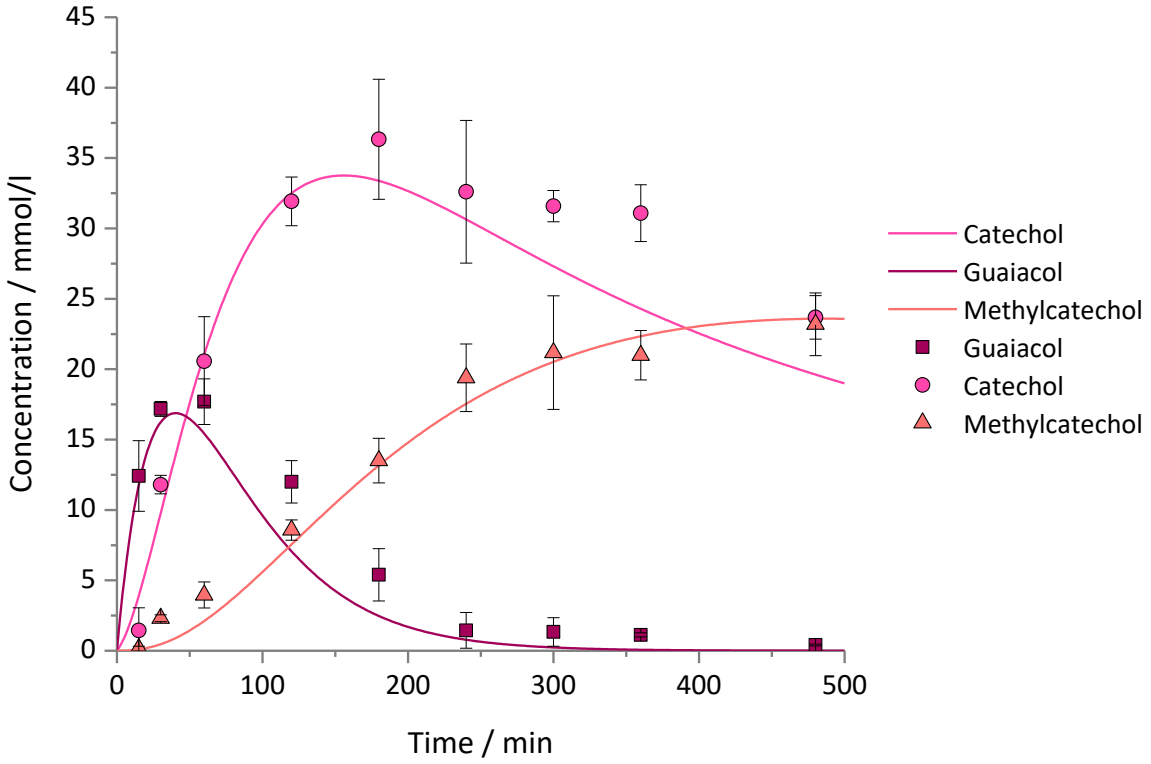

Figure 73: Experimental concentration profiles of guaiacol, catechol, and 4-methylcatechol over different residence times (0.25 – 8 h) at 300 °C (dots) compared to the modeled concentration profiles (lines) of the three components for Indulin AT.

At 350 °C, the model showed more deviation to the measured concentration profiles (appendix Figure 90). The first model fits not as well as at lower temperatures, which could be reasoned in the change in the cleavage reactions with different temperatures, see chapter 4.6.

Repeated modeled concentration profiles, with two Arrhenius plots for two temperature ranges (Figure 74), were compared a second time to the gained experimental results.

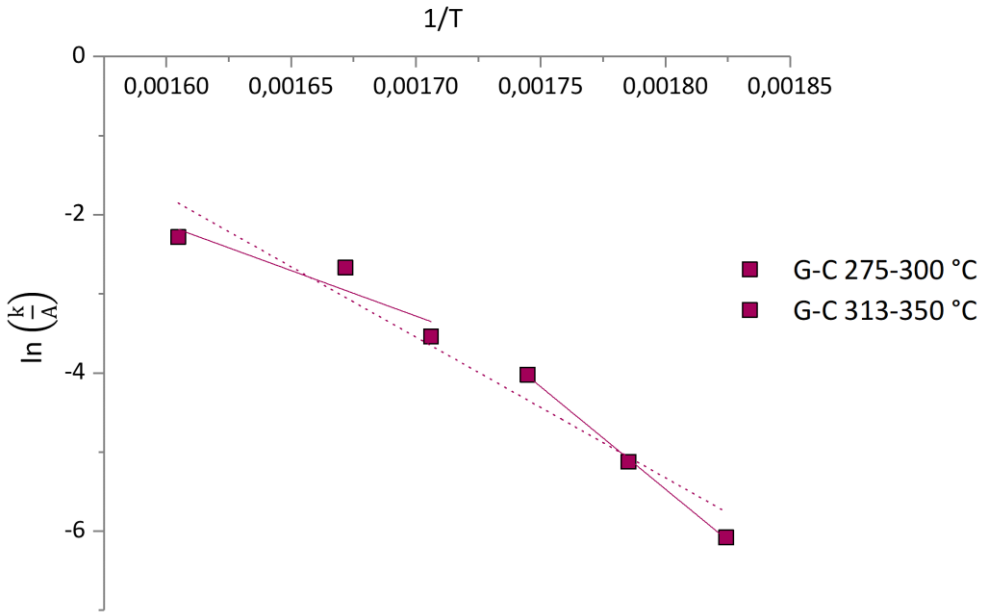

Figure 74: Arrhenius plot for one reaction and two temperatures ranges; Guaiacol to catechol (G-C). The natural logarithm of the calculated reaction rate constant over the inverse of the corresponding temperatures in Kelvin which delivers the activation energy out of the slope for 275-300 °C and 313-350 °C (straight lines) and the activation energy for the whole temperature range.

This leads to different activation energies, coefficients and reaction rates for the temperature ranges of 275 – 300 °C and 313 – 350 °C (see Table 11).

Table 11: Activation energies in J/mol for the main reactions (coniferyl alcohol to guaiacol “lg”, guaiacol to catechol “gc” and catechol to 4-methylcatechol “cmc”) calculated out of the Arrhenius plots.

E_A	Activation energy J/mol 275 - 300 °C	Activation energy J/mol 313 - 350°C
lg	5.65 E^{+04}	3.03 E^{+03}
gc	2.15 E^{+05}	9.57 E^{+04}
cmc	1.41 E^{+05}	-7.31 E^{+03}

The newly generated concentration profiles are shown in Figure 75 (and Figure 87 - Figure 90 in the appendix). With the new generated activation energies and constants, a new concentration profile is gained and can be compared to the other one.

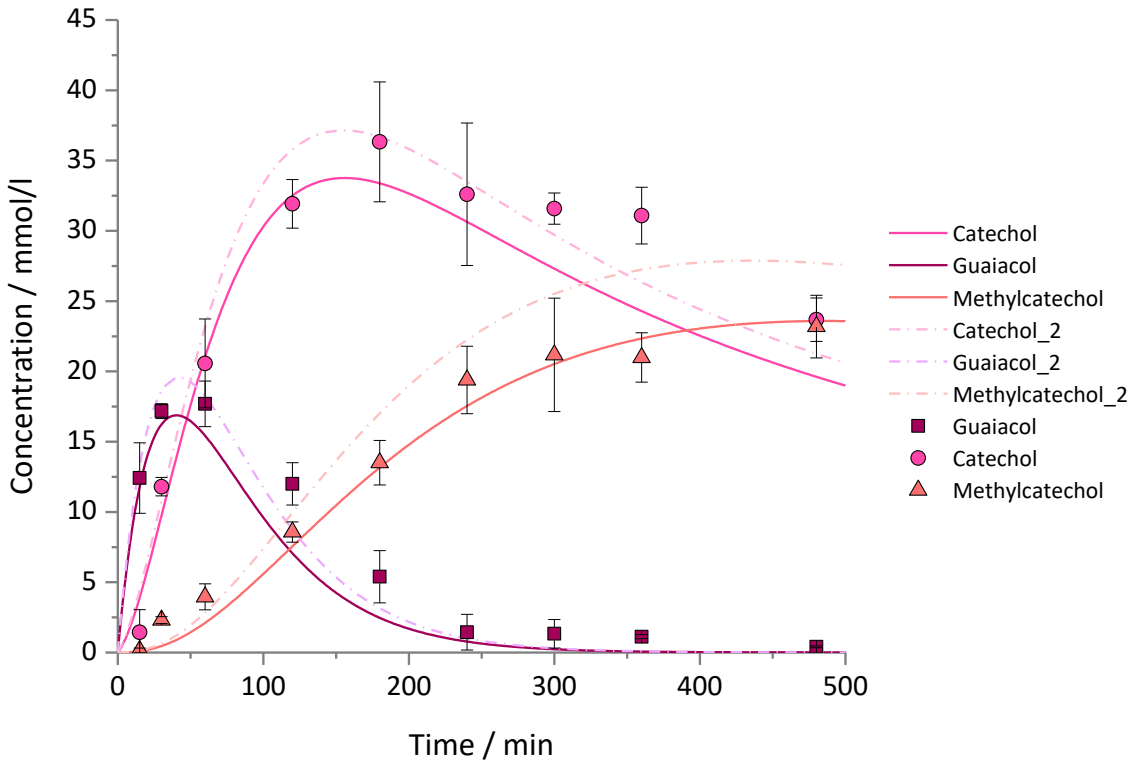

Figure 75: Experimental concentration profiles of guaiacol, catechol and 4-methylcatechol over different residence times (0.25 – 8 h) at 300 °C (dots) compared to the modeled concentration profiles (lines) of the three components and these compared to the modeled concentration profiles of the three components with a second activation energy for Indulin AT (dashed lines "_2").

Compared to the experimental gained concentration profiles the quality of the built model was evaluated by the coefficient of determination R^2 (Table 12).
The comparison of the model and the measured concentration profiles is over the whole range of residence times (0-24h). The noncontinuous experimental status makes it just possible to compare the profiles between 10 measured points. Here it must be considered that these also have an error and are not ideal. This delivers a rather vague R^2, however, it indicates the accuracy of the model.

Table 12: Coefficients of determination R^2 of the calculated concentration profiles to the experimentally measured concentrations for the modeled temperature range at 300 °C for one activation energy "_1" and two temperature ranges "_2".

T °C	guaiacol	catechol	4-methylcatechol
300_1	0.88	0.88	0.98
300_2	0.91	0.93	0.84

Contemplating the simplification of the kinetic, like no interaction between the different reactions, a determination coefficient over 0.7 is considered to describe the occurring kinetics of the model.

The built model is based on a lignin which only contains coniferyl alcohol as a monomeric unit. With the change of the origin lignin structure, not only by different bonds but also in the distribution of the monomeric building blocks, the reaction pathways can change and be influenced by each other. Catechol, for example, is not only built via coniferyl alcohol, furthermore, it is also a product of sinapyl and p-cumaryl alcohol [117][128][129]. So, the calculated results of the model must be corrected with a factor, which implies the products of the other monomeric building blocks of other biomass sources. To get this factor properly, further studies with these monomeric building blocks should be performed in the future, however, even by doing this the changes in the whole behavior by using real biomass cannot be included and must be fitted in a certain way. Because the used lignins show a large range in the basic contribution (Table 13) it is possible to build a factor of the used biomass sources for a first approximation:

Table 13: Monomeric units of Indulin AT, beech bark, Organosolv of beech wood of the FhG CBP, Organosolv of *Miscanthus* of the FhG ICT and Organosolv of poplar wood of the FhG ICT.[B]

Monomer basics	Indulin AT	Beech bark	Organosolv beech	Organosolv Miscanthus	Organosolv poplar
sinapyl alcohol	0 %	44.5 %	51.4 %	48.6 %	63.5 %
p-cumaryl alcohol	2.5 %	33.2 %	24.3 %	15.2 %	7.2 %
coniferyl alcohol	97.5 %	22.3 %	24.3 %	36.3 %	29.3 %

Under the assumption that the behavior of the other two monomeric units is in a certain way similar to the behavior of the degradation of coniferyl alcohol units, like, e.g. the building of catechol out of sinapyl and p-cumaryl alcohol units [117] the model for the first determined activation energies etc. was enhanced by including sinapyl and p-cumaryl alcohol as reactants, by calculating a factor. A factor for the product enhancement resulting in the other basic components (x & y) was built over the other four investigated lignins:

$$c_{measured} = c_{modeled\ Indulin} \cdot w_{coniferyl} + c_{modelled\ sinapyl} \cdot w_{sinapyl} + c_{modeled\ cumaryl} \cdot w_{cumaryl} \quad (5.20)$$

$$c_{modeled\ sinapyl} = c_{modeled\ Indulin} \cdot x \quad (5.21)$$

$$c_{modeled\ p-coumaryl} = c_{modeled\ Indulin} \cdot y \quad (5.22)$$

$$\frac{c_{measured}}{c_{modeled\ Indulin}} = w_{coniferyl\ alcohol} + x \cdot w_{sinapyl\ alcohol} + y \cdot w_{p-cumaryl\ alcohol} \quad (5.23)$$

$c_{measured}$	measured product concentration in concentration profiles
$c_{modeled\ Indulin}$	modeled product concentration of the Indulin AT model ≙ coniferyl alcohol amount
$c_{modeled\ sinapyl}$	modeled product concentration of the Indulin AT model ≙ coniferyl alcohol amount
$c_{modeled\ p-cumaryl}$	modeled product concentration of the Indulin AT model ≙ coniferyl alcohol amount
$w_{coniferyl\ alcohol}$	coniferyl alcohol amount % in used lignin gained over NMR
$w_{sinapyl\ alcohol}$	sinapyl alcohol amount % in used lignin gained over NMR
$w_{p-cumaryl\ alcohol}$	p-cumaryl alcohol amount % in used lignin gained over NMR
x	factor for the amount produced over sinapyl alcohol
y	factor for the amount produced over p-cumaryl alcohol

The factors deliver the amount of the product gained out of a different monomeric compound than coniferyl alcohol. The gained factors are:

Table 14: Gained factors for the amount produced over sinapyl alcohol “x” and p-cumaryl alcohol “y”.

x	0.47
y	1.01

Using this factors, the modeled concentration profiles could be built and compared with experimental results. The modeled concentration profiles of *Miscanthus giganteus* are shown in Figure 76. Especially the short residence times are represented well via the model.

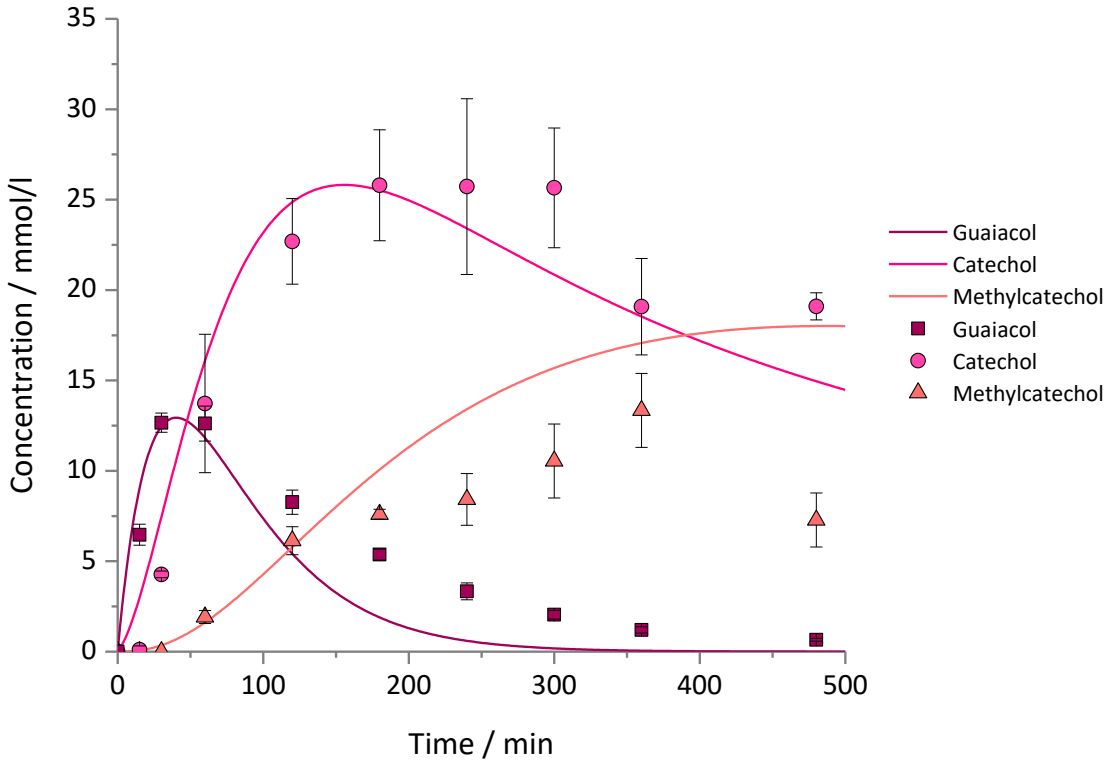

Figure 76: Experimental concentration profiles of guaiacol, catechol, and 4-methylcatechol over different residence times (0.25 – 8 h) at 300 °C (dots) compared to the modeled concentration profiles (lines) of the three components for *Miscanthus* organosolv lignin.

With longer reaction times the differences between the model and the experimental data are increasing. The same behavior can be observed for poplar organosolv lignin and beech wood organosolv lignin (see Figure 77 and Figure 78).

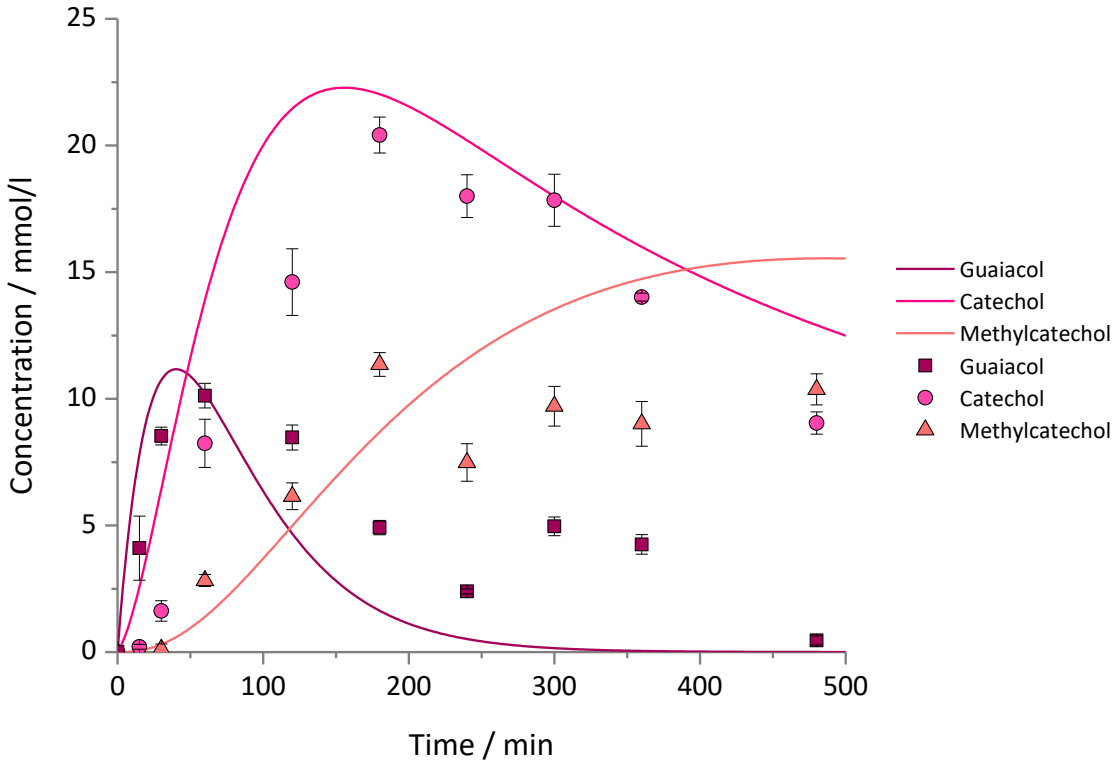

Figure 77: Experimental concentration profiles of guaiacol, catechol, and 4-methylcatechol over different residence times (0.25 – 8 h) at 300 °C (dots) compared to the modeled concentration profiles (lines) of the three components for poplar organosolv lignin.

Even with a mild isolation method to gain the lignin, the thermal degradation is influenced by it and can change the behavior of the reactions, which can hardly be included in the model. The different investigated lignins show similarity in its bonds, however, it is assumed that Indulin AT has a shorter chain length due to the Kraft process (see chapter 4.1). This leads to the assumption that the model can be transferred to every biomass because the bond distribution is more crucial than the chain length.

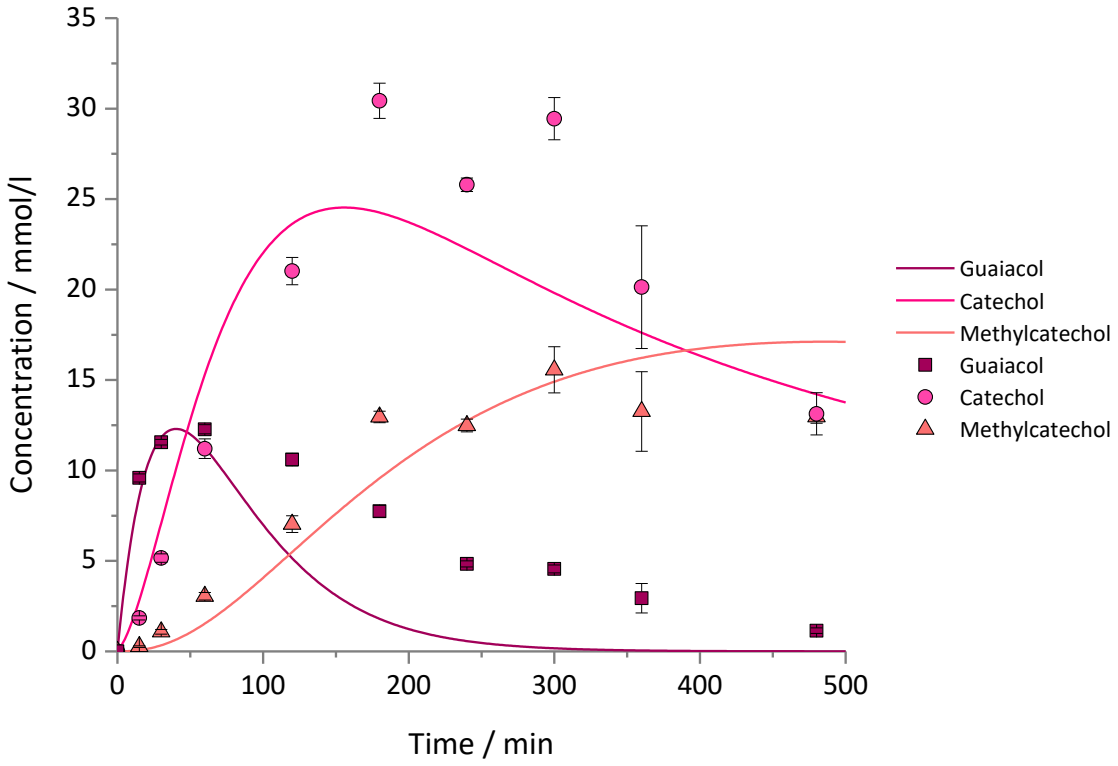

Figure 78: Experimental concentration profiles of guaiacol, catechol, and 4-methylcatechol over different residence times (0.25 – 8 h) at 300 °C (dots) compared to the modeled concentration profiles (lines) of the three components for beech wood organosolv lignin.

The different building blocks of lignin deliver different products, and these have also an influence on the reactions happening between the products, repolymerization and gasification reactions happening in the liquefaction process. Which also can be observed when bark is used as a starting material.

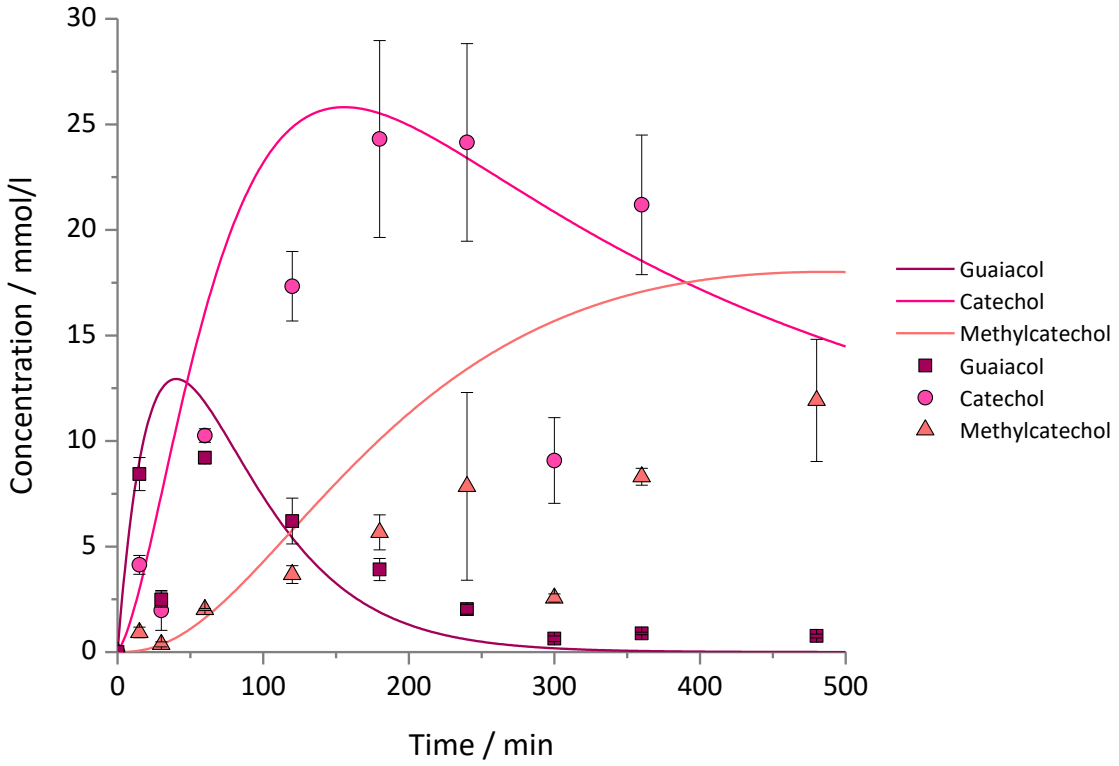

Figure 79: Experimental concentration profiles of guaiacol, catechol, and 4-methylcatechol over different residence times (0.25 – 8 h) at 300 °C (dots) compared to the modeled concentration profiles (lines) of the three components for bark lignin.

Bark contains a lot of different substances next to lignin, like tannins or extracts. This enlarges possible side reactions and interactions of the products and already enlarges the errors in the experimental measurements and results. It is also possible that the used bark amounts are not that homogenous, because bark itself is not homogenous, depending on the tree, an illness or an injury of the tree. So, it is not possible to get a common biomass contribution. This complicates the model, because of the variation in the starting numbers and the influence of different not considered reactions happening. However, it still represents the product concentration profiles over time (Figure 79), especially for catechol.

Experiments with different building blocks (ideally would be a biomass source built of only sinapyl alcohol and only p-cumaryl alcohol or model compounds) need to be done to improve these factors (x & y) and the reaction network. However, because of the variety in the structure of the investigated lignins (see Figure 7 and their isolation methods) it is estimated that the received factors are sufficient for more than these biomass sources. Moreover, the built model reflects the concentration profiles of different biomasses in a certain way, to get an idea of the necessary downstream processes in the hydrothermal liquefaction process to gain special chemicals in a certain quality.
The accordance of the concentration profiles over the whole investigated residence times improves with a briefer temperature range to calculate the activation energies, especially for the first reactions in the reaction network. For the temperatures, in-between only six different

residence times were applied, to have an idea of temperatures in between, but with enough data points, to have enough information. The modeling of the consecutive reactions is more influenced by the fact of the basic kinetic assumptions (e.g., first-order reaction, no interaction between the products). Also, with longer residence times it is more complicated, because of the, not considered, repolymerization and followed recleavage reactions, but for an industrial process, a process with residence times under 3 hours should be favored and so the model fits for the relevant reaction times.
Looking at the Arrhenius plots a partly non-Arrhenius behavior [116][120], see Figure 80, could be assumed.

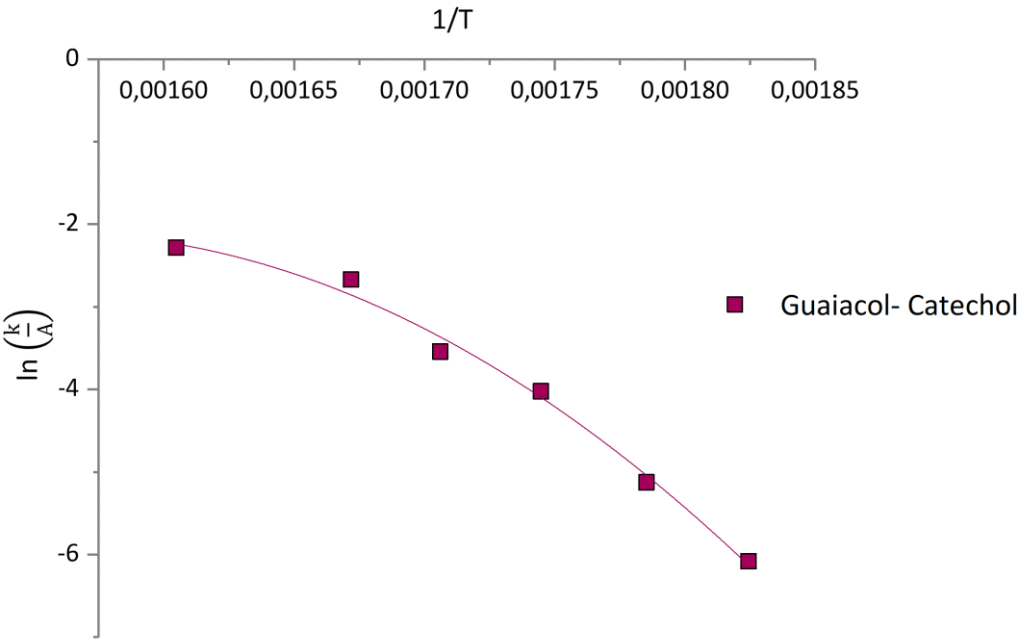

Figure 80: Arrhenius plot for the reaction; Guaiacol to catechol. The natural logarithm of the calculated reaction rate constant over the inverse of the corresponding temperatures (275-350 °C) in Kelvin. A non-Arrhenius behavior could be assumed because of the changes in the reaction mechanisms.

This could indicate a larger influence of temperature ranges on the reaction rates, most presumably because of the change in the ion product, the density and dielectric constant of water changing with the temperature [123][130][116].
Therefore, different activation energies for different temperature ranges can be calculated, and different concentration profiles modeled. Nevertheless, the overall calculation of the model based on one temperature range of 275-350 °C gives reasonable results and approximate composition of the product mixture.
By using biomass, the smallest change in reaction parameters, lead to a change of the model because of the change in the reaction network. This is why it is not possible to compare different kinetic parameters with each other [26]. Furthermore, a lot of calculated parameters or kinetic parameters received from model compounds like guaiacol, do not reflect the real lignin depolymerization and show different results than real biomass experiments [131].

Complex reactions are occurring especially under higher temperatures which makes it more complex to set up a model representing different reaction pathways including different starting structures [34]. However, the calculated parameters are in the range of some other models and reflect the experimental results [132][133].
This work aimed to realize a model with calculated kinetic factors, with the lowest amounts of fittings and fitting parameters, to get a real reflection of the product concentrations. To get an idea of the product mixture when different biomass sources are used in a hydrothermal cleavage process, different lignins were investigated. It is a challenging task to get such a model [80] because of the number of parallel reactions and interactions taking place. Nevertheless, even considering the fact of the simplifications assumed for the calculated model, it reflects the concentration profiles sufficient. Moreover, it can be assumed that lignin degradation is always following the same reaction pathways and can be roughly modeled and foreseen (Figure 81).

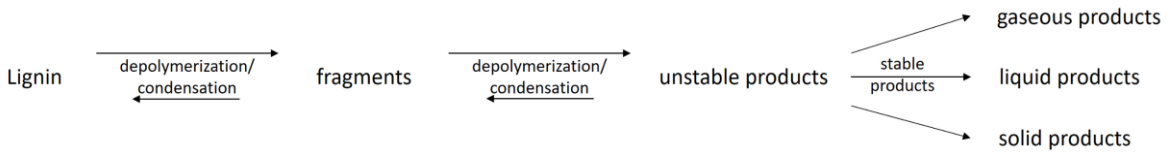

Figure 81: Lignin depolymerization/condensation scheme, pathways towards stable products [134].

This fact is presumably the reason why the models fit the measured concentration profiles so well. And, also, why the change in the Arrhenius plots is not always tremendous. Taking everything into consideration (different biomasses, complex product mixtures, huge reaction network, different lignin isolation processes and so on) the built model calculates useful results to predict the main monomeric component distribution.

Further concentration profiles for different temperatures and their determination coefficients can be found in the appendix.

6 Conclusion & Outlook

A Kraft Lignin, Indulin AT, was chosen as a reference and investigated in this work integrated into the Bioeconomy network. The entire process of hydrothermal liquefaction to obtain bifunctional components was studied in this thesis:

- Various biomasses (structure, analytics)
- Behavior/different parameters (KOH-influence, different lignins, temperature/ - residence time influence)
- Reaction network (incl. influence of internal back-mixing; loop reactor, plug flow, conti. tank, batch and external influences such as H_2 carriers, back-mixing, reaction pathways)
- Prediction of product composition - model (downstream better adjustable) (incl. - an extension of previous work reaction network, monomer product mix for different biomasses)

Depending on the origin of lignin, the bond types and monomeric basic units of the starting molecules differ. Under the same hydrothermal conditions, bark and Indulin AT and the other investigated lignins provide comparable catechol yields. Other products, such as a higher proportion of syringol with bark as a starting material, suggest that other monomeric units are present in the basic structure of bark lignin. However, because of their different monomeric units, the product spectra differ to the Indulin AT spectra.
For all investigated lignins a model based on coniferyl alcohol to predict the monomeric product spectra was built in this work. This was realized by experimental studies, like concentration profiles, the test of different reactor types, influences like back mixing or the addition of hydrogen carriers. However, the purification of the products is not developed by now. As side products of the hydrothermal splitting of lignin for the production of catechols, more than 50 other products emerge in addition to the desired product catechol.
The next step would be a purification of the product mixture, e. g. for the concentration of catechols. Several mechanisms would be conceivable, which have to be examined for their feasibility, later purity of the product and their consideration regarding the economy of the project:

- Polymer inclusion membranes [114]
- Membrane modules, size selection
- conversion to a stable intermediate molecule (cf. hydrogen with carbon dioxide to formic acid)
- Solid phase extraction, resins [135][136]
- Extraction

Polymer inclusion membranes, which can be embedded in the cycle process of the existing project in order to remove the recyclable material catechol from the reaction in a targeted manner for further recycling.

Using different membrane modules, purification can take place according to the molecular size and thus fractionation of the resulting product range can be achieved. In this way, more targeted applications such as the impregnation of wood, which is based on the molecular size, could also be better considered. Another possibility would be the further reaction to a stable intermediate product, which can be selectively removed from the mixture.

At the moment, there is a lot of potential for the use of biomass in many ways, Biomass has a high potential as a source for platform chemicals via hydrothermal liquefaction. Regarding in the context of a future bio-economy this will be even more important, as both are waste streams of the high-volume pulping industry and which are used mostly not chemically yet. This work has a focus on the development of a whole new value chain and a complete process, nevertheless, the basic reactions need to be understood well before a process design is possible. Hydrothermal liquefaction appears as a reasonable conversion technology because functional groups remain in the product molecules. The oligomeric compounds, which have not been investigated in detail until now, are promising products for chemical use. With different reaction times, temperatures and catalysts the reaction towards bifunctional molecules can be influenced. This could lead to a higher value generated for the wood and paper sector. Building a biorefinery on these foundations would be possible. The previous work has already yielded great insights, as an advantage of this work, the liquefaction process itself was better understood by examining different reactor systems. Internal analytical standards were achieved, and the analysis of oligomer components was improved. In particular, basic reactions to bifunctional compounds were clarified and modeled. Through the model, a monomer product composition can be predicted for different biomasses, and the necessary down streaming can be adapted.

Possible biorefineries and product lines made from sustainable raw materials are to be developed and implemented within the Bioeconomy Baden-Württemberg research network. Now, the main focus is on the use of renewable biomass as an alternative to fossil fuels. In this context, value creation chains are being developed which are to lead from the cultivation of biomass to the products.

7 References

[1] VCI, *Verband der Chem. Ind.* **2018**.
[2] U. Lüttge, M. Kluge, G. Thiel, *Botanik*, Wiley-VCH Verlag, Weinheim, **2010**.
[3] P. Sitte, E. W. Weiler, J. W. Kadereit, A. Bresinsky, C. Körner, *Lehrbuch Der Botanki Für Hochschulen*, Spektrum Akademischer Verlag, Heidelberg, **2002**.
[4] P. Jürgen, in *Gülzower Fachgespräche*, Fachagentur Nachwachsende Rohstoffe E.V., Gülzow, **2009**, pp. 18–41.
[5] W. G. Glasser, in *Gülzower Fachgespräche*, Fachagentur Nachwachsende Rohstoffe E.V., **2009**, pp. 42–44.
[6] M. Fache, B. Boutevin, S. Caillol, *ACS Sustain. Chem. Eng.* **2016**, *4*, 35–46.
[7] M. Ragnar, G. Henriksson, M. E. Lindstrom, M. Wimby, J. Blechschmidt, S. Heinemann, *Ullmann's Encycl. Ind. Chem.* **2014**, 1–92.
[8] P. S. B. Dos Santos, X. Erdocia, D. a. Gatto, J. Labidi, *Ind. Crops Prod.* **2014**, *55*, 149–154.
[9] M. Bunzel, J. Ralph, *J. Agric. Food Chem.* **2006**, *54*, 8352–8361.
[10] D. Forchheim, *Optimization of the Reaction Parameters of a CSTR and a PFR (Batch) for the Recovery of Phenol from Hydrothermal Biomass Liquefaction*, **2013**.
[11] J. Peng, F. Lu, J. Ralph, *J. Agric. Food Chem.* **1998**, *46*, 553–560.
[12] J. Barbier, N. Charon, N. Dupassieux, A. Loppinet-Serani, L. Mahé, J. Ponthus, M. Courtiade, A. Ducrozet, A. A. Quoineaud, F. Cansell, *Biomass and Bioenergy* **2012**, *46*, 479–491.
[13] S. Kang, X. Li, J. Fan, J. Chang, *Renew. Sustain. Energy Rev.* **2013**, *27*, 546–558.
[14] D. Schmiedl, S. Endisch, E. Pindel, D. Rückert, S. Reinhardt, R. Schweppe, G. Unkelbach, *Erdol Erdgas Kohle incl Oil Gas Eur. Mag.* **2012**, *128*, 357.
[15] A. Kruse, N. Dahmen, *J. Supercrit. Fluids* **2015**, *96*, 36–45.
[16] E. Dinjus, a Kruse, *J. Phys. Condens. Matter* **2004**, *16*, S1161–S1169.
[17] A. Kruse, N. Dahmen, *J. Supercrit. Fluids* **2015**, *96*, 36–45.
[18] K. Tekin, S. Karagöz, S. Bektas, *Renew. Sustain. Energy Rev.* **2014**, *40*, 673–687.
[19] D. Forchheim, U. Hornung, A. Kruse, T. Sutter, *Waste and Biomass Valorization* **2014**, 1–10.
[20] K. Tekin, S. Karagöz, S. Bektaş, *Renew. Sustain. Energy Rev.* **2014**, *40*, 673–687.
[21] H. E. Jegers, M. T. Klein, *Ind. Eng. Chem. Process Des. Dev.* **1985**, *24*, 173–183.
[22] E. Dorrestijn, M. Kranenburg, D. Poinsot, P. Mulder, *Holzforschung* **1999**, *53*, 611–616.
[23] E. Weiss-Hortala, A. Kruse, C. Ceccarelli, R. Barna, *J. Supercrit. Fluids* **2010**, *53*, 42–47.
[24] P. Schulze, A. Seidel-Morgenstern, H. Lorenz, M. Leschinsky, G. Unkelbach, *Bioresour. Technol.* **2016**, *199*, 128–134.
[25] G. Unkelbach, E. Pindel, R. Schweppe, *Chemie-Ingenieur-Technik* **2009**, *81*, 1767–1771.
[26] T. Faravelli, A. Frassoldati, G. Migliavacca, E. Ranzi, *Biomass and Bioenergy* **2010**, *34*, 290–301.
[27] X. Wang, R. Rinaldi, *ChemSusChem* **2012**, *5*, 1455–1466.
[28] J. Kjällstrand, O. Ramnäs, G. Petersson, *J. Chromatogr. A* **1998**, *824*, 205–210.
[29] L. Donaldson, *IAWA J.* **2013**, *34*, 3–19.
[30] A. Kruse, M. Kirchherr, S. Gaag, T. A. Zevaco, *Chemie-Ingenieur-Technik* **2015**, *87*, 1707–1712.
[31] D. Steinbach, **2011**.
[32] N. Dahmen, U. Hornung, J. Schuler, D. Schmiedl, V. Rohde, *Chemie Ing. Tech.* **2016**, *88*, 1412–1412.
[33] H. J. Roth, A. Kleemann, *Arzneistoffsynthese.*, Thieme, **1982**.
[34] E. A. B. da Silva, M. Zabkova, J. D. Araújo, C. A. Cateto, M. F. Barreiro, M. N. Belgacem, A. E. Rodrigues, *Chem. Eng. Res. Des.* **2009**, *87*, 1276–1292.

[35] B. V. Babu, *Biofuels, Bioprod. Biorefining* **2008**, *2*, 393–414.
[36] A. Bridgewater, *Therm. Sci.* **2004**, *8*, 21–50.
[37] A. Fendt, T. Streibel, M. Sklorz, D. Richter, N. Dahmen, R. Zimmermann, *Energy & Fuels* **2012**, *26*, 701–711.
[38] E. Henrich, N. Dahmen, F. Weirich, R. Reimert, C. Kornmayer, *Fuel Process. Technol.* **2016**, *143*, 151–161.
[39] A. Kruse, *J. Supercrit. Fluids* **2009**, *47*, 391–399.
[40] J. Yanik, S. Ebale, A. Kruse, M. Saglam, M. Yüksel, *Fuel* **2007**, *86*, 2410–2415.
[41] A. Kruse, *Biofuels, Bioprod. Biorefining* **2008**, *2*, 415–437.
[42] P. Biller, R. B. Madsen, M. Klemmer, J. Becker, B. B. Iversen, M. Glasius, *Bioresour. Technol.* **2016**, *220*, 190–199.
[43] R. B. Madsen, P. Biller, M. M. Jensen, J. Becker, B. B. Iversen, M. Glasius, *Energy and Fuels* **2016**, *30*, 10470–10483.
[44] R. B. Madsen, R. Z. K. Bernberg, P. Biller, J. Becker, B. B. Iversen, M. Glasius, *Sustain. Energy Fuels* **2017**, *1*, 789–805.
[45] S. Feng, Z. Yuan, M. Leitch, C. C. Xu, *Fuel* **2014**, *116*, 214–220.
[46] R. Beauchet, F. Monteil-Rivera, J. M. Lavoie, *Bioresour. Technol.* **2012**, *121*, 328–334.
[47] M. Javad, M. Almassi, M. Ebrahimi-nik, *J. Energy Inst.* **2014**, DOI 10.1016/j.joei.2014.10.005.
[48] C. Xu, R. A. D. Arancon, J. Labidi, R. Luque, *Chem. Soc. Rev.* **2014**, *43*, 7485–7500.
[49] S. Cheng, C. Wilks, Z. Yuan, M. Leitch, C. Xu, *Polym. Degrad. Stab.* **2012**, *97*, 839–848.
[50] R. Singh, A. Prakash, S. Kumar, B. Balagurumurthy, A. K. Arora, S. K. Puri, T. Bhaskar, *Bioresour. Technol.* **2014**, *165*, 319–322.
[51] D. Zhou, S. Zhang, H. Fu, J. Chen, *Energy and Fuels* **2012**, *26*, 2342–2351.
[52] R. Shu, J. Long, Y. Xu, L. Ma, Q. Zhang, T. Wang, C. Wang, Z. Yuan, Q. Wu, *Bioresour. Technol.* **2016**, *200*, 14–22.
[53] M. Azadfar, A. H. Gao, S. Chen, *Int. J. Biol. Macromol.* **2015**, *75*, 58–66.
[54] P. J. Deuss, K. Barta, *Coord. Chem. Rev.* **2015**, *306*, 510–532.
[55] O. Gordobil, R. Moriana, L. Zhang, J. Labidi, O. Sevastyanova, *Ind. Crops Prod.* **2016**, *83*, 155–165.
[56] German Federal Government, **2012**, 108.
[57] A. Kupferschmid, **2001**, *Teil 4*.
[58] I. Miranda, J. Gominho, I. Mirra, H. Pereira, *Ind. Crops Prod.* **2012**, *36*, 395–400.
[59] S. Feng, S. Cheng, Z. Yuan, M. Leitch, C. Xu, *Renew. Sustain. Energy Rev.* **2013**, *26*, 560–578.
[60] M. Fleckenstein, **2016**.
[61] R. Katahira, H. Kamitakahara, T. Takano, F. Nakatsubo, *J. Wood Sci.* **2006**, *52*, 255–260.
[62] S. Bauer, H. Sorek, V. D. Mitchell, A. B. Ibáñez, D. E. Wemmer, *J. Agric. Food Chem.* **2012**, *60*, 8203–8212.
[63] M. Bunzel, J. Ralph, *J. Agric. Food Chem.* **2006**, *54*, 8352–8361.
[64] S. D. Mansfield, H. Kim, F. Lu, J. Ralph, *Nat. Protoc.* **2012**, *7*, 1579–1589.
[65] C. S. Lancefield, N. J. Westwood, *Green Chem.* **2015**, *17*, 4980–4990.
[66] J. Schäfer, **2016**.
[67] C. Nord, **2015**.
[68] P. Korntner, I. Sumerskii, M. Bacher, T. Rosenau, A. Potthast, *Holzforschung* **2015**, *69*, 807–814.
[69] M. Balakshin, E. Capanema, *J. Wood Chem. Technol.* **2015**, *35*, 220–237.
[70] R. El Hage, N. Brosse, L. Chrusciel, C. Sanchez, P. Sannigrahi, A. Ragauskas, *Polym. Degrad. Stab.* **2009**, *94*, 1632–1638.
[71] J. F. S. Pat, *Ullmann's Encycl. Ind. Chem.* **2001**, DOI 10.1002/14356007.b05_181.
[72] pss-polymer, **2016**.
[73] M. H. Gey, *Instrumentelle Analytik Und Bioanalytik*, Springer-Verlag, Berlin

Heidelberg, **2008**.
[74] N. Yan, C. Zhao, P. J. Dyson, C. Wang, L. T. Liu, Y. Kou, *ChemSusChem* **2008**, *1*, 626–629.
[75] J. Y. Kim, S. Oh, H. Hwang, U. J. Kim, J. W. Choi, *Polym. Degrad. Stab.* **2013**, *98*, 1671–1678.
[76] A. A. Artemyeva, T. Diprospero, I. P. Smoliakova, E. I. Kozliak, A. Kubátová, *Development and Optimization of LC / HRMS Methods for Characterization of Lignin and Its Thermal and Biological Degradation Products*, **2015**.
[77] T. Diprospero, A. Artemyeva, A. Kubátová, I. Smoliakova, *Preparation of Analytical Standards for Identification of Lignin Degradation (Lignin Degradation Products Characterizatrion)*, Dakota, **2015**.
[78] A. A. Artemyeva, E. I. Kozliak, A. Kubátová, *Development and Optimization of SEC / HRMS Method for Characterization of Lignin and Its Thermal Degradation Products*, Dakota, **2015**.
[79] J. L. Sánchez, J. Salafranca, S. Moles, J. F. Palomo, C. Martínez, N. Gil-Lalaguna, C. Dueso, A. Gonzalo, *Eur. Biomass Conf. Exhib. Proc.* **2017**, 1005–1011.
[80] F. Jin, *Application of Hydrothermal Reactions to Biomass Conversion*, **2014**.
[81] J. Schuler, U. Hornung, J. Sauer, **2017**, pp. 987–991.
[82] J. Schuler, U. Hornung, N. Dahmen, J. Sauer, *GCB Bioenergy* **2018**, 1–13.
[83] Wahyudiono, M. Sasaki, M. Goto, *Chem. Eng. Process. Process Intensif.* **2008**, *47*, 1609–1619.
[84] D. Forchheim, *Optimization of the reaction parameters in a batch reactor and a CSTR for the recovery of phenol from hydrothermal biomass liquefaction,* Karlsruher Institut für Technologie, **2013**.
[85] J. Hagen, *Technische Katalyse*, Wiley-VCH, Weinheim, **1997**.
[86] J. Hagen, *Chemiereaktoren: Auslegung Und Simulation*, **2004**.
[87] H. S. Fogler, *Elements of Chemical Reaction Engineering*, Pearson Education Inc., **2006**.
[88] A. Kruse, C. Lietz, *Chemie Ing. Tech.* **2002**, *74*, 1140–1144.
[89] A. Kruse, H. Ederer, D. Ernst, B. Seine, *Chemie Ing. Tech.* **2008**, *80*, 1809–1814.
[90] M. Baerns, *Technische Chemie*, Wiley-VCH, **2013**.
[91] M. Instruments, **2017**.
[92] A. Kruse, E. Dinjus, *J. Supercrit. Fluids* **2007**, *41*, 361–379.
[93] M. Ernst, *Praxissemsterreport - Untersuchungen Zur Hydrothermalen Spaltung von Lignin*, Heilbronn, **2017**.
[94] A. Funke, F. Reebs, A. Kruse, *Fuel Process. Technol.* **2013**, *115*, 261–269.
[95] J. Schuler, U. Hornung, A. Kruse, N. Dahmen, J. Sauer, *J. Biomater. Nanobiotechnol.* **2017**, *08*, 96–108.
[96] B. Saake, R. Lehnen, *Ullmann's Encycl. Ind. Chem.* **2012**, 16.
[97] A. Toledano, L. Serrano, J. Labidi, *J. Chem. Technol. Biotechnol.* **2012**, *87*, 1593–1599.
[98] S. Karagöz, T. Bhaskar, A. Muto, Y. Sakata, T. Oshiki, T. Kishimoto, *Chem. Eng. J.* **2005**, *108*, 127–137.
[99] D. R. Robert, M. Bardet, G. Gellerstedt, E. L. Lindfors, *J. Wood Chem. Technol.* **1984**, *4*, 239–263.
[100] H. Zhu, Y. Chen, T. Qin, L. Wang, Y. Tang, Y. Sun, P. Wan, *RSC Adv.* **2014**, *4*, 6232–6238.
[101] R. Meusinger, A. M. Chippendale, *Ullmann´s Encycl. Ind. Chem.* **2012**, *31*, 150–153.
[102] D. Fengel, G. Wegener, *Wood : Chemistry, Ultrastructure, Reactions*, Kessel Verlag, **2003**.
[103] A. R. Robinson, S. D. Mansfield, *Plant J.* **2009**, *58*, 706–714.
[104] B. El Khaldi-Hansen, M. Schulze, B. Kamm, in *Anal. Tech. Methods Biomass*, Springer International Publishing, Cham, **2016**, pp. 15–44.
[105] A. Behr, D. W. Agar, J. Jörissen, A. J. Vorholt, Springer-Verlag GmbH, *Einführung in*

Die Technische Chemie, **2010**.
[106] E. Dinjus, A. Kruse, N. Tröger, *Chemie-Ingenieur-Technik* **2011**, *83*, 1734–1741.
[107] A. Kruse, R. Grandl, *Chemie Ing. Tech.* **2015**, n/a-n/a.
[108] J. Schuler, U. Hornung, N. Dahmen, J. Sauer, *Chemie Ing. Tech.* **2018**, *90*, 1151–1151.
[109] M. Schwiderski, A. Kruse, R. Grandl, D. Dockendorf, *Green Chem.* **2014**, *16*, 1569.
[110] A. Kruse, A. Funke, M. M. Titirici, *Curr. Opin. Chem. Biol.* **2013**, *17*, 515–521.
[111] N. Boukis, V. Diem, U. Galla, E. Dinjus, *Combust. Sci. Technol.* **2006**, *178*, 467–485.
[112] A. Sinag, A. Kruse, V. Schwarzkopf, *Eng. Life Sci.* **2003**, *3*, 469–473.
[113] C. Falco, Sustainable Biomass-Derived Hydrothermal Carbons for Energy Applications, Universität Potsdam, **2012**.
[114] M. O'Rourke, R. W. Cattrall, S. D. Kolev, I. D. Potter, *Solvent Extr. Res. Dev.* **2009**, *16*, 1–12.
[115] J. G. Van Bennekom, R. H. Venderbosch, D. Assink, H. J. Heeres, *J. Supercrit. Fluids* **2011**, *58*, 99–113.
[116] A. Kruse, E. Dinjus, *Zeitschrift fur Phys. Chemie* **2005**, *219*, 341–366.
[117] L. Du, Z. Wang, S. Li, W. Song, W. Lin, *Int. J. Chem. React. Eng.* **2013**, *11*, 135–145.
[118] J. R. Cooper, R. B. Dooley, **2007**, *10*, 1–7.
[119] M. Osada, O. Sato, M. Watanabe, K. Arai, M. Shirai, *Energy and Fuels* **2006**, *20*, 930–935.
[120] W. Buehler, E. Dinjus, H. J. Ederer, A. Kruse, C. Mas, **2002**, *22*, 37–53.
[121] U. Grigull, *Sonderdruck aus Brennstoff--Wärme-Kraft* **1983**, *35*, 289–293.
[122] Wahyudiono, M. Sasaki, M. Goto, *J. Mater. Cycles Waste Manag.* **2011**, *13*, 68–79.
[123] T. L. K. Yong, M. Yukihiko, *Ind. Eng. Chem. Res.* **2013**, *52*, 9048–9059.
[124] S. S. Toor, L. Rosendahl, A. Rudolf, *Energy* **2011**, *36*, 2328–2342.
[125] M. Y. Lui, B. Chan, A. K. L. Yuen, A. F. Masters, A. Montoya, T. Maschmeyer, *ChemSusChem* **2017**, *10*, 2140–2144.
[126] M. E. Sad, C. L. Padró, C. R. Apesteguía, *Appl. Catal. A Gen.* **2008**, *342*, 40–48.
[127] "Followreaction; http://www.chemgapedia.de/vsengine/vlu/vsc/de/ch/13/vlu/kinetik/grundlagen/komplexe_reaktionen.vlu/Page/vsc/de/ch/13/pc/kinetik/grundlagen/folgereaktion1.vscml.html," **2017**.
[128] E. B. Ledesma, N. D. Marsh, A. K. Sandrowitz, M. J. Wornat, *Proc. Combust. Inst.* **2002**, *29*, 2299–2306.
[129] A. A. Mullery, J. N. Hoang, A. T. Nguyen, C. D. Luong, E. B. Ledesma, *J. Anal. Appl. Pyrolysis* **2017**, *123*, 83–91.
[130] N. Akiya, P. E. Savage, *Chem. Rev.* **2002**, *102*, 2725–2750.
[131] G. Jiang, D. J. Nowakowski, A. V. Bridgwater, *Thermochim. Acta* **2010**, *498*, 61–66.
[132] B. Zhang, H. J. Huang, S. Ramaswamy, *Appl. Biochem. Biotechnol.* **2008**, *147*, 119–131.
[133] J. E. White, W. J. Catallo, B. L. Legendre, *J. Anal. Appl. Pyrolysis* **2011**, *91*, 1–33.
[134] F. P. Bouxin, A. McVeigh, F. Tran, N. J. Westwood, M. C. Jarvis, S. D. Jackson, *Green Chem.* **2015**, *17*, 1235–1242.
[135] P. S. R. Waldvogel, in *Statusseminar FNR*, Mainz, **2017**.
[136] D. Schmitt, C. Regenbrecht, M. Hartmer, F. Stecker, S. R. Waldvogel, *Beilstein J. Org. Chem.* **2015**, *11*, 473–480.
[137] C. Beyer, D. Lorch, J.-N. Gerdes, *Kontinuierlicher Prozess Zur Gewinnung von Catechol Aus Lignin*, Karlsruhe, **2017**.
[138] "Pyrocatechol ≥99% | Sigma-Aldrich," **2018**.

[A] with J. Schäfer, Department of Food Chemistry and Phytochemistry KIT.

[B] with M. Fleckenstein, University of Göttingen. Wood Biology & Wood Products.

FIGURES

TABLES

8 Appendix

8.1 Gas chromatography - analysis of the gaseous phase

Table 15: Calibrated gases; using standard gas mixtures to determine the quantity of these.

hydrogen	methane
carbon dioxide	propene
ethane	propane
oxygen	carbon monoxide
nitrogen	i-butane
n-butane	

GC-Method for the measurements:
The oven equilibration time is 1 min, with a maximum temperature of 250 °C, the slow fan is disabled. The runtime of each analysis is 46 minutes. The oven program heats it to 50 °C for 10 min, then 4 K/min to 90 °C for 0 min and then 25 K/min to 150 °C for 12 min and 50 K/min to 230 °C for 10 min.
The front inlet heater is set at a temperature of 250 °C with 2.7 bar as pressure. The septum flow is 18 ml/min, with a septum purge flow of 3 ml/min. The split ratio is 28 : 1 with a flow of 0 ml/min. The heater of the FID is set at a temperature of 300 °C with a hydrogen flow of 35 ml/min, an air flow of 400 ml/min and a makeup gas (helium) flow of 1 ml/min. The TCD heater is set at a temperature of 250 °C with a reference flow of 25 ml/min and a makeup gas (helium) flow of 1 ml/min.

8.2 Gas chromatography - analysis of the liquid phase

Table 16: Calibrated components; using pure components in gas chromatography qualities.

cyclopentanone	guaiacol
furfural	4-ethylphenol
2-methyl-yclopentanon	4-methyl-guaiacol
phenol	catechol
o-cresol	4-methyl-catechol
p-cresol	4-ethylguaiacol
4-ethylcatechol	syringol
vanillin	

GC-Method for the measurements:
The front inlet has an initial temperature of 275 °C and a pressure of 2.4 bar. The split ratio is 30.8 : 1, with a split flow of 61.6 ml/min. The total helium flow is 65.7 ml/min. The capillary

column is a Restek 13323 Rtx-1 MS, for max. 350 °C with a nominal length of 30 m, the nominal diameter of 250 µm and a nominal film thickness of 25 µm. The initial flow is 2 ml/min with a nominal initial pressure of 2.4 bar and an average velocity of 46 cm/sec. The FID has a temperature of 310 °C, with a hydrogen flow of 41 ml/min and an air flow of 450 ml/min. The constant makeup gas flow (nitrogen) is 5 ml/min.

8.3 Sample preparation of the liquid samples for the GC measurements

The extraction is performed with ethyl acetate as an extraction agent. By acidifying the solution to a pH value of 3 to 4, the phenol form is present which can be extracted from the water phase to the organic solvent used for extraction.
The acidification is performed with sulfuric acid (~5 vol.%) because a better phase separation can be achieved with sulfuric acid.
The phases are separated, and the organic extract is used for the GC analytic. The extraction is carried out with 0.52 ml of ethyl acetate, which contains an internal standard (pentadecane). The aqueous phase is mixed with the ethyl acetate and left to settle for about an hour. Then the mixture gets centrifuged to separate the phases, and the organic phase is used for further analytics.

8.4 Equations used for the calculation of the sample concentrations [10]

For the evaluation of the amounts of the respective components before the extraction, following distribution coefficients (Table 17) and equations (1 – 4) are used.

Table 17: Distribution coefficients of the calibrated components for the extraction, as a preparation for the measurement of the liquid product mixture.

cyclopentanone	0.52	guaiacol	0.92
furfural	0.48	4-ethylphenol	0.80
2-methyl-yclopentanon	0.76	4-methyl-guaiacol	0.78
phenol	0.95	catechol	0.82
o-cresol	1.00	4-methyl-catechol	0.70
p-cresol	0.97	4-ethylguaiacol	0.78
4-ethylcatechol	0.87	syringol	0.75
vanillin	0.74		

$$c_{\text{sample}} = \frac{(c_{\text{raw}} \cdot f_{\text{ISDT}} \cdot f_{\text{dilution}} \cdot f_{\text{volume}})}{DC} \qquad (8.1)$$

c_{sample} concentration of the compound in the sample

c_{raw} concentration of the extract

f_{ISDT} factor of the distribution of the internal standard

$f_{dilution}$ factor of the sample dilution

f_{volume} factor of the extraction volume

DC distribution coefficient (gained in previous work)

$$f_{\mathrm{ISTD}} = \frac{c_{\mathrm{ISTD}}}{c_{\mathrm{ISTD\ in\ sample}}} \tag{8.2}$$

c_{ISTD} concentration of the internal standard in the measurement

$c_{ISTD\ in\ sample}$ concentration of the internal standard in the sample

$$f_{\mathrm{dilution}} = \frac{v_{\mathrm{sample}}}{v_{\mathrm{ethyl\ acetate}}} \tag{8.3}$$

v_{sample} volume of the sample

$v_{ethyl\ acetate}$ volume of the ethyl acetate

$$f_{\mathrm{volume}} = \frac{v_{\mathrm{sample\ for\ extraction}}}{v_{\mathrm{ethyl\ acetate\ for\ extraction}}} \tag{8.4}$$

$v_{sample\ for\ extraction}$ volume of the sample used in the extraction step

$v_{ethyl\ acetate\ for\ extraction}$ volume of the ethyl acetate used in the extraction step

8.5 SEC polydispersity M_w/M_n

Table 18 gives the results of the whole peak of the synthesized oligomer. The smaller the polydispersity M_w/M_n is, the consistent the molecules are. The polydispersity of the measured samples (400 °C @ one h: 3.3; 300 °C @ one h: 8.1 and 30 min: 7.0) are higher, so there is a higher variety of the molecules.

Table 18: The weight average molecular weight M_w, the number average molecular weight M_n, the polydispersity M_w/M_n, the whole retention volume and the area of the RI signal of the measured synthesized oligomer.

Peak	1
M_w (Da)	772
M_n (Da)	407
M_w/M_n	1.9
Ret Vol (ml)	14.3
RI Area (mV/ml)	306.5

8.6 Biomass structure data

Table 19: Elemental analysis of the used bark and Indulin AT with ash contents at 550 °C and 1000 °C.

	C wt.%	H wt.%	N wt.%	S wt.%	ash-550 %	ash-1000 %
Bark	47.8	5.7	0.8	0.1	6.9	4.8
Indulin AT	61.6	5.6	1.4	1.7	3.8	2.4

Table 20: Monomer units of Indulin AT, beech bark, Organosolv of beech wood of the FhG CBP, Organosolv of *Miscanthus* of the FhG ICT and Organosolv of poplar wood of the FhG ICT.[B]

Monomer basics	Indulin AT	Beech bark	Organosolv beech	Organosolv *Miscanthus*	Organosolv poplar
Sinapyl alcohol	0 %	44.5 %	51.4 %	48.6 %	63.5 %
p-cumaryl alcohol	2.5 %	33.2 %	24.3 %	15.2 %	7.2 %
Coniferyl alcohol	97.5 %	22.3 %	24.3 %	36.3 %	29.3 %

8.7 Additional model data (R^2, concentration profiles and kinetic parameters)

Table 21: Coefficients of determination R^2 of the calculated concentration profiles to the experimentally measured concentrations for the modeled temperature range (275-350 °C).

T °C	guaiacol	catechol	4-methylcatechol
275	0.95	0.78	0.90
287	0.92	0.87	0.74
300	0.88	0.88	0.98
313	0.90	0.96	0.88
325	0.91	0.95	0.80
350	0.34	0.75	-0.40

Table 22: Coefficients of determination R^2 of the calculated concentration profiles to the experimentally measured concentrations for the second modeled temperature range (275-350 °C).

T °C	guaiacol	Catechol	4-methylcatechol
275	0.86	0.93	0.78
287	0.68	0.95	0.93
300	0.91	0.93	0.84
313	0.91	0.90	0.90
325	0.88	0.87	0.86
350	0.37	0.15	-1.79

Table 23: Coefficients of determination R^2 of the calculated concentration profiles to the experimentally measured concentrations for the modeled temperature range (275-350 °C).

T °C	phenol	o-cresol	p-cresol	4-methylguaiacol	4-ethylguaiacol	4-ethylcatechol
275	0.80	1.00	1.00	0.82	0.53	0.89
287	0.76	1.00	1.00	0.69	0.38	0.88
300	0.54	0.03	0.78	0.72	-0.09	0.92
313	0.84	1.00	1.00	0.89	0.93	0.70
325	0.82	1.00	0.98	0.96	0.98	0.73
350	0.89	0.66	0.68	0.62	-0.68	0.76

Table 24: Coefficients of determination R^2 of the calculated concentration profiles to the experimentally measured concentrations for the second modeled temperature range (275-350 °C).

T °C	phenol	o-cresol	p-cresol	4-methylguaiacol	4-ethylguaiacol	4-ethylcatechol
275	-0,72	0,47	0,82	0,70	0,37	0,85
287	0,17	-0,68	0,57	0,42	-0,23	0,86
300	0,44	0,87	0,71	0,79	0,43	0,82
313	-0,24	0,25	0,83	0,52	0,31	0,83
325	-0,39	-0,19	-4,37	0,54	0,13	0,68
350	0,56	0,74	0,77	0,57	-1,44	0,65

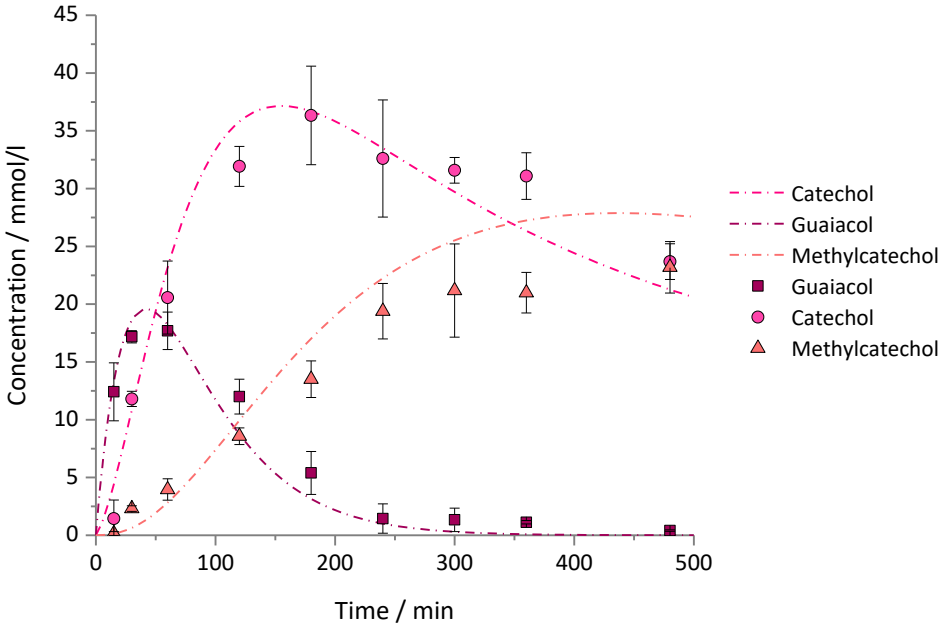

Figure 82: Experimental concentration profiles of guaiacol, catechol, and 4-methylcatechol over different residence times (0.25 – 8 h) at 300 °C (dots) compared to the modeled concentration with the second activation energy profiles of the three components for Indulin AT.

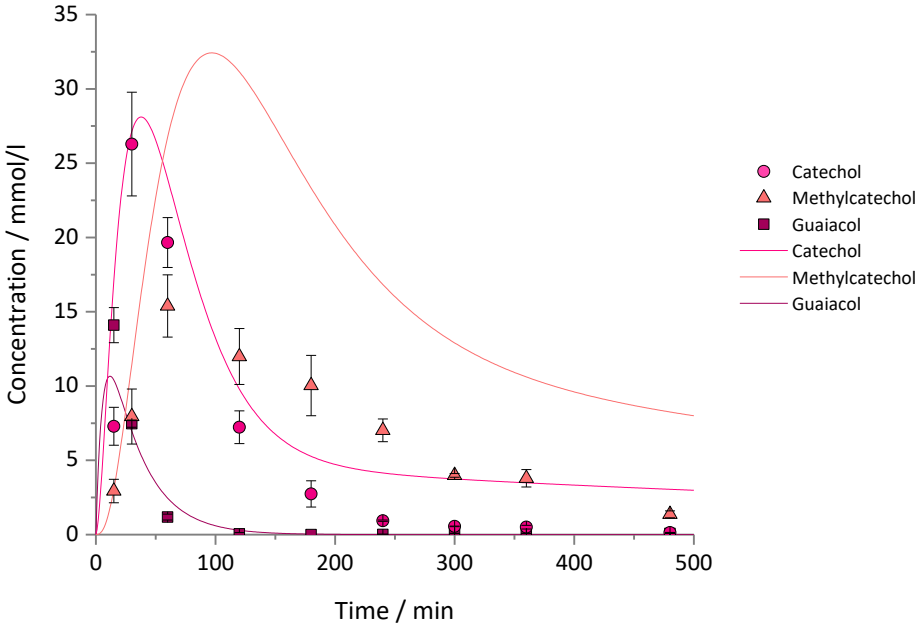

Figure 83: Experimental concentration profiles of guaiacol, catechol, and 4-methylcatechol over different residence times (0.25 – 8 h) at 350 °C (dots) compared to the modeled concentration profiles of the three components for *Miscanthus* organosolv lignin.

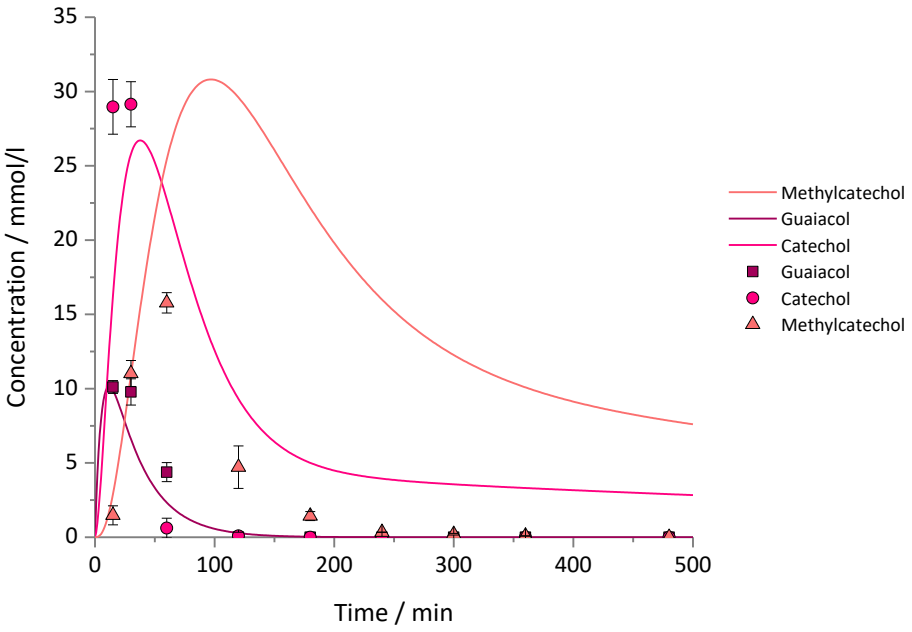

Figure 84: Experimental concentration profiles of guaiacol, catechol, and 4-methylcatechol over different residence times (0.25 – 8 h) at 350 °C (dots) compared to the modeled concentration profiles of the three components for beech wood organosolv lignin.

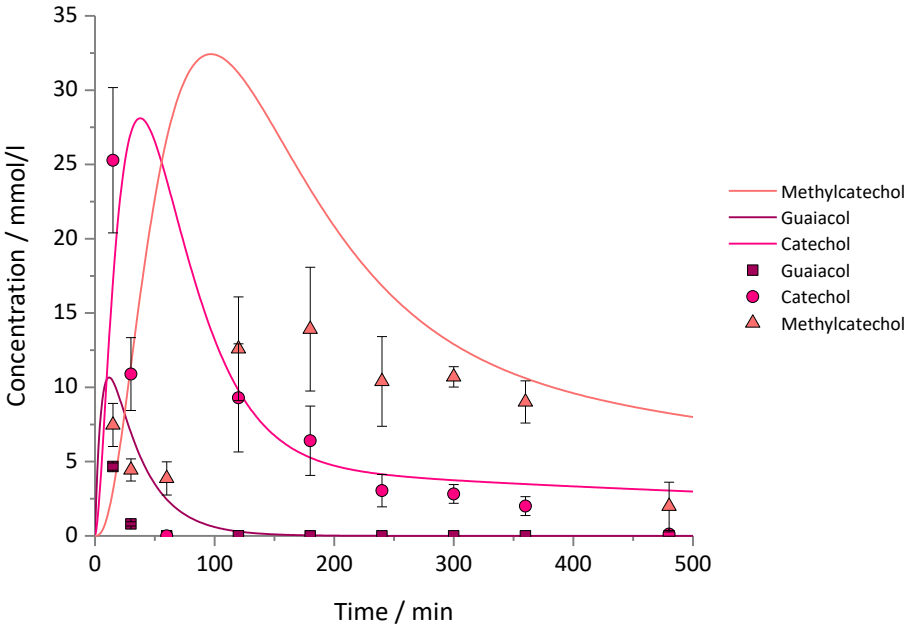

Figure 85: Experimental concentration profiles of guaiacol, catechol, and 4-methylcatechol over different residence times (0.25 – 8 h) at 350 °C (dots) compared to the modeled concentration profiles of the three components for beech bark lignin.

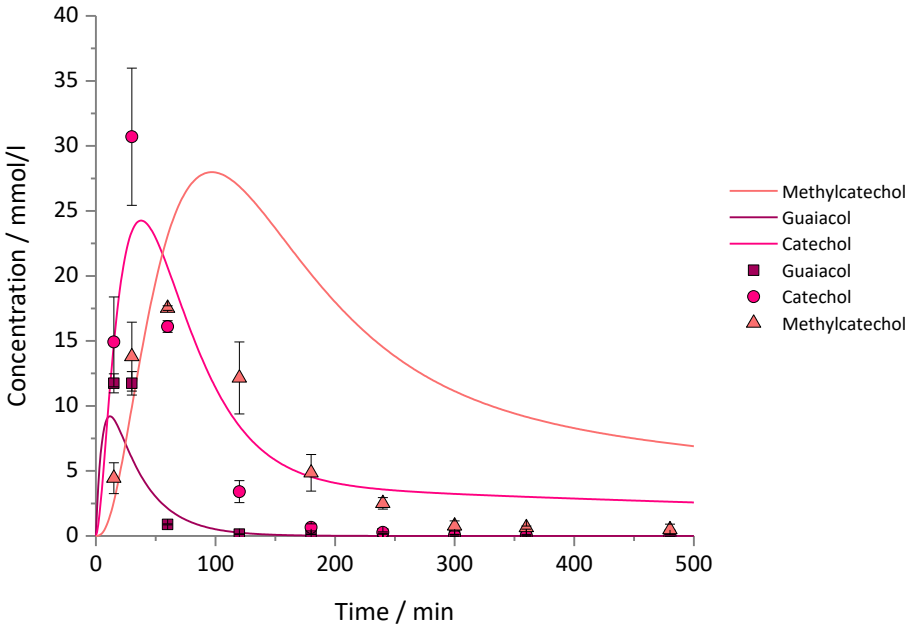

Figure 86: Experimental concentration profiles of guaiacol, catechol, and 4-methylcatechol over different residence times (0.25 – 8 h) at 350 °C (dots) compared to the modeled concentration profiles of the three components for poplar organosolv lignin.

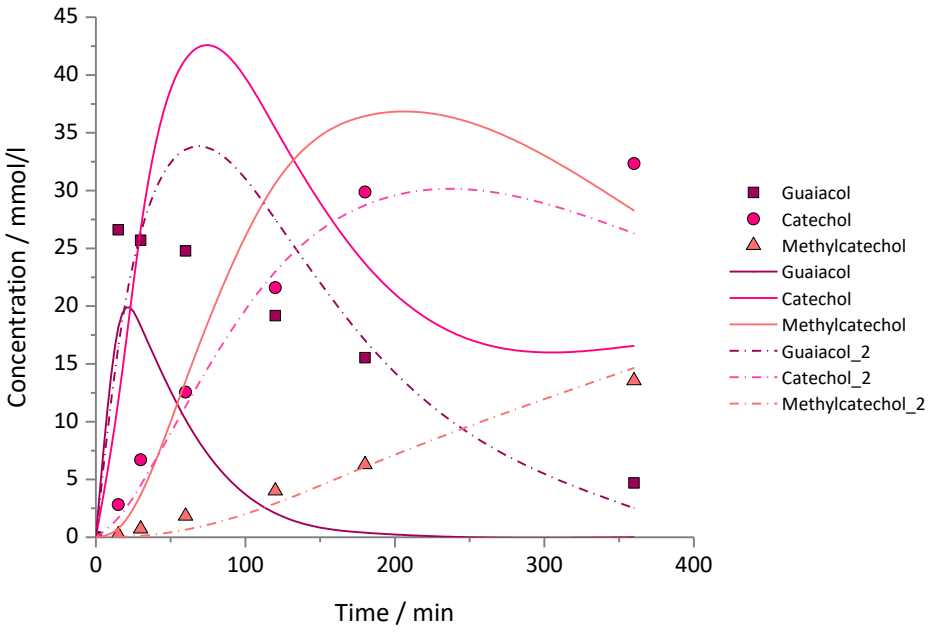

Figure 87: Experimental concentration profiles of guaiacol, catechol, and 4-methylcatechol over different residence times (0.25 – 8 h) at 287 °C (dots) compared to the modeled concentration profiles of the three components and these compared to the modeled concentration profiles of the three components with a second activation energy for Indulin AT.

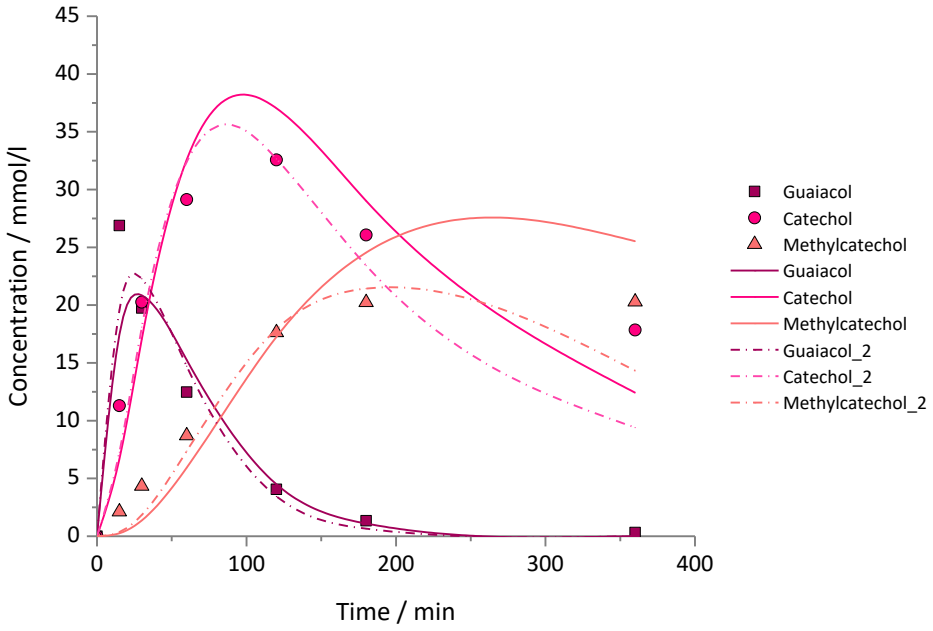

Figure 88: Experimental concentration profiles of guaiacol, catechol, and 4_methylcatechol over different residence times (0.25 – 8 h) at 313 °C (dots) compared to the modeled concentration profiles of the three components and these compared to the modeled concentration profiles of the three components with a second activation energy for Indulin AT.

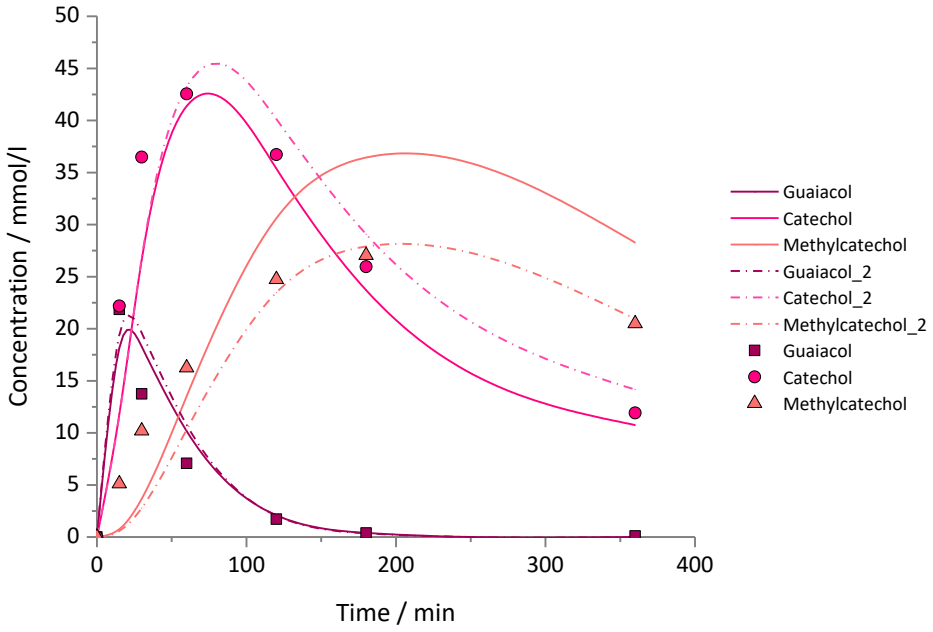

Figure 89: Experimental concentration profiles of guaiacol, catechol, and 4-methylcatechol over different residence times (0.25 – 8 h) at 325 °C (dots) compared to the modeled concentration profiles of the three components and these compared to the modeled concentration profiles of the three components with a second activation energy for Indulin AT.

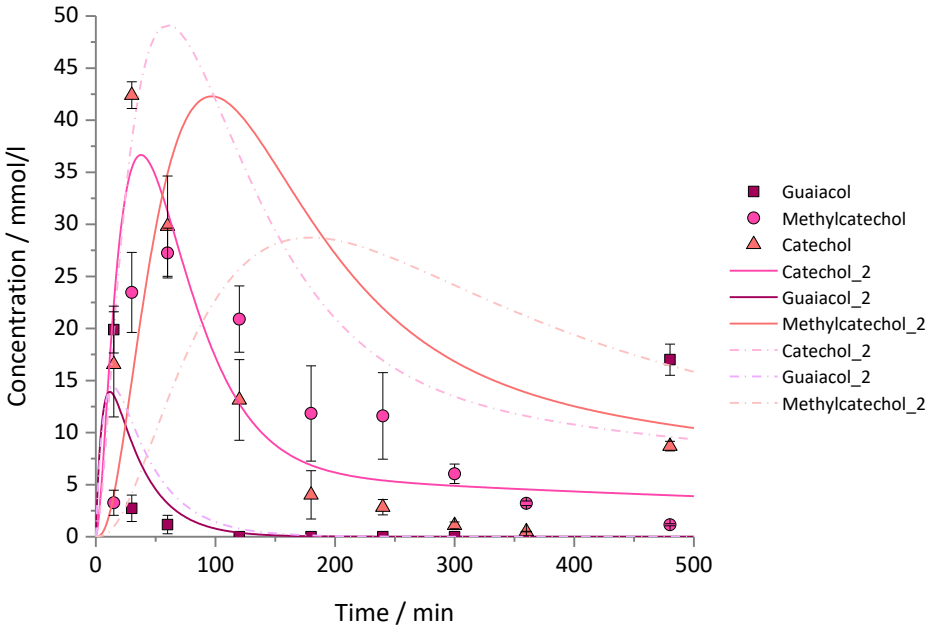

Figure 90: Experimental concentration profiles of guaiacol, catechol, and 4-methylcatechol over different residence times (0.25 – 8 h) at 350 °C (dots) compared to the modeled concentration profiles of the three components and these compared to the modeled concentration profiles of the three components with a second activation energy for Indulin AT.

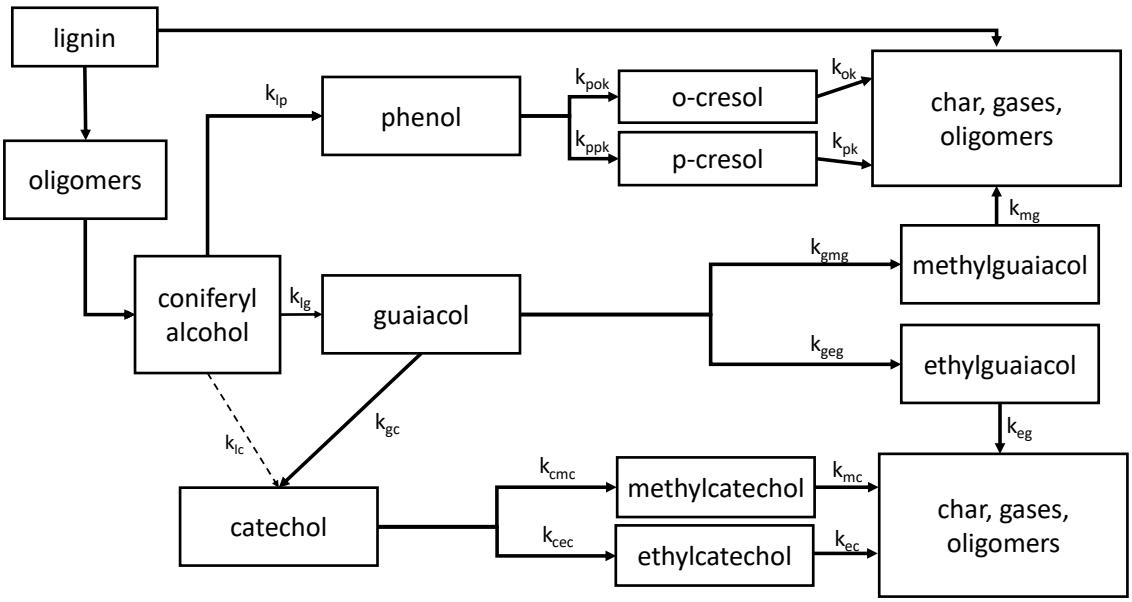

Figure 91: Modeled reaction network.

Table 25: Activation energies in J/mol for the reactions calculated out of the Arrhenius plots of one temperature range (287-350 °C, with k_{lc} . -1.10 E^{-03})

	Activation energy J/mol	pre-exponential factor 1/min
k_{lp}	3.43 E^{+03}	1.28 E^{+01}
k_{lg}	3.06 E^{+04}	1.29 E^{+01}
k_{cmc}	1.19 E^{+05}	2.50 E^{+08}
k_{cec}	6.80 E^{+04}	2.99 E^{+03}
k_{gc}	1.48 E^{+05}	3.91 E^{+11}
k_{ec}	8.17 E^{+04}	2.88 E^{+05}
k_{eg}	5.09 E^{+04}	1.70 E^{+03}
k_{geg}	5.51 E^{+04}	3.92 E^{+02}
k_{mc}	8.00 E^{+04}	6.00 E^{+04}
k_{gmg}	5.37 E^{+04}	3.59 E^{+02}
k_{mg}	4.09 E^{+04}	2.28 E^{+02}
k_{ok}	5.77 E^{+04}	4.00 E^{+02}
k_{pok}	7.51 E^{+04}	4.45 E^{+03}
k_{ppk}	9.88 E^{+04}	5.94 E^{+05}
k_{pk}	1.28 E^{+05}	2.77 E^{+08}

Table 26: Activation energies in J/mol for the reactions calculated out of the Arrhenius plots of two temperature ranges.

275 - 300 °C	Activation energy J/mol	pre-exponential factor 1/min		313 - 350 °C	Activation energy J/mol	pre-exponential factor 1/min
k_{lp}	-1.65 E^{+05}	1.16 E^{-17}		k_{lp}	-6.07 E^{+04}	2.83 E^{-07}
k_{lg}	5.65 E^{+04}	3.30 E^{+03}		k_{lg}	3.03 E^{+03}	5.38 E^{-02}
k_{cmc}	1.41 E^{+05}	3.26 E^{+10}		k_{cmc}	-7.31 E^{+03}	1.89 E^{-03}
k_{cec}	4.38 E^{+04}	1.70 E^{+01}		k_{cec}	9.87 E^{+04}	1.33 E^{+06}
k_{gc}	2.15 E^{+05}	7.39 E^{+17}		k_{gc}	9.57 E^{+04}	1.18 E^{+07}
k_{ec}	3.21 E^{+04}	8.00 E^{+00}		k_{ec}	1.78 E^{+05}	5.77 E^{+13}
k_{eg}	-1.74 E^{+05}	1.45 E^{-18}		k_{eg}	6.44 E^{+04}	3.11 E^{+04}
k_{geg}	-1.92 E^{+05}	3.04 E^{-21}		k_{geg}	7.86 E^{+04}	5.37 E^{+04}
k_{mc}	1.53 E^{+05}	3.32 E^{+11}		k_{mc}	-2.58 E^{+04}	4,44 E^{-05}
k_{gmg}	5.69 E^{+04}	6.83 E^{+02}		k_{gmg}	2.11 E^{+04}	1.00 E^{+00}
k_{mg}	5.23 E^{+04}	2.51 E^{+03}		k_{mg}	7.52 E^{+03}	3,05 E^{-01}
k_{ok}	3.76 E^{+05}	2.90 E^{+32}		k_{ok}	9.70 E^{+04}	6.87 E^{+05}
k_{pok}	2.05 E^{+05}	6.35 E^{+15}		k_{pok}	7.78 E^{+04}	6.61 E^{+03}
k_{ppk}	1.17 E^{+05}	2.78 E^{+07}		k_{ppk}	1.12 E^{+05}	8.62 E^{+06}
k_{pk}	5.90 E^{+04}	9.10 E^{+01}		k_{pk}	1.44 E^{+05}	6.46 E^{+09}

8.8 Process evaluation [137]

To estimate the catechol sales price for economic extraction from the hydrothermal lignin degradation process, a laboratory process has been scaled up to industry size in a scale-up course. The specification to produce 50 tons of catechol per day delivered the remaining process streams. Using the mass and energy balances investment and manufacturing costs could be determined. The period of observation is 13 years, three of them are pure investment years. They are followed by a ten-year operating period at the end of it, all process plants have been written off. To get the retail price for catechol was calculated in the way, that its sale covers all running costs. These costs include fixed and variable production costs and investment costs.

The calculations were performed for two different lignins; Indulin AT and an Organosolv lignin. The starting conditions of the lab experiments are given in Table 27. The scaled-up process shall be a plug flow reactor.

Table 27: Initial values for the calculations. Price refers to the lignin. The catechol yield is quantity related. Organosolv is a specially manufactured product while Indulin AT is in the waste stream.

Lignin	Price €/kg	Pressure bar	Temperature °C	Residence time h	Yield Plug flow %
Indulin AT	50	150	300	3	27
Indulin AT	50	190	350	0.5	29
Organosolv	350	150	300	3	29
Organosolv	350	190	350	0.5	24

The specifications came from a 25 ml batch process in which 1.66 g of dry lignin with 12.5 mL of a 1 wt.% KOH solution were set to a suspension. This resulted in a partial solution. The procurement of the associated material values was taken from different literature. It was already designed for the standard conditions as extremely difficult to determine heat capacities, densities, and viscosities. Heat capacities for the suspension were determined according to their mass fraction.

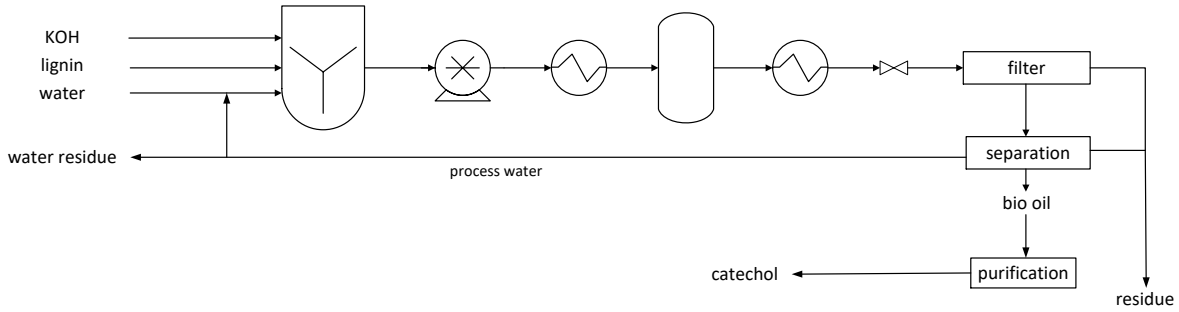

Figure 92: Flowsheet of the planned and calculated process set up with a plug flow reactor.

In the beginning, all reactants are mixed in a stirred tank and then promoted by a feed pump as a suspension. The pump also generates a high required pressure difference. Then the feed is brought to a supercritical state with a heater. In this state, the suspension gets into the flow tube. Through a heat exchanger, the product stream is cooled to room temperature after the reactor and an expansion valve pressure relaxes the mixture to atmospheric pressure. The product stream consists of an aqueous phase, which contains catechol as well as solids, ashes and a gas phase. The gas phase consists mostly of CO_2 and a meager amount of hydrocarbons. Restoring standard conditions is required because these components have too little density difference under HTL conditions to separate them. The solids are filtered from the product stream in a filter. The product phase is finally separated in a water and bio-oil phase, and the catechol gets purified in a “black-box”, no information of the downstream process is available right now. For the catechol separation a black-box was assumed and with a factor of twice of the invest costs included. The remaining water is returned to the process, with a small stream of water leaving the process as wastewater to prevent rising impurities. The calculations delivered catechol prices in €/kg, which are shown in Table 28.

Table 28: Interest-free manufacturing and investment costs due to the produced catechol quantity of ten years vs. the current selling price.

	Residence time h	Indulin AT €/kg	Organosolv €/kg	Actual price €/kg
Plug flow	0.5	2 829	21 521	170 [138]
	3	3 094	20 740	

The calculated process leads to a catechol price of 2 829 €/kg which is 17 times of the Sigma Aldrich price, which is already a much higher price, than bulk ware. Without using all gained products, the process is not feasible by now.